Biochemical and functional characterization of novel RNA-binding proteins interacting with SMN in motor neuron-derived cells

Janik Laframboise

Thesis submitted to the

Faculty of Graduate and Postdoctoral Studies

in partial fulfillment of the requirements

for the MSc degree in Cellular and Molecular Medicine

January 9, 2013

Cellular Molecular Medecine

Faculty of Medicine

University of Ottawa

Abstract

Spinal muscular atrophy is an autosomal recessive genetic disease that results from the loss and/or degeneration of alpha motor neurons in the lower part of the spinal cord. With ~ 1 in 6000 live births per year being affected, this disease is the second leading cause of infant death and is caused by the loss or decrease of the Survival of Motor Neuron protein (SMN). While a lot is known about the role that SMN plays in the cytoplasmic assembly of spliceosomal small nuclear ribonucleoproteins (snRNPs), it remains a crucial question in the field to gain a better understanding of what specific/distinct function(s) SMN might have in motor neurons. We have identified novel interactions between SMN and two RNA-binding proteins (RBPs) known to be components of axonal RNA granules. More specifically, we demonstrated that SMN interacts with HuD and SERBP1 in a direct fashion in foci-like structures along neurites of motor neuron-derived cells. We have also demonstrated that the SMN/HuD interaction is required for the localization of HuD into RNA granules in neurites of motor neuron-derived cells. Furthermore, I have shown that SERBP1 is down-regulated in the absence of normal levels of SMN and, most importantly, that over-expression of SERBP1 can rescue SMA-like neuronal defects using a cell culture model of the disease. These findings may help shed light on the non-canonical molecular pathway(s) involving SMN and RBPs in motor neurons and underscores the possible therapeutic benefits of targeting these RBPs in the treatment of SMA.

Table of contents

List of Figures

List of Abbreviations

ARE – AU-rich RNA element

A-SMN – axonal SMN

BSA – Bovine serum albumin

CARM1 – Coactivator-associated arginine methyltransferase 1

CB – Cajal bodies

cDNA – complementary Deoxyribonucleic acid

DMEM – Dulbecco's modified Eagle's medium

ELAV-like family of protein – Embryonic lethal abnormal vision-like family of protein

ESE – Exonic splicing factor

ESS – Exonic splicing enhancer

FBS – Fetal bovine serum

GAP-43 – Growth associated protein 43

GAPDH – Glycerol-3-phosphate dehydrogenase

GAR – glycine/arginine-rich

GDNF – Glial cell-derived neurotrophic factor

GST – Gluthatione S-transferase

HABP4 – Hyaluronan binding protein 4

hnRNP – heterogeneous nuclear Ribonucleoprotein protein

HRP – Horseradish peroxidase

KSRP – KH-type plicing regulatory protein

MN-1 – motor neuron-like

mRNA – messenger Ribonucleic acid

mRNP – messenger Ribonucleoprotein particle

NLS – nuclear localization signal

NMJ – Neuromuscular junction

OD – optical density

PAI-RBP1 – Plasminogen activator inhibitor type 1 mRNA binding protein

PBS – Phosphate buffered saline

PBS-T – Phosphate buffered saline and tween

PCR – Polymerase chain reaction

PGM – proline/glycine/methionine-rich

PMSF – Phenylmethanesulphonylfluoride

PRMT – Protein arginine methyltransferase

PVDF – Polyvinylidene difluoride

qPCR – quantitative Polymerase chain reaction

RBP – RNA-binding protein

RG – Arginine-glycine

RGG box – Arginine-glycine-glycine box

RNA – Ribonucleic acid

RNP – Ribonucleoprotein

RRM – RNA recognition motif

RT-PCR – Reverse transcriptase polymerase chain reaction

SERBP1 – Serpine mRNA binding protein 1

SDS – Sodium dodecyl sulfate

SDS-PAGE – Sodium dodecyl sulfate – polyacrylamide gel

SMA – Spinal muscular atrophy

S*mn* – Survival of motor neuron gene

SMN – Survival of Motor Neuron protein

snRNP – small nuclear Ribonucleoprotein particle

SUMO – Small ubiquitin modifiers

TDRD3 – Tudor domain containing protein 3

tri-snRNP – triple small nuclear Ribonucleoprotein

U snRNA – Uridine-rich small nuclear RNA

UTR – Untranslated region

Acknowledgements

I would first like to thank my ultimate mentor; Dr. Jocelyn Côté for is guidance throughout this amazing learning experience and for giving me the opportunity to become an accomplished researcher. Thank you for your patience, your support and understanding in difficult times and finally for being a great researcher who's love for science is transparent and inspiring. I would like to also take this opportunity to express my gratitude to my advisory committee members, Dr. Martin Holcik and Dr. Bernard Jasmin, for their help and guidance throughout this project.

I would also like to thank my lab colleague, for their support, knowledge and encouragement. Dr. M. Baldwin, Dr. G. Sanchez, H. Tadesse, A. Morettin, A. Fanous and G. Paris, as well as former coworkers, Dr. H. Valderrama, Dr. I. Goulet and L. Hubers. A special thanks to Lisa who guided me through my first lab experiences and provided me with all the tools to become an accomplished researcher.

Finally, I want to thank my family (I. Gravelle, P. Larente, J. Laframboise, J. Cadieux) and friends (G. Paris, E. Sauvé, E. Demers, E. Buteau, M. Demers, R. Gravelle) for their patience, encouragement and support. Thanks to my mother and father who made this learning experience possible and to my life partner Ian for his infinite patience.

Chapter 1. Introduction

1.1 Proximal Spinal muscular atrophy (SMA)

1.1.1 Classification of Proximal spinal muscular atrophy

Proximal spinal muscular atrophy (SMA) is a common autosomal recessive genetic disease found in humans with a carrier frequency of 1 in 40 and an incidence of 1 in 6000 (Monani 2005; Pearn 1980). It is a leading cause of infant mortality, second only to cystic fibrosis (Monani 2005). This devastating disease was first described more than a century ago by Werdnig and Hoffman and was characterized by a loss of anterior horn cells resulting in progressively increasing weakness and death at an early age (Werdnig 1892; Hoffmann 1892). This disease specifically affects alpha-motor neurons in the anterior horn of the spinal cord leading to atrophy of the proximal muscles of the limbs and trunk (Melki 1997; Monani 2005). SMA progresses by a diffuse symmetric weakness of proximal muscles, which then worsens into paralysis and finally leads to death by respiratory distress (Melki 1997; Roberts et al. 1970). The patients suffering from this disease are also marked by a decrease in deep reflexes (Lefebvre et al. 1998). Moreover, SMA is characterized by a broad range of phenotypes which Byers and Banker divided into 3 groups based on the maximum muscle function achieved (Byers and Banker 1961). The current clinical classification used by researchers is comprised of 5 types based on age of onset and maximum muscle function achieved which is more closely related to life expectancy. Type 0 is considered the most severe SMA and patients usually have respiratory distress and limited life expectancy. Type 1 patients that are classified as having severe SMA, cannot sit

without being supported, are younger than 6 months and have a life expectancy of approximately 2 years. Type 2 patients are between the ages of 6 months and 18 months and are able to sit without support. Type 3 is composed of infants older than 18 months that can walk. Finally, Type 4 patients are usually older than 10 years old when disease manifests itself and they have a normal life expectancy (Brzustowicz et al. 1990; Monani 2005). Additionally, there are other forms of SMA (i.e. not caused by SMN) that are genetically distinct and affect different neuron and muscle types. There is an autosomal dominant form (Sambuughin et al. 1998; van der Vleuten et al. 1998), a recessive form that affect specifically the distal muscles (Viollet et al. 2002) and a severe form of SMA with respiratory distress (Grohmann et al. 2001).

1.1.2 The genetic cause of proximal SMA

The chromosomal localization of the causative gene and large range of phenotypes presented by SMA suggested that a genetic cause might be difficult to uncover (Pearn 1980). However, the origin that gave rise to the pathology was surprisingly simple. SMA is caused by mutation (5%) or deletion (95%) of the survival of motor neuron gene (*SMN1*) that encodes a ubiquitously expressed protein called Survival of motor neuron (SMN) which has been implicated in RNA metabolism (Figure 1; Lefebvre et al. 1995). The *SMN1* gene is responsible for the production of nearly all the full length functional SMN protein; however there is another copy of this gene termed *SMN2* that shares a high level of homology (Lefebvre et al. 1995). These two genes are different by 5 nucleotides in their sequences and a single base pair change of a C to a T in exon 7 of the *SMN2* gene causes the skipping of this exon, which leads to the production of an unstable and rapidly degraded protein (Lefebvre et al. 1995). In spite of this, the *SMN2* gene contributes 10% of the full

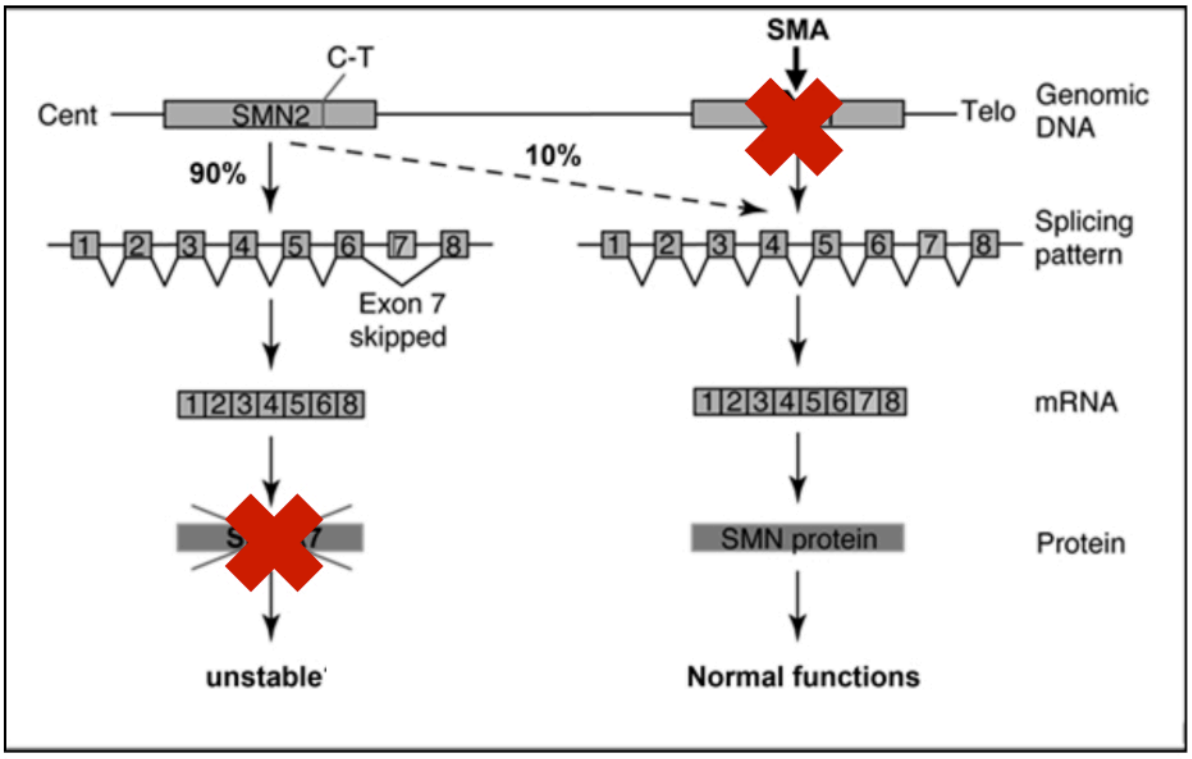
SMA
C-T
Cent
SMN2
Telo
Genomic DNA
90%
10%
Splicing pattern
1 2 3 4 5 6 7 8
Exon 7 skipped
1 2 3 4 5 6 8
1 2 3 4 5 6 7 8
mRNA
SMN protein
Protein
unstable
Normal functions

Figure 1. The genetic cause of proximal Spinal Muscular Atrophy (SMA). SMN genomic locus in healthy individuals and in SMA type 1 patients. In healthy patients the *SMN1* gene produces the full length functional SMN protein, whereas in SMA type 1 patients this gene is mutated or completely deleted which leads to a drastic decrease in full length functional SMN protein levels. The *SMN2* gene is responsible for only 10% of the production of the SMN protein since in exon 7 there is a single base pair change of a C to a T that results in its skipping, and leads to the production of a truncated protein that is unstable and rapidly degraded (modified from Khoo et al., *Trends Biotechnol,* 2003).

length functional SMN protein in cells (Figure 1) (Coovert et al. 1997; Lefebvre et al.1997). The Cartegni and Krainer laboratories demonstrated that the single base pair change between *SMN1* and *SMN2* in exon 7 disrupts an enhancer sequence which abolishes the binding of the ASF/SF2 splicing factor and causes skipping of this exon (Cartegni and Krainer 2002). However, the Kashima and Manley laboratories reported that the change from a C to a T in exon 7 creates an exonic splicing silencer (ESS) which permits the hnRNP A1 splicing factor to bind and silence the exon (Kashima and Manley 2003). It is possible that both of these mechanisms play a role since the end result is the same; skipping of exon 7 (Monani 2005). The genome at the location of the *SMN2* gene is susceptible to recombination and duplication events; therefore it is possible that patients can have more than one copy of the *SMN2* gene present. Moreover, the *SMN2* gene produces 10 percent of the full length functional SMN protein; therefore the severity of the disease is inversely correlated with the *SMN2* gene copy number. This may also contribute to the diverse range of clinical presentation observed for SMA (Feldkotter et al. 2002; McAndrew et al. 1997).

1.2 The survival of motor neuron protein (SMN)

1.2.1 The Survival of motor neuron protein.

SMN is a ubiquitously expressed protein that is composed of 294 amino acids and resolves at a molecular weight of 38 KDa on a SDS-PAGE gel. The *SMN* gene is comprised of nine exons and 8 introns (Figure 2A). The N-terminal region of this protein has been shown to bind to Gemin2. An amino acid domain encoded by exon 2b and a tyrosin/glycine-rich motif encoded by exon 6 allows the dimerization of SMN (Young et al.

2000). Furthermore, exon 2a and 2b encode for a domain that has been demonstrated to bind to nucleic acid *in vitro* (Briese et al. 2005). Although somewhat controversial, the localization of SMN to the cytoplasm has been linked to a domain encoded by exon 7 (van Bergeijk et al. 2007; Wolstencroft et al. 2005; Zhang et al. 2007b; Zhang et al. 2003). The middle region of the SMN protein contains a 60 amino acid domain, termed the Tudor domain, that is encoded by exon 3 and in its core has a barrel-like structure (Figure 2A). This barrel-like structure is composed of beta-sheets that form a hydrophobic pocket with a large amount of negatively charge residues which allow protein-protein interactions (Selenko et al. 2001). Specifically, the Tudor domain of SMN allows the interaction with methylated arginines residues in substrate proteins (Barth et al. 2003; Brahms et al. 2001; Cheng et al. 2007; Cote and Richard 2005; Kim et al. 2006). In the snRNP assembly process (discussed below), it is this domain that mediates the interaction of the SMN complex with core Sm proteins (Chari et al. 2008). Importantly, mutations in the Tudor domain of SMN are found in human patients with severe forms of SMA and these mutations inhibit its capacity to interact with methylated arginines, therefore highlighting its implication in the etiology of the disease (Cote and Richard 2005; Tadesse et al. 2008).

1.2.2 Arginine methylation

As mentioned above, the Tudor domain allows SMN to interact with arginine methylated proteins, and mutations of this domain have been linked to the SMA pathology (Cote and Richard 2005). This specific post-translational modification is catalysed by a family of protein termed the protein arginine methyltransferases (PRMT). These enzymes catalyse the transfer of a methyl group from a donor (S-adenosyl methionine) to a nitrogen

atom of the guanidino group on an arginine. This increases the bulkiness of the arginine residue and its hydrophobicity without changing its charge (Pahlich et al. 2006). A first methyl group is added to the arginine forming a mono-methylated intermediate; while a second methyl group is added in most cases to generate a dimethylated arginine (Figure 2B). There are two types of arginine dimethylation reactions, namely asymmetric dimethylation and symmetric dimethylation that are carried out by type I and type II PRMT, respectively (Figure 2B). The type III PRMT is composed of only PRMT7 and is characterised by a single addition of a methyl group, therefore forming a mono-methylated arginine (Bedford 2007). Importantly, we count up to 9 different PRMTs in mammals that are almost all ubiquitously expressed, apart from PRMT8 which is expressed only in neurons, and play crucial roles in the regulation of numerous cellular processes. They usually recognize and methylate an arginine (R)-glycine (RG) rich sequence known as the GAR motif (Najbauer et al. 1993). However, one member of this family, PRMT4, also known as coactivator-associated arginine methyltransferase 1 (CARM1), has a higher level of specificity for an R in a 'non RG' context. This R is most often surrounded by a so-called 'PGM motif', which is rich in proline, glycine and methionine residues (Cheng et al. 2007). Furthermore, PRMT6 recognizes the consensus GAR motif and can also recognize and methylate RR motifs (Xie et al. 2007). Lastly, PRMT5 and 7 can methylate isolated arginines in non-consensus regions.

Arginine methylation can regulate a number of processes, including subcellular localization of proteins, transcription, protein-protein interaction, protein-RNA interactions as well as cell differentiation (Bedford et al. 2000; Bedford and Richard 2005). Arginine methylation is most known for its role in the regulation of transcription by its action on the

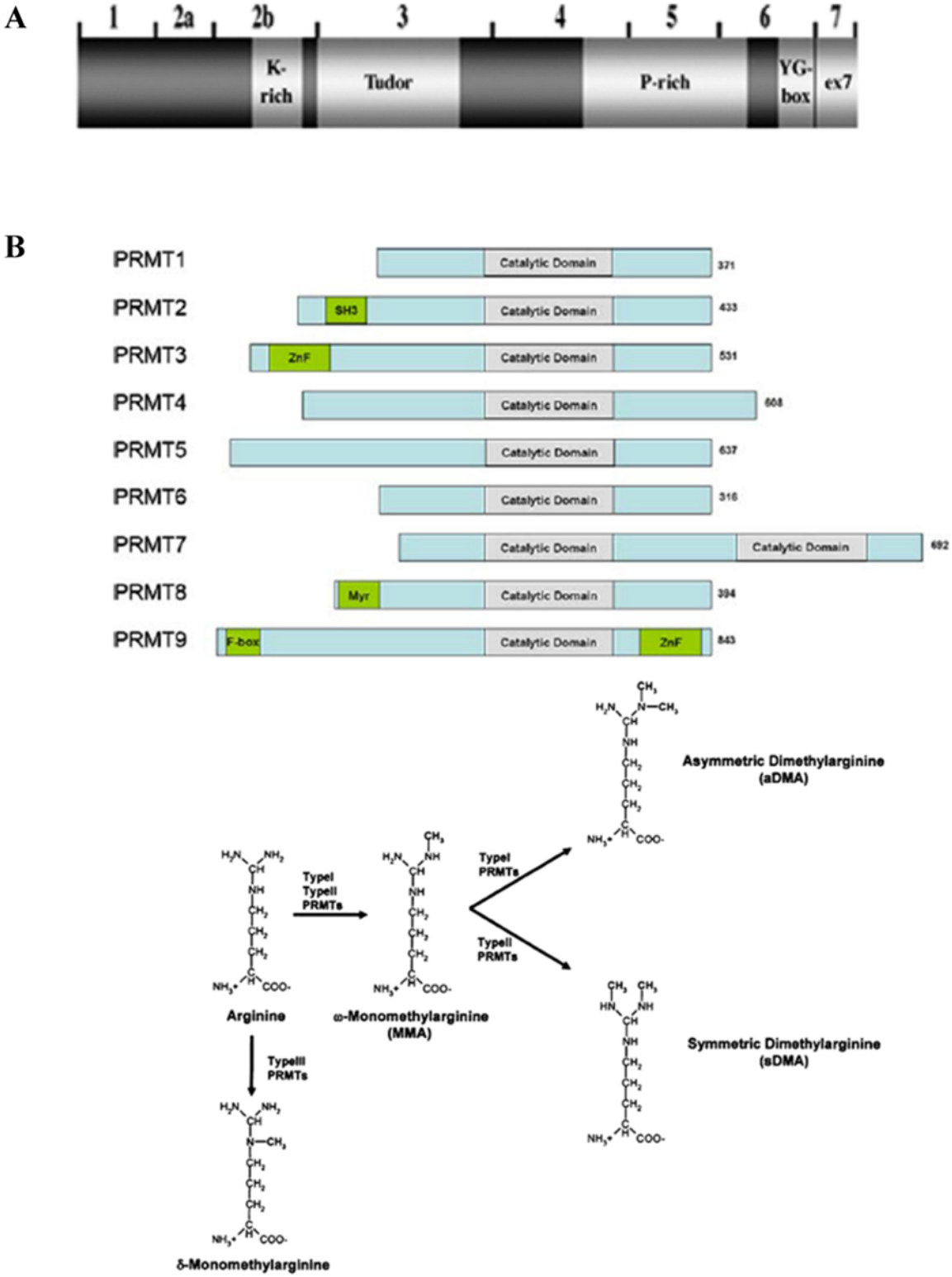
A
1
2a
2b
3
4
5
6
7
K-rich
Tudor
P-rich
YG-box
ex7
B
PRMT1
PRMT2
PRMT3
PRMT4
PRMT5
PRMT6
PRMT7
PRMT8
PRMT9
Catalytic Domain
SH3
ZnF
Myr
F-box
371
433
531
608
637
316
692
394
843
Arginine
ω-Monomethylarginine (MMA)
Asymmetric Dimethylarginine (aDMA)
Symmetric Dimethylarginine (sDMA)
δ-Monomethylarginine
TypeI TypeII PRMTs
TypeI PRMTs
TypeII PRMTs
TypeIII PRMTs

Figure 2. The SMN protein and arginine methylation. A. Schematic representation of the full length SMN protein. Numbers 1 to 7 represent the different exons that encodes the indicated protein domains (modified from Renvoise et al., *J. Cell Sci.,* 2006). **B.** Protein arginine methylation is catalysed by a family of protein known has protein arginine methyltransferases (PRMTs). Nine of these proteins have been characterized in mammals to date (top panel). Following the catalysis of the formation of a monomethyl-arginine, type I transfers a second methyl group to the same nitrogen which generates an asymmetrical dimethylation whereas type II transfers a methyl group to the second nitrogen producing a symmetrical dimethylation (modified from Wolf, *Cell. Mol. Life Sci., 2009).*

remodeling of chromatin, through modification of histone tails (Chen et al. 1999; Mowen et al. 2001; Wang et al. 2001; Yun and Fu 2000). Importantly, arginine methylation of RNA-binding proteins (RBPs) has been demonstrated to influence their subcellular localization and interaction with their RNA targets. For example, it has been shown that methylation of HuD by CARM1 negatively affects the binding activity of HuD to p21 mRNA (Fujiwara et al. 2006; Hubers et al. 2011). Additionally, it was shown that methylation of HuR can positively regulates its RNA binding activity to Sirtuin 1 mRNA (Calvanese et al. 2010). Apart from its role in the regulation of RNA-binding activities, arginine methylation has also been linked with neuronal differentiation. When the methyltransferase activity is inhibited in PC12 cells, a defect was observed at the level of neurite outgrowth following treatment with nerve growth factors (NGF) (Cimato et al. 1997). This demonstrates that methylation may be crucial for the differentiation process of these cells.

1.2.3 The canonical function of SMN: snRNP biogenesis

In the subcellular context, SMN localizes to both the cytoplasm and nucleus (Monani 2005). Precisely, early work demonstrated that SMN binds to heterogeneous nuclear ribonucleoproteins (hnRNPs) and that it localizes to nuclear bodies termed Cajal bodies (Liu et al. 1997). SMN also localizes to foci-like structure in the nucleus which can colocalize in some instances with Cajal bodies. These structures termed Gemini of Cajal bodies or more commonly referred to as ‘gems’, are not present in all types of cells and their cellular function is still largely unknown. It is thought that gems are a cluster of SMN proteins and some associated proteins that are not exported to the cytoplasm due to the absence of post-translation modifications needed for this export (Carvalho et al. 1999;

Hebert et al. 2002). Furthermore, Cajal bodies are rich in transcription factors, factors implicated in the post-transcriptional modification of nuclear RNAs and small ribonucleoproteins (snRNPs). Therefore, SMN could possibly play a crucial role in RNA metabolism (Monani 2005). Evidence has shown that SMN is involved in the assembly and maturation of snRNPs (Figure 3) (Pellizzoni 2007). SMN forms a multi-protein complex containing Gemin proteins and Unrip collectively called the core SMN complex. In this complex, SMN increases the efficiency and specificity of snRNP assembly by acting like a chaperone molecule (Akamatsu et al. 2005). Furthermore, SMN, Gemin7 and Gemin8 form the backbone of the complex and therefore create a binding platform for all the binding partners of the core complex. Several Gemin proteins are present in the SMN complex. Gemin2, Gemin3 and Gemin8 can interact directly with the SMN proteins, while, Gemin4 and Gemin5 are recruited to the complex via their interaction with Gemin3 and Gemin2, respectively. Gemin8 can interact with Gemin7 and Gemin4 and latter recruits Unrip and Gemin6 (Figure 3, top panel) (Cauchi 2010; Ogawa et al. 2009; Otter et al. 2007). The size of SMN does not allow the association of all these proteins; therefore SMN oligomerizes to form a higher-order complex of 20S to 80S (Lorson et al. 1998). Moreover, the SMN complex plays an essential role in the assembly of the splicing machinery by promoting the formation of cytoplasmic complexes between core Sm proteins, which are a heptameric ring of Sm proteins that forms around a conserved sequence present on Uridine-rich small nuclear RNAs (U snRNAs) (Pellizzoni 2007). Additionally, Gemin5 confers specificity to U spliceosomal snRNAs by recognizing the Sm site and an adjacent 3'-terminal stemloop structure found in all pre-snRNAs; therefore allowing the Sm core to interact only with the proper RNAs (Yong et al. 2010). This association between the SMN complex and Sm proteins is facilitated by symmetrical arginine dimethylation of the C-

The SMN complex

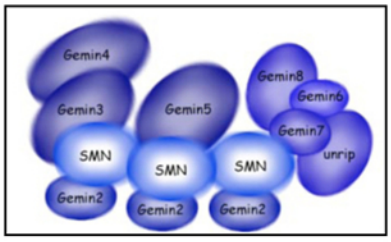

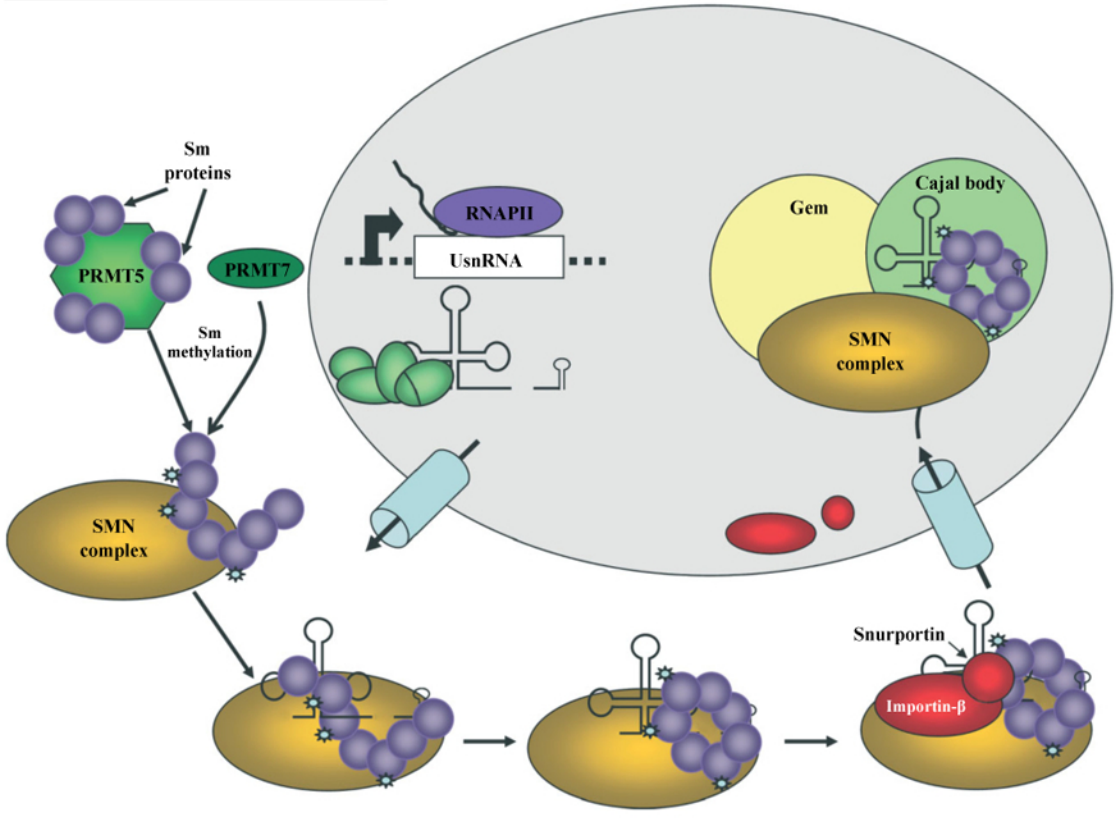

Figure 3. The role of the SMN core complex in snRNP biogenesis. Uridine-rich small nuclear RNAs (U snRNAs) are first transcribed and exported to the cytoplasm where they are recognized and bound by the SMN complex (Gemin5). This complex is composed of SMN proteins, Gemins and Unrip (top panel). The role of the SMN complex is to facilitate and promote the specific assembly of Sm proteins and U snRNAs into snRNPs. Following arginine methylation of SmD1, SmD3 and SmB/B' by PRMT5 (and potentially PRMT7) which renders them better substrates for the Tudor domain of SMN, it directs the Sm core to the SMN complex. The complex composed of the SMN complex, Sm proteins and U snRNA is then translocated into the nucleus in foci-like structures known as the Cajal bodies where, after further maturation, they can participate in pre-mRNA splicing (modified from Pellizzoni, *Embo Rep.,* 2007 and Coady and Lorson, *Wiley Interdiscip. Rev. RNA,* 2011).

terminal domain of SmD1, SmD3 and SmB/B' by the 20S PRMT5 methylosome complex, facilitating their interaction with the Tudor domain of SMN (Meister et al. 2001). Importantly, plCln, a member of the PRMT5 complex, was recently shown to be responsible for the recruitment of Sm proteins to the SMN complex. Binding of the SMN complex to the Sm proteins causes the dissociation of plCln and catalyze ring closure on the specific snRNA (Chari et al. 2008). Additionally, Gemin2, which is part of the SMN complex, acts like an arm that gathers 5 of the 7 Sm proteins, positioning them in a pentamer fashion ready for the Sm core assembly. Gemin2 also blocks the pre-mature association between the Sm core and RNA (Zhang et al. 2011). Following transport of the snRNP complexes from the cytoplasm to the nucleus and further maturation within Cajal bodies, they are now ready to participate in splicing (Figure 3; bottom panel) (Mouaikel et al. 2003; Narayanan et al. 2004). It surprisingly took a long time before defects in splicing were observed in SMA-like conditions, even though SMN plays a crucial role in snRNP biogenesis. In an early study, Pellizzoni and colleagues demonstrated a dominant-negative form of SMN, SMNΔN27, which provoked a reorganization of snRNPs in the nucleus and inhibited pre-mRNA splicing *in vitro* suggesting that defects in splicing may contribute to SMA (Pellizzoni et al. 1998). It wasn't until 2005 that Wan and colleagues demonstrated a correlation between the levels of SMN and snRNP assembly in cells deficient for SMN (Wan et al. 2005). More recently, Gabanella and colleagues supported this notion by demonstrating that there were defects in snRNP assembly in tissues from SMA mice; therefore linking the assembly defects to the SMA pathology (Gabanella et al. 2007). More recently, changes in the stoichiometry of specific snRNAs and more importantly, pre-mRNA splicing defects in numerous transcript have been reported (Zhang et al. 2008). Additionally, in lymphoblast from SMA patients, a marked decrease in tri-snRNPs and

splicing defects in minor introns have also been reported (Boulisfane et al. 2011) Since then, numerous defects in splicing and also alternative splicing have been documented (Baumer et al. 2009; Campion et al. 2010; Jodelka et al. 2010; Ruggiu et al. 2012). Nevertheless, the reasons why motor neurons are specifically affected by the drastic decrease in SMN protein levels in SMA remains unclear. Perhaps SMN modulates downstream pathways that are crucial to motor neurons making them more susceptible to a decrease in SMN protein level. Another reasonable explanation is that SMN has a function that is independent of its role in snRNP assembly which would be specific to motor neurons.

1.2.4 The non-canonical function of SMN: why are motor neurons more sensitive to low levels of SMN?

Numerous hypotheses have been brought forth to explain why motor neurons are more sensitive to a decrease in the SMN protein. The implication of SMN in motor neuron-specific activities could explain the specificity of this pathology and recently, there is growing evidence to support this hypothesis. It has been demonstrated that the activity of SMN in snRNP assembly is elevated in embryonic and early postnatal spinal cord development, but it decreases dramatically when myelination occurs and is maintained at a low steady state (Gabanella et al. 2005). Furthermore, in humans, during the development of the central nervous system, the localization of SMN changes from being predominantly in the nucleus, where it participates in snRNP assembly, to a more axonal localization (Giavazzi et al. 2006). In agreement with this localization, it has been observed that SMN

colocalizes with cytoskeletal filaments in axons (Pagliardini et al. 2000). Intriguingly, using fluorescently tagged SMN granules, a bidirectional movement dependent on the cytoskeleton has been observed. More specifically, the long range transport of these SMN containing granules is inhibited by depolymerisation of microtubules and the short range transport is decreased dramatically upon disruption of F-actin (Zhang et al. 2003). Another team of researchers also demonstrated that SMN can be transported in a retrograde and anterograde fashion at a speed of 2 μm/second. This is in agreement with the motor protein-dependent fast axonal transport (Fallini et al. 2010). Furthermore, a novel splicing isoform of SMN termed axonal-SMN (a-SMN) which is essentially the Tudor domain of SMN and a few additional amino acids at its C-terminus, was discovered and is expressed in foci-like structures along the axons where it promotes axonogenesis (Setola et al. 2007). These granular foci are thought to be RNA granules which are multiprotein complexes reported to transport RNA-binding proteins and their specific mRNA targets along the growing axons (Elvira et al. 2006a; Lee 2012). This transport allows the local translation of some specific mRNAs implicated in neurite outgrowth (Schuman 1999). Additionally, several RNA-binding proteins have been reported to localize to neuronal RNA granules along the axons, like for example KSRP, HuD, hnRNP Q/R and Staufen 2 (Elvira et al. 2006a). There is evidence that some components of the SMN core complex are present in SMN containing axonal granules (Fallini et al. 2011; Sharma et al. 2005; Todd et al. 2010; Zhang et al. 2006). Even though, some of the well known components of the SMN complex such as the Gemins, are present, it seems that the Sm proteins are absent, further supporting the possibility that SMN plays a role in motor neuron axons that is independent of its role in snRNP assembly (Fallini et al. 2011; Sharma et al. 2005; Todd et al. 2010; Zhang et al. 2006).

1.3 RNA binding proteins and regulation of mRNA transport

1.3.1 The RNA binding protein HuD

RNA binding proteins constitute a large proportion of RNA containing granules since they are responsible for, among other things, the localization and stability of mRNA (Deschenes-Furry et al. 2006). Our lab is interested in the RNA-binding protein HuD which is part of the ELAV-like family of proteins. This family of proteins was first identified as a target of autoantibodies found in patients affected with paraneoplastic cephalomyelitis (Dalmau et al. 1990). Hu proteins are the mammalian homologues of the ELAV protein found in *Drosophila* (Robinow et al. 1988), which when deleted, results in an abnormal vision phenotype and embryonic lethality. The Hu family of proteins is comprised of four members which include HuC (PLE21), HuD and HuB (He1-N1) that are all specifically expressed in neurons and HuR (HuA) which is ubiquitously express (Hinman and Lou 2008). The Hu proteins are considered classical RBPs since they contain three RNA recognition motifs (RRMs), which are 90% homologous, separated by a hinge region between the second and the third RRM (Figure 4A). The RRM binds to mRNA targets (Hinman and Lou 2008) while the hinge region contains a nuclear export signal which allows the shuttling back and fourth from the nucleus to the cytoplasm (Kasashima et al. 1999). The RRM1 of HuD predominantly binds to the mRNA target, whereas the RRM2 does aid in binding of the target transcript, but is mostly important for the stabilization of the RNA-protein interaction. The RRM3 is involved in the stabilization of the RNA-protein

A

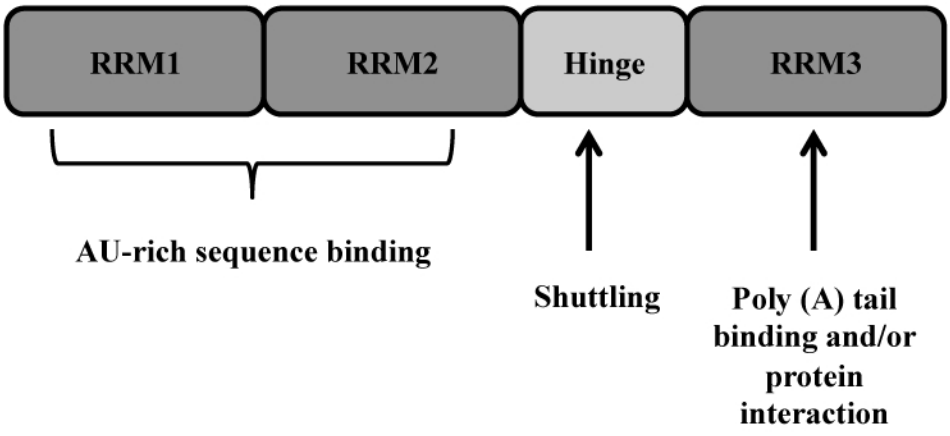
RRM1
RRM2
Hinge
RRM3
AU-rich sequence binding
Shuttling
Poly (A) tail binding and/or protein interaction

B

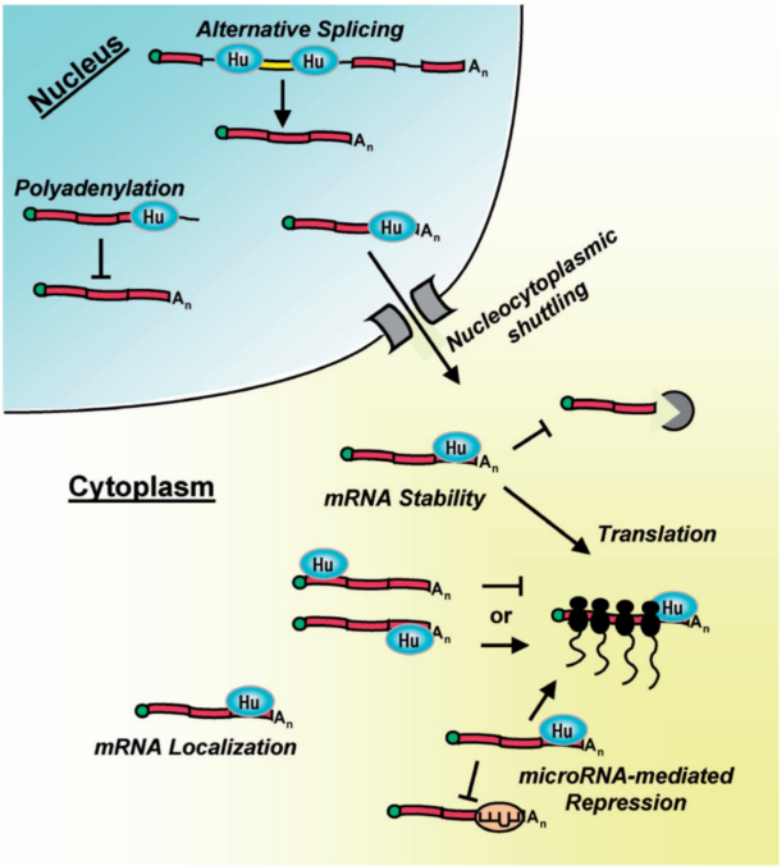
Nucleus
Alternative Splicing
Hu
Hu
An
Polyadenylation
Nucleocytoplasmic shuttling
Cytoplasm
mRNA Stability
Translation
or
mRNA Localization
microRNA-mediated Repression

Figure 4. The ELAV-like family of proteins. A. Schematic representation of the full length Hu proteins which consist of tree RNA recognition motifs (RRM1, RRM2, RRM3) separated by a Hinge region (Hinge) between the second and the third RRM (modified from Hinman et al., *Cell mol. Life Sci.,* 2008). **B.** Illustration of the numerous functions of Hu proteins showing its role in many post-transcriptional events carried out in both the nucleus and the cytoplasm (modified from Hinman et al., *Cell mol. Life Sci.,* 2008).

interaction and also binds the poly(A) tail (Kasashima et al. 2002). It has also been proposed that the RRM3 could be involved in protein-protein interactions since HuD, HuC and HuB have been shown to dimerize (Kasashima et al. 2002). Moreover, AU rich elements (AREs) located in the 3' untranslated region (UTR) of target transcripts allows the Hu proteins to recognize the different mRNA targets (Hinman and Lou 2008). Most ARE-binding proteins have the effect of destabilizing their target transcripts, however the Hu family of proteins stabilize their targets; therefore increasing their half life (Aranda-Abreu et al. 1999; Deschenes-Furry et al. 2003; Deschenes-Furry et al. 2006; Mobarak et al. 2000). One mechanism through which HuD increases mRNA stability is by blocking the association of destabilizing RBPs when it forms oligomers on mRNA targets (Fialcowitz-White et al. 2007). But the regulation of mRNA stability is very complex since destabilizating RBPs and stabilizating RBPs compete for binding to specific mRNA targets, therefore the half-life of the mRNA is dependent on the relative abundance of each of these types of RBPs (Barreau et al. 2006; Lal et al. 2004). Lastly, HuD has also been linked to the regulation of translation (Fujiwara et al. 2012; Fukao et al. 2009), where it would mediate a bridging interaction between the poly(A) tail and eIF4A.

It has been shown that Hu proteins are amongst the earliest marker of neuronal differentiation and therefore it is not surprising that these proteins play a crucial role in neuronal development (Anderson et al. 2001; Antic and Keene 1997; Figueroa et al. 2003; Perrone-Bizzozero and Bolognani 2002). In our laboratory we are particularly interested in studying the role of HuD in this process. Within neurons, HuD is expressed in the cellular body, axons and growth cones (Aronov et al. 2002; Okano and Darnell 1997; Smith et al. 2004). It has been shown that HuD, through its interaction with target transcripts such as c-

fos, N-myc, p21, neuroserpin and MARKs, plays a crucial role in the processes of neuronal development and differentiation (Figure 4B) (Chagnovich et al. 1996; Wein et al. 2003). Furthermore, in HuD knockout mice, neuronal cells do not exit the cell cycle in a normal fashion leading to a decreased neurite production, suggesting that HuD is crucial for the differentiation of neuronal cells through the regulation of cell cycle exit and cell lineage commitment (Akamatsu et al. 2005). Moreover, HuD stabilizes many targets, such as GAP-43 and Tau, that are implicated in the formation of neuronal processes (Aranda-Abreu et al. 1999; Chung et al. 1997; Mobarak et al. 2000). Additionally, it has been demonstrated in E19 cortical neurons, PC12 cells and retinoic acid induced embryonic stem cells that HuD's expression accelerates neurite outgrowth (Anderson et al. 2000; Anderson et al. 2001; Kasashima et al. 1999). Furthermore, when overexpressed, HuD significantly stimulates long neurite formation and increased levels of GAP-43 (Anderson et al. 2001). Whereas when HuD is knockdown in PC12 cells there is a decrease in the production of neurites even in the presence of nerve growth factor (Mobarak et al. 2000). Taken together, these results demonstrate that the neuronal specific Hu protein, HuD, through its stabilizing effect on target transcripts and its positive effects on neurite outgrowth, plays a pivotal role in the development of the nervous system. Some evidence has been brought to light demonstrating that HuD might also play a role in the adult nervous system. In fact, HuD has been linked to plasticity of the nervous system. It has been shown that following spatial learning tasks there is an increase in HuD levels in hippocampal neurons. This is also accompanied by a dramatic increase in GAP-43 transcript levels (Pascale et al. 2004; Quattrone et al. 2001). Furthermore, it has also been demonstrated that HuD is linked to axonal regeneration since after a crush of the DRG sensory neurons and facial neurons there is an increase in HuD protein levels that remain elevated for a duration of 21 days.

This elevation of HuD is also accompanied by an increase in GAP-43 mRNA levels (Anderson et al. 2003). Taken together, HuD is a neuronal protein that is implicated in many aspects of neuronal development, maintenance and axonal regeneration. These observations demonstrate its importance for a proper functioning nervous system.

1.3.2 The RNA-binding protein SERBP1

The Serpine mRNA binding protein 1 (SERBP1) is a protein that has been identified by several groups and has several acronyms, including PAI-RBP1, HABP4, CGI-55. Currently the function of SERBP1 is unknown. It was first named PAI-RBP1 since it bound the cyclic nucleotide-responsive sequence in type-1 plasminogen activator inhibitor mRNA (Heaton et al. 2001). Analysis done on one of the isoforms of SERBP1, CGI-55, predicted a nuclear localization signal (NLS), two coiled-coil motifs, and five lysines that have the potential to be modified by small ubiquitin modifiers (SUMO) (Kobarg et al. 1997). Furthermore, it has recently been demonstrated that SERBP1 has three possible arginine methylation sites. Specifically, the N-terminus contains an arginine rich sequence, an arginine glycine (RG)-rich segment is located in the middle of the protein and finally at the C-Terminus end there is an Arginine-glycine-glycine box (RGG box) (Lee et al. 2012). Interestingly, it has been shown that SERBP1 interacts with PRMT1 in HeLa cells and upon AdOx treatment, an indirect methyltransferase inhibitor, there is a significant decrease in this interaction. Furthermore, PRMT1 methylates SERBP1 at the middle RG and the C-terminal RGG. When PRMT1 activity was inhibited by AdOx treatment or when PRMT1 is depleted by siRNA, there was a significant translocation of SERBP1 in the nucleus (Lee et al. 2012). Therefore, methylation of SERBP1 significantly impacts its intracellular

localization. Moreover, it has been demonstrated that the TDRD3 protein, known to contain a Tudor domain which is responsible for the interaction with methylated proteins, interacts with SERBP1 and localizes to stress granules. It is then possible that SERBP1 is implicated in RNA regulation since stress granules are important in translational regulation upon cellular stress (Goulet et al. 2008). Additionally, SERBP1 has also been linked to processing of mRNA as it localizes to Cajal bodies and interacts with pre-mRNA, mRNA, spliceosomes and U2 small nuclear RNP auxiliary factor U2AF65, further supporting the possible function of SERBP1 in splicing (Prigge et al. 2009). Finally, SERBP1 has been found in a screen performed on rat brains for proteins present in RNA granules. As mentioned above, RNA granules are a complex of proteins that have the role of transporting RNA molecules along the neurites for local translation of mRNA, therefore SERBP1 may play a role in the differentiation process of neuronal cells (Elvira et al. 2006b). Taken together, SERBP1 is a methylated RNA-binding protein that can interact with proteins that harbor a Tudor domain and is linked to numerous RNA regulation functions including transport of RNA granules along the neurites.

1.4 Rationale, Hypothesis and objectives

1.4.1 Rationale

SMN has a wide assortment of interacting partners that are implicated in numerous different cellular processes. Therefore, it has been postulated that SMN might play essential roles in other cellular processes in motor neurons, apart from its housekeeping role in snRNP biogenesis. We then decided to investigate the possible interacting proteins of SMN

by carrying out a proteomic screen in an attempt to shed light on putative non-canonical functions of SMN. We uncovered that SMN might interact with two RNA-binding proteins, HuD, which is implicated in a number of neuronal processes from neuronal differentiation to plasticity and SERBP1, a protein with largely unknown functions. SMN is known to interact with arginine methylated RBPs such as KSRP and FMRP (Piazzon et al. 2008; Tadesse et al. 2008) which have been linked to the transport of mRNPs in axons during neuronal differentiation. We have demonstrated that HuD can be methylated by CARM1 and recent work done by the Lee laboratory showed that SERBP1 is methylated by PRMT1 (Lee et al. 2012), therefore it is possible that HuD and SERBP1 are interacting partners of SMN. Additionally, HuD and SERBP1 have been shown to be components of RNA granules (Elvira et al. 2006b), which play an important role in neuronal differentiation by promoting transport and regulating local translation of specific mRNAs in growth cones. Therefore, we propose that the interactions between SMN and HuD as well as the interaction between SMN and SERBP1, might be implicated in the assembly and/or transport of RNA granules in neurites of motor neurons. These findings would shed light on a cellular function for SERBP1, since it has not yet been associated with a specific physiological cellular function. Additionally, this would help elucidate the possible novel function(s) of SMN in motor neurons and, in turn, provide crucial information to help understand the motor neuron-specificity of SMA.

1.4.2 Hypothesis

I propose that SMN interacts with RNA binding protein HuD and SERBP1 and that these interactions promote motor neuron differentiation.

1.4.3 Objectives

- Complete the biochemical and functional characterization of the interaction between HuD and SMN in motoneuron-derived MN-1 cells.
- Biochemical and functional characterization of a novel interaction between SMN and the RNA-binding protein SERBP1 in motoneuron-derived MN-1 cells.

Chapter 2. Materials and Methods.

2.1 Cell culture, differentiation and generation of stable knockdown cell lines

MN-1 cells were cultured in Dulbecco's modified eagle medium (DMEM) containing 10% fetal bovine serum (FBS; Thermoscientific), 2% penicillin/streptomycin (Multicell; Wisent) and 25 μg/mL plasmocin (Invivogen). They were cultured at 37 ºC with 5% CO2 and cells were passaged at approximately 85% confluency. For protein extraction, GST pulldowns and Immunoprecipitation, cells were plated at 50% confluency and incubated overnight. For immunofluorescence, BiFC and transfection, cells were plated at 30% confluency and incubated overnight.

MN-1 cells were differentiated using a differentiation media containing 2% FBS, 50 μM Transretinol (Sigma) and 10 μg/mL of GDNF (Cedarlane). The maintenance media was first discarded and cells were washed with 1X phosphate buffered saline solution (1X PBS). The 1X PBS was then replaced with the differentiation media and cells were

incubated for 24 to 48 hours prior to extraction of proteins or mRNA (as described in the section 2.2 and 2.6, respectively).

To generate a stable knockdown of CARM1 in MN-1 cells, a target sequence was selected using the online 'RNAi Explorer' design algorithm (http://www.genelink.com/sirna/shRNAi.asp), and from this, the following 2 oligos (Sens mCARM1 oligo: 5'-GATCGGCTACATGCTCTTCAATGAACGAATGCTCTCAA-GAGGAGCATTCGTTCATTGAAGAGCATGTAGCTTTTTTGA; Antisense mCARM1 oligo: 5'-AGCTTCAAAAAAGCTACATGCTCTTCAATGAACGAATGCTCCTCTTGAGAGCAT T-CGTTCATTGAAGAGCATGTAGC) were hybridized, digested, and subcloned into the *Bam*H1 and *Hin*dIII sites of the pRS shRNA vector (OriGene). For the SMN stable knockdown, a predesigned microRNA-adapted shRNA lentiviral vector targeting a sequence in the 3'UTR of mouse SMN mRNA (GIPZ #RMM4431, OpenBiosystems) was used. The pRS-1 (Origene) and pGIPZ (OpenBiosystems) empty vectors, respectively, were used as controls for the selection process. Lipofectamine 2000 (Invitrogen) was used for DNA transfections according to manufacturer instruction. Selection was achieved using 4 μg/ml puromycin dihydrochloride (Sigma). Pools obtained following 2 weeks of selection regiment were then maintained in 2 μg/ml of puromycin.

2.2 Isolation of proteins, SDS-PAGE and Western blot

Cells from 100 mm plates were first washed with 1X PBS and then lysed with radioimmunoprecipitation (RIPA) lysis buffer (10 mM Tris pH 7.4, 100 mM NaCl, 1 mM

ethylene tetraacetic diamine acid (EDTA), 1% nonyl phenoxypolyethoxylethanol 40 (NP-40), 0.5% sodium deoxycholate (NaDOC), 0.1% sodium dodecyl sulfate (SDS)). The extracts were then mixed intermittently and put at one ice for 15 minute to insure proper lysis. The extract was centrifuge at maximum speed for 15 minutes and the supernatant was collected. The protein quantification was done using the Bradford method (BioRad) according to manufacturer protocol. Bovine serum albumin (BSA) was used to generate a standard curve. To quantify the proteins, the optical density (OD) was measured using a spectrophotometer with a wavelength of 595 nm. The concentrations of proteins were obtained by extrapoling the OD value to the standard curve. Equal concentration of protein contained in the numerous extracts were then mix with a equal amount of 2X Laemmli buffer (25% glycerol, 125 mM Tris HCl pH 6.8, 4% SDS, 700 mM β-mercaptoethanol, 0.1% bromophenol Blue). The extracts were boiled at 95 ºC for 10 minutes and loaded in a 12% SDS-polyacrylamide gel electrophoresis (SDS-PAGE). Resolved protein were then transferred onto an Immunobilon-P polyvinylidene difluoride (PVDF; Millipore: 0.45 μm pores) membrane. The membrane was blocked for one hour in 5% non-fat milk in 1X PBS with 0.05% Tween 20 (PBS-T). The primary antibody mixed in 2% non-fat milk in PBS-T was then added onto the membrane for one hour at room temperature or overnight at 4 ºC depending on the antibody. Primary antibody includes HuD (1:1000; Santa Cruz), GAPDH (glyceraldehydes 3-phosphate dehydrogenase) (1:5000; Covance), SMN (1:3000; BD Biosciences), SERBP1 (1:1000; Abnova), GST (1:3000), Tubulin (1:1000; Sigma). After the incubation period, the membrane was washed 3 times for 5 minutes with PBS-T. The secondary horseradish peroxidase (HRP) conjugated antibody (goat anti-mouse or goat anti-rabbit; Jackson Immunoresearch Labs) was added for one hour at room temperature.

The membrane was again washed 3 times for 5 minutes with PBS-T before the exposition on film (Clonex) using chemiluminescent HRP substrate (Millipore).

2.3 Production of recombinant proteins

Escherichia coli BL21 (Stratagene) were transformed with the various cDNA construct (GST-Tag, GST-SMN Tudor and GST-SMN Tudor E134K). One colony was picked and cultured overnight at 37 ºC in 100 mL of Lysogeny broth (LB; Fisher Scientific) containing 100 µg/mL of ampicillin (Sigma). The next day, the 100 mL of bacteria was transferred to 900 mL of LB and incubated at 37 ºC for an hour. Isopropyl-D-thiogalactopyranoside (IPTG; Wisent) at a final concentration of 0.1 µM was added to the bacteria. There were then allowed to grow for 3 more hours before being centrifuged at 4000 rpm for 30 minutes. The pellets were resuspended in 10 mL of cold 1X PBS with complete protease inhibitors and sonicated five times for 15 secondes at 4 ºC. The extracts were then centrifuge for 20 minutes at 12000 rpm. 1% Triton X-100 and 500 µL of glutathione agarose beads (Sigma) was added to the supernatant and allowed to tumble overnight at 4 ºC. The next day, the beads were centrifuge at 2500 rpm for 2 minutes and 2 washed with 1X PBS containing 1% triton were done. Two other washes were done using 1X PBS. For the GST pulldown experiment, proteins were not eluded from the beads to simplify the experimental process. The beads were kept in 50% slurry in 1XPBS at 4ºC. The concentrations of the proteins were quantified by SDS-PAGE followed by a commassie dye. The gel was distained overnight using a methanol and acetic acid solution. An image of the distained gel was taken using the Gel Logic 200 imaging system (Kodak).

The proteins were eluted from the beads for the Far Western experiment. The beads were centrifuged at maximum speed for 30 seconds and the supernatant was discarded. An equal amount of a 10mg/mL glutathione in 1X PBS with complete protease inhibitor solution was added to the beads. The beads were shook vigorously and placed at 37ºC for 1 minute. The beads were then centrifuge at maximum speed for 30 seconds and the supernatant was collected. The three previous steps were done 10 times and the final extract was dialysed overnight at 4 ºC in 2 L of cold 1X PBS. The extracts were then concentrated using a 0.45 μM filter (Millipore). The Bradford experimental procedure was used to quantify the protein (as described in section 2.2).

2.4 GST pulldown

MN-1 cells were lysed as describe previously in section 2.1 using a 1% Triton X-100 lysis buffer (10 mM Tris HCl pH 7.4, 150 mM NaCl and 1% triton). For each pulldown, 500 ug of proteins was used and lysis buffer was added to give a final volume of 1mL. Approximately 5 μg of the different beads (GST-Tag, GST-SMN Tudor, GST-SMN Tudor E134K) were added to the extract and the pulldown was then allowed to tumble overnight at 4 ºC. Four washes with 1 mL of the lysis buffer followed by a wash with 1 mL 1X PBS was then done and the beads were resuspended in equal amount of 1X PBS. An equal amount of 2X Laemmli buffer was added to the beads and the extracts were run on a 12% SDS- PAGE gel and transferred onto a PVDF membrane as described in the section 2.2. Resulting membrane was blotted with the anti-GST antibody and anti SERBP1 antibody.

2.5 Immunoprecipitation and Far Western

The proteins from MN-1 cells were extracted has described in section 2.2. For each immunoprecipitation (IP), 500 µg of protein was used and RIPA lysis buffer was added to a final volume of 1 mL. A 10% input was also aliquoted and kept at -20 ºC until the IP was run on a gel. Either 1 µg of IgG or 5 µg of HuD or SMN was added to the lysate. The IP's were tumbled at 4ºC overnight. The next day, 30 µL of slurry Protein A/G sepharose beads (Sigma) was added to the IP's for an hour. The beads were then washed with 1 mL of RIPA lysis buffer 5 times for 5 minutes. Beads were resuspended in 30 µL of Laemmli buffer and ran on a 12% SDS-PAGE gel and transferred as described in section 2.2. The resulting membrane was blotted with anti-HuD, anti-SERBP1. The membrane was then stripped and reblotted with anti-SMN antibody.

For the Far Western, an IP was done as described previously, however 1000 µg of protein were used and the antibody added to the IP was anti-SERBP1 or anti-HuD. The SDS-PAGE and the Western Blotting was done has previously described in section 2.2. The type of membrane used was nitrocellulose (GE Water and Process technologies: 45 microns). The membrane was blocked overnight at 4 ºC and probed with GST-SMN Tudor protein in 2% non-fat milk also overnight at 4 ºC. The proteins were produced has previously described in section 2.3. The membrane was washed 3 times for 5 minutes with PBS-T and then blotted with anti-GST antibody for one hour. The secondary goat anti rabbit was incubated for one hour and the membrane was exposed on film with the help of HRP substrate. As a control, anti-HuD or anti-SERBP1 was also blotted for one hour after the membrane had been stripped.

2.6 RNA extraction and Reverse transcription

The RNA was isolated from a 100mm plate using Trizol reagent (Invotrogen) according to the manufacturer protocol. The RNA was resuspended in a rational amount of DEPC treated water depending on the size of the pellet obtained, and then was quantified using a spectrophotometer with a wavelength of 260 nm. DEPC treated water was used as a negative control. 1 μg of RNA was incubated with 1 μM oligo dT for 10 minutes at 65 ºC. Reverse transcription was then done on the respective sample using 0.5 mM deoxyribonucleotide (dNTPs; Invitrogen), 20 U RNasin (Promega), and 10 U AMV reverse transcriptase enzyme (Promega) in AMV reverse transcriptase buffer. The samples were incubated for 1 hour at 42 ºC.

Polymerase chain reactions (PCR) were done using 25 ng of the respective cDNA, 2 X GoTaq green master mix (Promega) and 400 nM of the respective forward and reverse primers. The PCR conditions for GAPDH, γ-actin, β-actin, GAP-43 and Tau are shown in appendix 1. The primers used were:

GAPDH (F) 5'-ACCACAGTCCATGCCATCAC-3',

GAPDH (R) 5'TC-CACCACCCTGTTGCTGTA-3',

γ-actin (F) 5'-ACAGCTTTACCACCACTGCTGAGA- 3',

γ-actin (R) 5'-ACTCCTGCTTGCTGATCCACATCT-3',

β-actin (F) 5'- TCTTGGGTATGGAATCCTGTGGCA-3',

β-actin (R) 5'- ACTCCTGCTTGCTGATCCACATCT-3',

GAP-43 (F) 5'- TTTGTTTCTTGGTGTTGTTATGGC-3',

GAP-43 (R) 5'- GAACGAACATTGCACACACA-3',

Tau (F) 5'- GGTCGAAGATTGGCTCTACTG-3',

Tau (R) 5'- GCCAAGGAAGCAGACACTTC-3'.

2.7 DNA plasmids

First, in order to identify YFP fragments that can associate to form a bimolecular fluorescent complex, we generated the bicistronic expression vectors. The constructs encoding N-YFP (Nyfp-) or the C-terminal fragment of YFP (Cyfp) were generated as follows: The DNA sequence enconding EGFP was removed by restriction endonuclease digestion using *Nhe*I and *Bsp*EI and replaced with a sequence encoding the N-terminal region (1-154 amino acids: Nyfp) and C-terminal region (155-238 amino acids: Cyfp) of YFP. A linker sequence (RSIAT) was also engineered to prevent disruption of protein folding in the context of the fusion. The Nyfp and Cyfp fragments were generated using PCR with pEYFP-C1 vector (Clontech) as a DNA template and the following primers:

Nyfp-1-154 (5'-gcatgctagcatggtgagcaagggcgag-3')

and 5'-atgctccgga**agtagcaatagaacg**catgatatagacgttgtg-3')

Cyfp-155-238 (5'-gcatgctagcatggccgacaagcagaagaac-3'

and 5'-atgctccgga**agtagcaatagaacg**gtacagctcgtccatgcc-3').

The *Nhe*I and *Bsp*EI sites are underlined and the RSIAT sequence is indicated in bold letters. These vectors were used for the Bimolecular Fluorescense complemention system (BiFC). The BiFC constructs expressing Nyfp-H/SMN and HuD/SMN-Cyfp were constructed by a two-step subcloning strategy. First, the cDNA encoding HuD was removed from myc-pcDNA-HuD (a gift from Dr. Bernard Jasmin, University of Ottawa) digested with *Bam*HI and *Xho*I. The resulted DNA fragment was then inserted in the *Bgl*II and *Sal*I sites of N-YFP and C-YFP respectively. Wild type and mutant SMN cDNA sequences were removed from EGFP-C1-SMN (122) by restriction endonuclease digestion following the same strategy as described above. For the SERBP1 fusion constructs, the SERBP1 sequence was removed from the myc-pcDNA-SERBP1 vector with *Eco*RI and *Xho*I restriction endonuclease enzymes (New England Biolabs). The vector containing the N-yfp and C-yfp fragments generated above was digested with *Eco*RI and *Sal*I (New England Biolabs) and the coding sequence of SERBP1 was ligated with the T4 ligase (Promega) according to manufacturer protocol in this specific vector.

2.8 Immunofluorescence and Biofluorescence complementation assay

MN-1 cells were first plated in 6 well plates at 30% confluency on glass coverslips and the next day, cells were left untreated or were treated with differentiating media as described previously in section 2.1. Cells were first washed with 1X PBS three times and then incubated with 4% paraformaldehyde (PFA; Fisher Scientific) for 10 minutes. Three washes with 1X PBS were done and cells were incubated with 0.5% triton in 1X PBS for 5 minutes. Following 3 washed with 1X PBS, the primary antibody was incubated for one hour. Primary antibodies used include: HuD (1:300, Santa Cruz), SMN (1:300, BD

Sciences), SERBP1 (1:300, Abnova). Three washes with 1X PBS were done. Finally, the cells were incubated for an hour in the dark with alexa fluor secondary antibody goat anti mouse (594 nm) or goat anti rabbit (488nm) (1:300, Life Technology). The coverslips were then washed three times prior to being mounted on a microscope slide with Vectashield containing DAPI (Vector laboratories). The cells were visualized using Zeiss 40X objective of a Zeiss Axo Imager.Z1 microscope. Furthermore, an AxioCam HRm camera was used to take the images. Finally, Adobe Photoshop CS2 (Adobe) was used to merge the different filters used to create the final image.

MN-1 cells were first transfected with the different fusion construct separately. These include: Nyfp-SMN, Nyfp-E134K, Nyfp-SERBP1, Cyfp-HuD and Cyfp-SERBP1. MN- 1 cells were also co-transfected with either Nyfp-SMN - Cyfp-SMN, Nypf-HuD - Cyfp-HuD, Nyfp-SERBP1 - Cyfp-SERBP1, Nyfp-SMN – Cyfp-HuD, Nyfp-SMN – Cyfp-SERBP1, Nyfp-E134K – Cyfp-HuD or Nyfp-E134K – Cyfp-SERBP1. An empirical ratio of 2:1 (Nyfp:Cyfp) was used to co-transfect a total of 1 ug of cDNA. The transfections were performed using Lipofectamine Plus reagent (Life Technology) according to the manufacturer's protocol. The cells were incubated for 24 hour prior to the fixation and imaging that was performed as previously described.

2.9 Sucrose density gradient fractionation

MN-1 cells were first plated in 150mm plates at 25% confluency and incubated overnight. Next, the cells were first washed with ice cold 1X PBS and then lysed with a low-salt lysis buffer (20 mM Tris-HCl pH 7.5, 10 mM NaCl, 3 mM MgCl2, 1 mM

rRNasin, 1 mM dithiothreitol, 0.3% Triton X-100, 50 mM sucrose (Fisher Scientific)). The extracts were then centrifuge at 10 000g at 4 ºC for 10 minutes. Another centrifugation this time at maximum speed for 10 minutes was performed. A sucrose gradient (15-45% (w/w)) was prepared in 25 mM Tris HCl pH 7.5, 25 mM NaCl and 5 mM MgCl2 using a Hoefer Scientific instrument. One and two tenth mL extract was put onto a 10.6 mL sucrose gradient and centrifuge at 85 784.83g for two hours using a SW40 swing out rotor. After the centrifugation without brakes, the 1 mL fractions were collected using a fraction collector (Brandel-Amersham) and the quality of the extracts was monitored at a 254 nm wavelength using an ISCO UA-6 UV detector. The RNA and the proteins were precipitated using a 0.1 M NaCl and 2.5 volumes of ethanol solutions. The protein and RNA were isolated using the Trizol (Life Technology) reagent according to the manufacture protocol. The total RNA was resuspended with 30 uL of DEPC water and the proteins were resuspended with 100 uL of Laemmli buffer. The proteins were run on a 12% SDS-PAGE gel and transferred onto a PVDF membrane as previously described in section 2.2. A reverse transcription was done on the total RNA as described previously. Then the cDNA obtained was diluted 20 times and a PCR was done using GOTAq (Promega), 25 ng of cDNA and the respective foward and reverse primers at a concentration of 400 nM. The product obtained by the PCR was run on a 2% agarose gel (Life Technology). The imaging of the gel was done using a Gel logic 200 imaging system (Kodak).

2.10 Rescue experiment

Vector control and shSMN stable knockdown MN-1 cells were first plated at a 25% confluence and incubated overnight. The next morning, the pcDNA-3.1-myc-SERBP1 was transfected using the Lipofectamine Plus reagent as described by the manufacturer protocol

and incubated overnight. Cells were then differentiated as described in section 2.1 and left incubating for 24h. An average of 5 pictures of various area of each plate were taken using an Axiovert 40 CFL microscope with a magnification of 40X and using a canon power shot G6 camera. The total number of cells of each frame was counted. The cells with neurites double the length of the cell body and the cells with branching were then counted and a percentage of cells with neurites and branching were calculated by dividing these numbers by the total number of counted cells. The proteins were extracted, run on a SDS-PAGE gel and subjected to immunoblotting (as described in section 2.2) to verify the expression levels of the pcDNA-3.1-myc-SERBP1.

HuD interacts with the survival motor neuron protein and can rescue spinal muscular atrophy-like neuronal defects.

Lisa Hubers, Hector Valderrama-Carvajal, Janik Laframboise, Janie Timbers, Gabriel Sanchez and Jocelyn Côté.*

Received for publication August 29, 2010, and revised form, November 15, 2010.

I performed co-Immunoprecipitation experiment (Figure 1A) and Far Western/Blot Overlay experiments (Figure 1E). I participated in the preparation of cells and acquisition of images for the indirect fluorescence (Figure 2B) and Biomolecular Fluorescence Complementation assay (Figure 2C, 2D, 2E). Finally, I contributed to the extraction of protein and RNA for the Sucrose gradient experiments as well as the resulting Western Blot and RT-PCR. Lisa Hubers and Hector Valderrhama-Carvajal performed all other experiments presented in this manuscript, with occasional assistance from Janie Timbers and Gabriel Sanchez and guidance from Dr. J. Côté.

3.1 SMN interacts directly with the RNA-binding protein HuD and regulates its localization into RNA granules in motor neuron-derived cells.

Since HuD is well-known to be implicated in numerous crucial neuronal pathways, I have previously hypothesized that SMN mediate its specific role in motor neurons through an interaction with HuD, which our lab has identified as a putative interacting protein using mass spectrometry (unpublished data, J. Côté Laboratory). A previous graduate student initiated the characterization of the interaction between SMN and HuD, and showed that it could indeed interact using GST-pulldown experiments (Lisa Hubers, M. Sc.). However there remained a few important outstanding questions to be studied. First, I determine whether there was an interaction in a cellular context and if this interaction was dependent on the presence of RNA or regulated by arginine methylation, since the Tudor domain is known to recognize arginine methylated proteins. Furthermore, it was also crucial to determine if the interaction is direct and where this physical interaction occurs in differentiated motor neurons. Lastly, determining the functional consequence of this interaction was also important to assess, in the hope to possibly uncover a novel non-canonical function of SMN in motor neurons.

3.1.1 HuD can interact directly with SMN.

In order to determined whether the interaction between endogenous SMN and HuD actually exist in motor neuron-like cells, I performed co-immunoprecipitation experiments (co-IP) (Figure 5). Specifically, HuD was immunoprecipitated from wild type (WT) motor neuron-derived cells (MN-1) and the resulting immunoprecipitate was resolved by SDS-PAGE, transferred onto a PVDF membrane and probed for the presence of endogenous

A

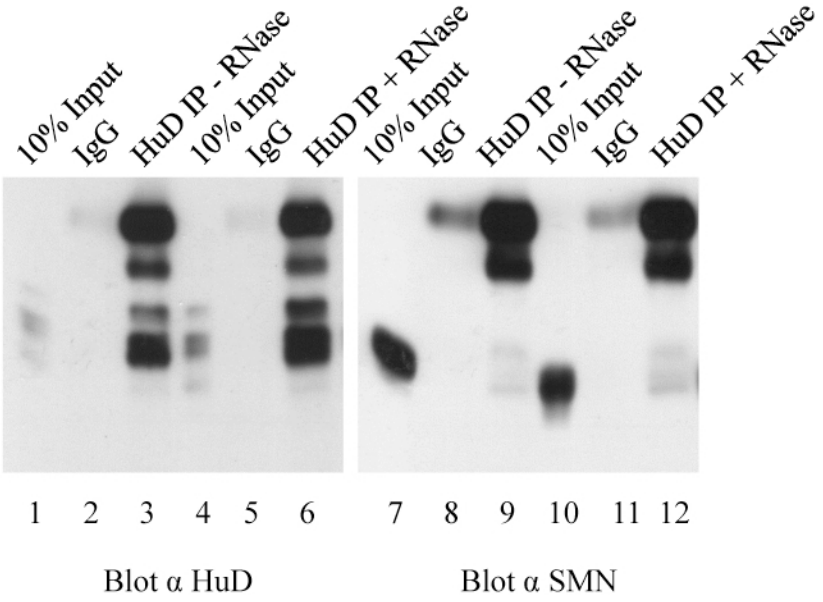
10% Input
IgG
HuD IP - RNase
10% Input
IgG
HuD IP + RNase
10% Input
IgG
HuD IP - RNase
10% Input
IgG
HuD IP + RNase
1 2 3 4 5 6 7 8 9 10 11 12
Blot α HuD
Blot α SMN

B

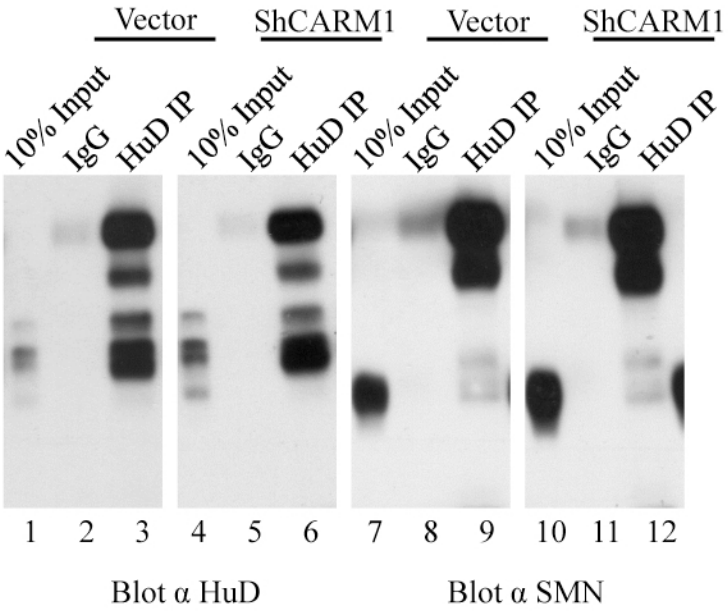
Vector
ShCARM1
Vector
ShCARM1
10% Input
IgG
HuD IP
10% Input
IgG
HuD IP
10% Input
IgG
HuD IP
10% Input
IgG
HuD IP
1 2 3 4 5 6 7 8 9 10 11 12
Blot α HuD
Blot α SMN

Figure 5. SMN and HuD interact in motor neuron-derived MN-1 cells extracts. A. SMN and HuD interact in extracts prepared from MN-1 cells and the interaction is potentially not dependent on an mRNA molecule, as determined by co-immunoprecipitation (co-IP) experiments. An IP of endogenous HuD was performed using WT MN-1 cells lysates treated or untreated with RNase A and analysed by western blot for the presence of HuD (left panel; lanes 1-6). The membrane was stripped and blotted for SMN (lane 7-12). 10% of the amount of lysates used for IPs was loaded and the IP was done with purified non-immunogenic mouse immunoglobulins G (IgGs) as a negative control (n = 3). **B.** The methylation status of HuD by CARM1 does not affect the interaction with SMN. Co-IPs of endogenous HuD were performed in vector control and CARM1 stable knockdown cell lines and subjected to Western blot analysis for the presence of HuD (right panel; lanes 1-6). The membrane was stripped and blotted for the presence of SMN (n = 3; right panel; lanes 7-12).

SMN using Western blotting. This experiment strongly suggests that there is an interaction between HuD and SMN, which is consistent with the proteomic screen and previous results obtained in the laboratory (Figure 5A; lanes 7 to 9). Interestingly, it was demonstrated in our recently published paper (Hubers et al. 2011), that the SMN/HuD interaction was sensitive to the RNase A treatment in GST-pulldown experiments, suggesting that the interaction might be mediated by an mRNA transcript. To assess if this was also the case for the endogenous interaction, cell lysates were treated with RNase A prior to being subjected to co-IP experiments as above. Strikingly, there was no effect on the levels of interaction between HuD and SMN following RNase A treatment (Figure 5A; lanes 10 to 12), implying that, in a cellular context, the interaction is not dependent on the presence of an mRNA molecule. It has also been described for HuD (Hubers et al. 2011) and other RNA-binding proteins, that the interaction between RBPs and SMN is methylation-dependent and hence, suggesting that the interaction is dependent on the Tudor domain of SMN (Cote and Richard 2005; Tadesse et al. 2008). Therefore, a co-IP was performed on vector control MN-1 cells and shCARM1 stable knockdown cells, since CARM1 is the PRMT responsible for methylating HuD at arginine 248 (Figure 5B) (Hubers et al. 2011). Strikingly, there was no apparent effect on the level of interaction between HuD and SMN with a ~ 50% to 60% CARM1 depletion (Figure 5B, lanes 10 to 12), suggesting that the interaction might not be dependent on methylation of HuD by CARM1. Next, to determine if this interaction between SMN and HuD is direct a Blot overlay experiment was carried out (Figure 6). A large scale IP of HuD was performed, resolved on a SDS-PAGE gel and transferred on a nitrocellulose membrane. The membrane was then probed with purified GST-SMN Tudor proteins and subsequent anti-GST Western Blot demonstrated that there was, at least *in vitro*, a direct interaction with HuD. Taken together, I observed with these

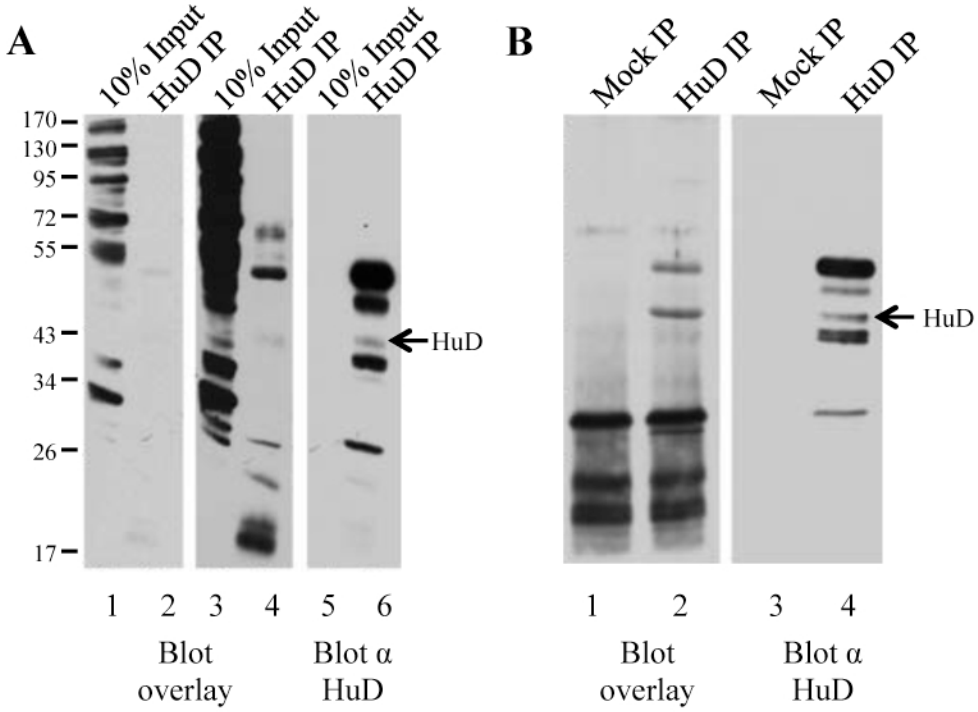
A
10% Input
HuD IP
10% Input
HuD IP
10% Input
HuD IP
170
130
95
72
55
43
34
26
17
HuD
1 2 3 4 5 6
Blot overlay
Blot α HuD
B
Mock IP
HuD IP
Mock IP
HuD IP
HuD
1 2 3 4
Blot overlay
Blot α HuD

Figure 6. The Tudor domain of SMN can bind HuD directly *n vitro*. HuD from MN-1 cells extracts interacts with the Tudor domain of SMN in a direct fashion *in vitro* as determined using a Blot Overlay assay. **A.** A large scale IP of HuD was performed, resolved on a SDS-PAGE gel, transferred on a Nitrocellulose membrane and probed with purified GST-SMN Tudor protein. Anti-GST immunoblotting was performed and shorter (panel 1 and 2) and longer (panels 3 and 4) exposures are shown. The same membrane was then stripped and reprobed with anti-HuD antibodies to determine the position of HuD (panels 5 and 6). A 10% input was used as a positive control. **B.** A second blot overlay assay was done using a larger concentration of the starting lysate. A mock IP, where the antibody was omitted, was used as a negative control. Note that the Tudor domain of SMN interacts with a slower migrating form of HuD (n = 3, indicated with an arrow).

first series of experiments, that the interaction was in fact present *in situ* and that, *in vitro*, the interaction can be direct. Additionally, I also showed that this specific interaction is potentially not dependent on the presence of mRNA and does not seem to be dependent on the methylation of HuD by CARM1.

3.1.2 The SMN/HuD interaction occurs in the cytoplasm and in foci-like structures along the axons.

Now that a physical interaction was demonstrated between HuD and SMN in motor neuron-derived cells, the colocalization of HuD and SMN in motor neuron-derived cells was assessed (Lisa Hubers). The intracellular localization of SMN and HuD in fixed cells is well-established (Aranda-Abreu et al. 1999; Kasashima et al. 1999; Liu and Dreyfuss 1996). SMN localizes mostly in the cytoplasm and concentrates in bright nuclear foci corresponding to Gems and/or Cajal bodies. In contrast, HuD is diffusely distributed throughout the cytoplasm at steady state. Indirect immunofluorescence microscopy for SMN and HuD was performed on MN-1 cells induced to differentiate through the addition of trans-retinol and GDNF for 48 hrs. Both HuD and SMN were found in granular foci along neuritic extensions (Figure 7). Interestingly, in neurites, 36.4 ± 9.5 % of HuD foci also contained SMN, and 48.9 ± 15 % of SMN foci contained HuD (Figure 7, bar graph). In order to confirm and also determine where in the cells the HuD and SMN physical interaction occurs, we used the Biomolecular Fluorescence Complementation (BiFC) approach (Kerppola 2006). This assay has now been used extensively to detect non-covalent interactions between proteins of many different structural classes in virtually every

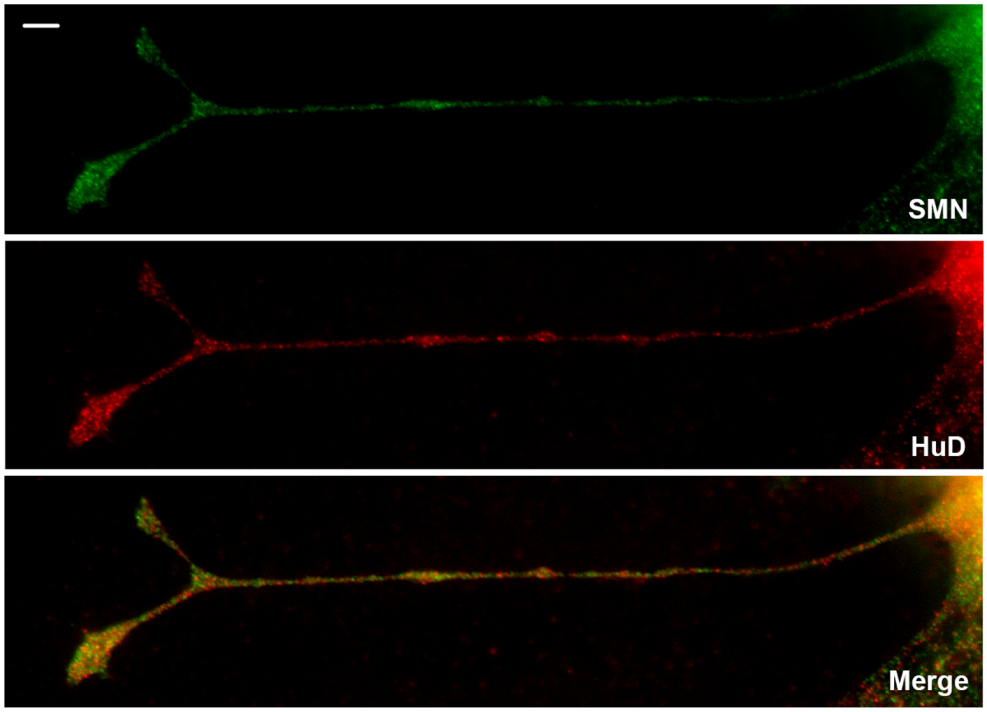
SMN
HuD
Merge

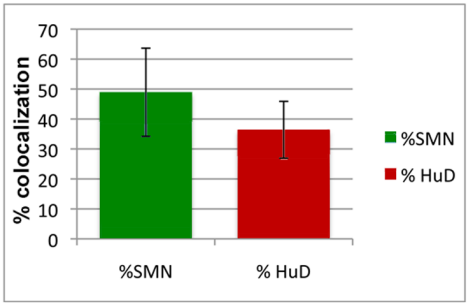
% colocalization
70
60
50
40
30
20
10
0
%SMN
% HuD
%SMN
% HuD

Figure 7. SMN and HuD colocalize in axons of motor neuron-derived cells. HuD and SMN colocalize in foci-like structures along neurites of MN-1 cells. Images taken at 63X and focused on axons of differentiated MN-1 cells. 36.4 ± 9.5 % of the HuD foci contained SMN whereas 48.9 ± 15% of SMN foci contained HuD. The Bar graph shows the mean percentages of signals co-localizing ± SEM. Bar, 20 um (n = 20 neurites).

subcellular compartment (Kerppola 2009 and references therein). More specifically, the BiFC experiment consisted of co-transfecting MN-1 cells with two fusion constructs containing the N-terminal of the yellow fluorescent protein (Nyfp) fused to the first putative protein and the C-terminal of the yellow fluorescent protein (Cyfp) fused to the second putative protein. If there is a non-covalent interaction between the two proteins, the Nyfp and the Cyfp will be at an appropriate distance permitting the YFP molecule to properly form and emit a discernible signal (Figure 8). Therefore, cDNAs encoding HuD or SMN (wild type and E134K mutant allele) were subcloned to create a fusion with either the N-terminal fragment of yellow fluorescent protein, YFP (Nyfp-HuD/SMN) or the C-terminal fragment of YFP (HuD/SMN-yfpC). Proper expression of each fusion protein was confirmed by immunoblotting (Figure 10A) and all fusion constructs were transfected individually to validate the BiFC approach. No discernible signal was observed showing that all signal observed when two fusion constructs are co-transfected will be indicative of an actual protein-protein interaction between the pair being tested (Figure 9). Since both SMN and HuD are known to oligomerize (Kasashima et al. 2002; Lorson et al. 1998), N- and C-terminal YFP fragment fusion constructs of either HuD or SMN were first co-transfected in undifferentiated MN-1 cells in order to validate the system. Combining HuD with HuD resulted in a diffused cytoplasmic fluorescent signal similar to the distribution obtained for endogenous HuD (Figure 10, panels A to C). Similarly, combining SMN-YFP fusion constructs resulted in a typical endogenous SMN intracellular distribution (Figure 10, panels D to F). Together, these controls show that the BiFC approach can be used to detect protein-protein interactions in cells, and most importantly reveal where in the cell these interactions are taking place. Next, the Nyfp-HuD and SMN-yfpC constructs were co-transfected in undifferentiated MN-1 and 24-48 hours post-transfection, cells were fixed

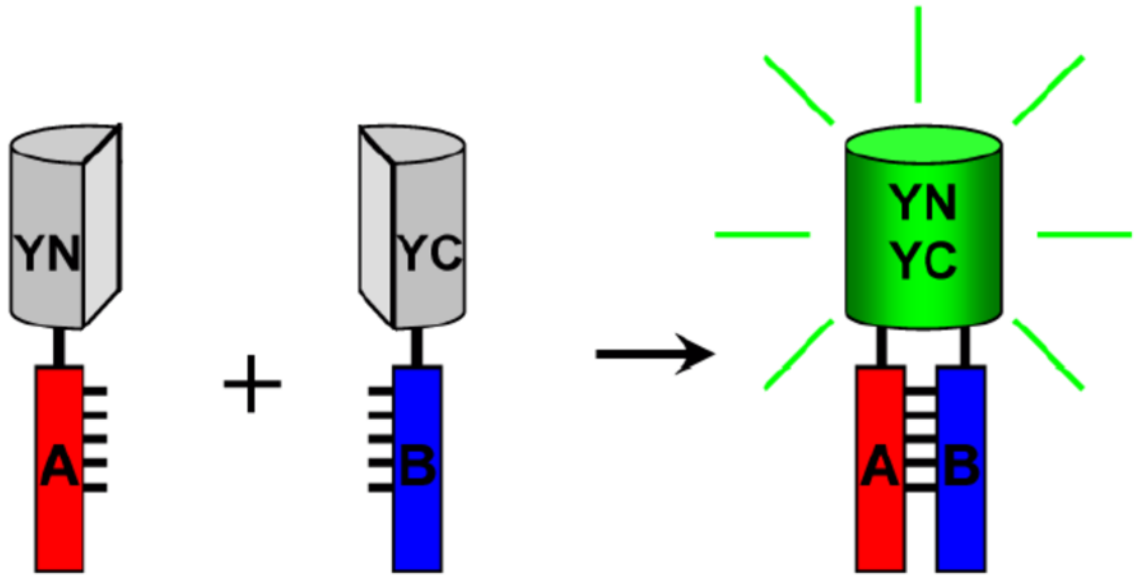
YN
A
+
YC
B
YN
YC
A
B

Figure 8. Bimolecular Fluorescence Complementation assay. Schematic representation of the Bimolecular Fluorescence Complementation Assay (BiFC). Two fusion constructs are generated so that the C-terminal of the Yellow Fluorescent Protein (YFP) is linked to the first putative protein and the N-terminal YFP is fused to the second putative protein respectively. Hence, if the two proteins are interacting in a non-covalent fashion, the YFP protein is properly reconstituted and a signal is discernable (modified from Kerppola, *Chem. Soc. Rev.,* 2006).

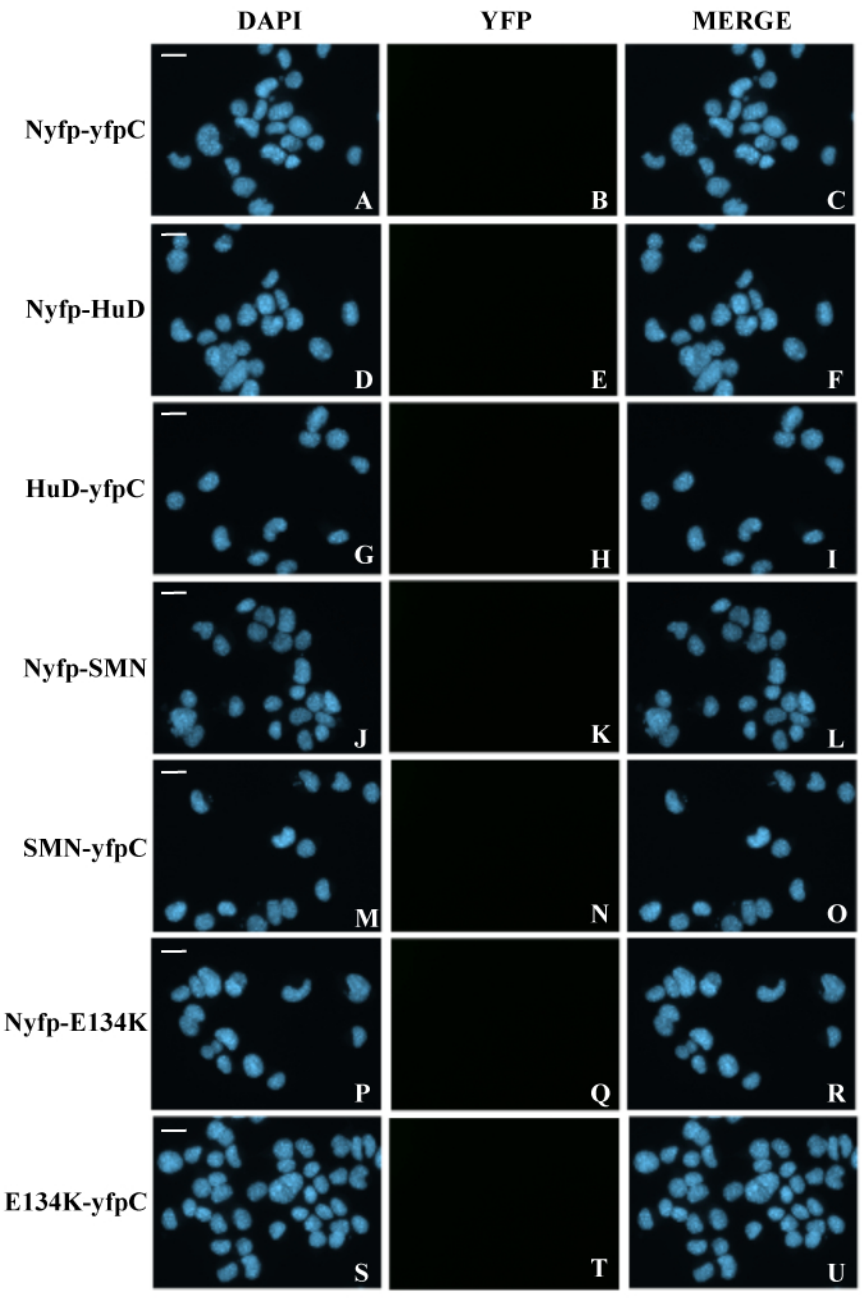
DAPI
YFP
MERGE
Nyfp-yfpC
A
B
C
Nyfp-HuD
D
E
F
HuD-yfpC
G
H
I
Nyfp-SMN
J
K
L
SMN-yfpC
M
N
O
Nyfp-E134K
P
Q
R
E134K-yfpC
S
T
U

Figure 9. Expression of individual BiFC fusion constructs or combination of parental Nyfp and yfpC proteins does not reconstitute YFP fluorescence. The identity of the respective expression vectors transfected in MN-1 cells is indicated on the left. Cell nuclei were counter-stained with DAPI. Bar is 20 μm (n = 3).

and visualized under a fluorescence microscope. As predicted, SMN and HuD interacted with each other in cells, resulting in a reconstituted YFP signal with a mostly diffuse cytoplasmic distribution (Figure 11, panels A to C). All cells positive for a YFP signal showed similar distribution suggesting the HuD/SMN interaction occurs predominantly in the cytoplasm with some degree of interaction in the nucleus, however not in nuclear Gems/Cajal bodies. As an internal control for this assay, SMN fusion constructs harboring the E134K Tudor domain mutation were also engineered. This mutation does not prevent the SMN protein from localizing to the cytoplasm and Cajal bodies, although it often leads to accumulation of mutant proteins in an increased number of Gems (Mohaghegh et al. 1999; Renvoise et al. 2006). Consistent with this, combination of wild type SMN and SMN-E134K yielded a YFP signal resembling normal endogenous SMN distribution (Figure 10, panels G to I), while mutant proteins together most often led to an increased number of nuclear foci (Figure 10, panels J to L). In contrast, combining HuD and mutant SMN-E134K fusion proteins did not yield any detectable fluorescence (Figure 11, panels D to F). The same experiment was also performed with MN-1 cells induced to differentiate 18 hours post-transfection and processed for fluorescence microscopy after 48 hours in differentiation media. As seen in undifferentiated cells, all YFP-positive cells showed a diffuse cytoplasmic signal, although the YFP signal was also observed within discrete foci localized to neurites of differentiated cells (Figure 11, panels G to L). Taken together, these results confirmed a direct interaction between SMN and HuD that mostly occurs in the cytoplasm and within neurites of differentiated motoneuron-like cells.

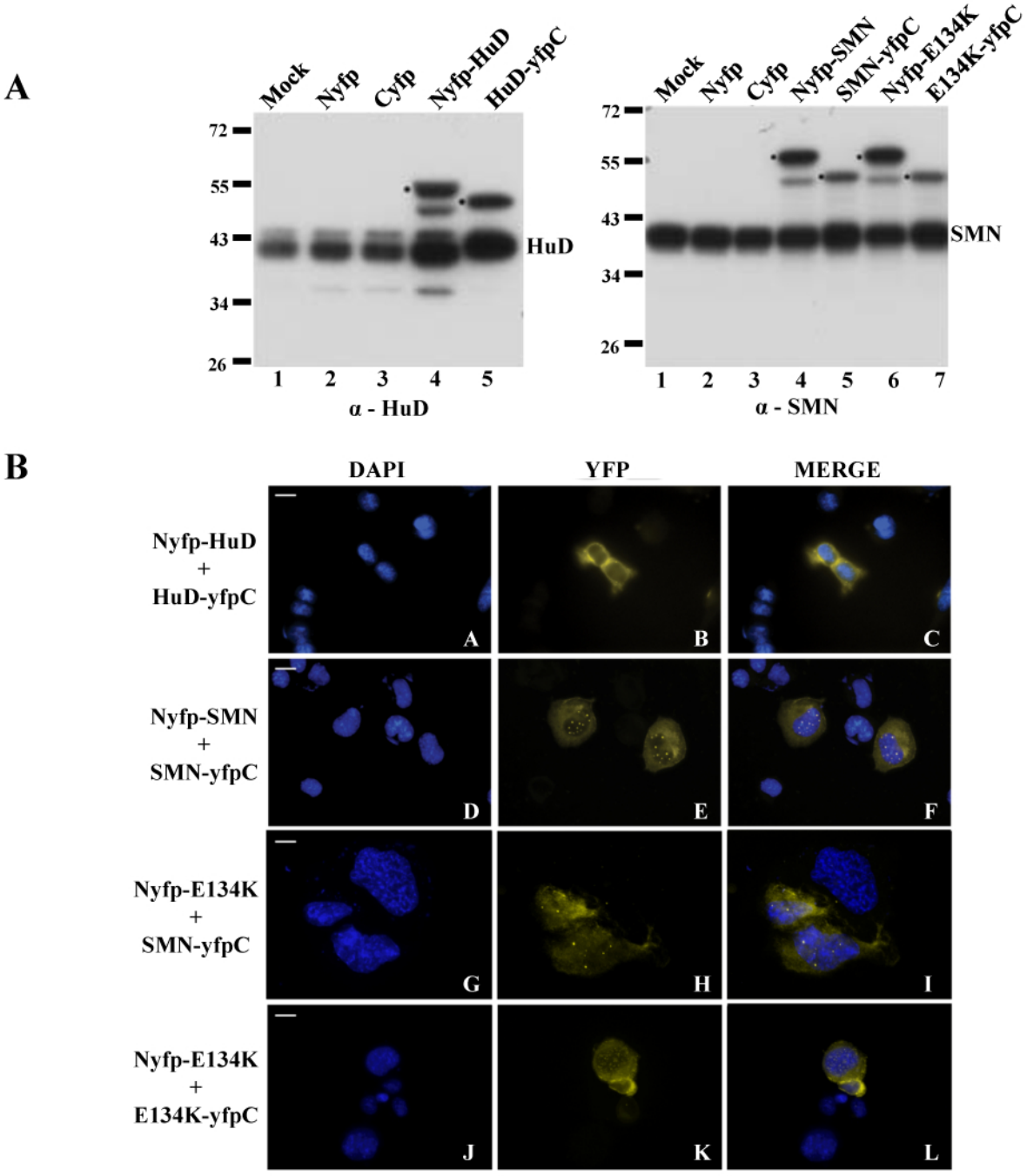
A
Mock
Nyfp
Cyfp
Nyfp-HuD
HuD-yfpC
72
55
43
34
26
HuD
1 2 3 4 5
α - HuD
Mock
Nyfp
Cyfp
Nyfp-SMN
SMN-yfpC
Nyfp-E134K
E134K-yfpC
72
55
43
34
26
SMN
1 2 3 4 5 6 7
α - SMN
B
DAPI
YFP
MERGE
Nyfp-HuD + HuD-yfpC
A
B
C
Nyfp-SMN + SMN-yfpC
D
E
F
Nyfp-E134K + SMN-yfpC
G
H
I
Nyfp-E134K + E134K-yfpC
J
K
L

Figure 10. SMN and HuD homodimerizes in motor neuron-derived cells. A. The expression levels of each fusion construct were assessed by immunoblotting using anti-HuD and anti-SMN antibodies. The endogenous HuD and SMN proteins are indicated on the right and the expressing constructs are indicated with a '•'. **B.** MN-1 cells were co-transfected with the indicated N-YFP and C-YFP fusion constructs. The co-transfection of the C- and N- terminal of either HuD or SMN demonstrates a intracellular and endogenous localization that is well established for the two proteins respectively (NYFP-HuD + CYFP-HuD/ NYFP-SMN + CYFP-SMN) (panel A to F). Furthermore, CYFP-SMN and NYFP-E134K or CYFP-E134K and CYFP-E134K were co-transfected, and suggests that the mutation of the Tudor domain (SMN-E134K) does not affect the homodimerisation of the SMN protein (panel g to l), although the co-transfection of both Tudor mutants together results in an increased number of nuclear foci likely corresponding to Gems. Bar 20 µm (n = 3).

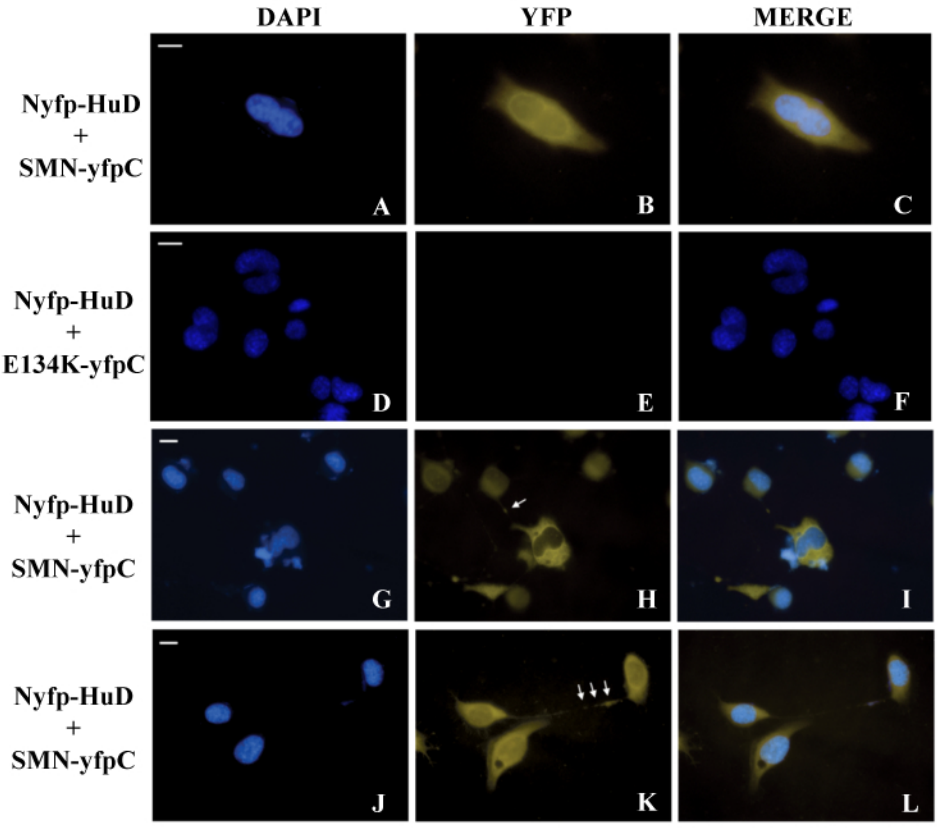
DAPI
YFP
MERGE
Nyfp-HuD
+
SMN-yfpC
A
B
C
Nyfp-HuD
+
E134K-yfpC
D
E
F
Nyfp-HuD
+
SMN-yfpC
G
H
I
Nyfp-HuD
+
SMN-yfpC
J
K
L

Figure 11. HuD and SMN physically interact in undifferentiated and differentiated motor neuron-derived cells. Cyfp-SMN and Nyfp-HuD were co-transfected in undifferentiated MN-1 cells and suggests that SMN and HuD protein interact directly in the cellular context. The localization of the interaction is mostly cytoplasmic with some degree of interaction in the nucleus (panel A to C). When Cyfp-E134K, a well known mutation of the Tudor domain of SMN and Nyfp-HuD were also co-transfected, it completely abolishes the interaction (panel D to F). When cells were co-transfected with Cyfp-SMN and Nyfp-HuD and were differentiated with a cocktail of Trans-Retinol and GDNF, the interaction between HuD and SMN localizes in the cytoplasm but importantly, in foci-like structures along extended neurites (panel G to L). Bar 20 μm (n = 3).

3.1.3 SMN is implicated in the localization of HuD and KSRP into RNA granules.

HuD is found in the cytoplasm, but also in neuronal processes, where it resides in so-called RNA granules with some of its mRNA targets (Anderson et al. 2003; Antic and Keene 1998). Thus, we next determined if SMN may influence HuD function in neurites (Hector Valderrama-Carvajal, Janik Laframboise). Control (empty vector) and shSMN knockdown MN-1 cultures were induced to differentiate using RA/GDNF treatment for 48 hours. This specific MN-1 cell line (shSMN) is stably expressing a shRNA targeting the 3'untranslated region of SMN and are expressing a 30% to 50% decrease of SMN protein levels compared to the empty shRNA vector control. Cytoplasmic extracts from Mock and differentiated cells were then resolved through sucrose density gradient fractionation (Figure 12). It was previously reported that the 'heavy' fraction at the bottom of the gradient actually contains RNA granules (Krichevsky and Kosik 2001). In order to validate this approach, the fractions were first probed using a series of well-accepted markers for mRNPs (Tubulin), ribosomal subunits (data not shown), and RNA granules (KSRP and HuD), which allowed identification of those respective fractions in the sucrose gradients (Figure 12, respective panels). An accumulation of KSRP and HuD was observed in these fractions upon differentiation of control MN-1 cells (Figure 12, respective panels), further supporting that fractions 11-13 indeed contained RNA granules components. In contrast, no accumulation of KSRP was observed in heavy sucrose gradient fractions when MN-1 shSMN cultures were induced to differentiate whereas for HuD a small amount is still present (Fig. 12, right, respective panels). These results implicates that SMN is required for proper recruitment of HuD (and KSRP) in dense neuronal RNA granules. Interestingly, SMN was also detected in RNA granules, consistent with its interaction with HuD (and KSRP) in punctate foci in neurites (Figure 12).

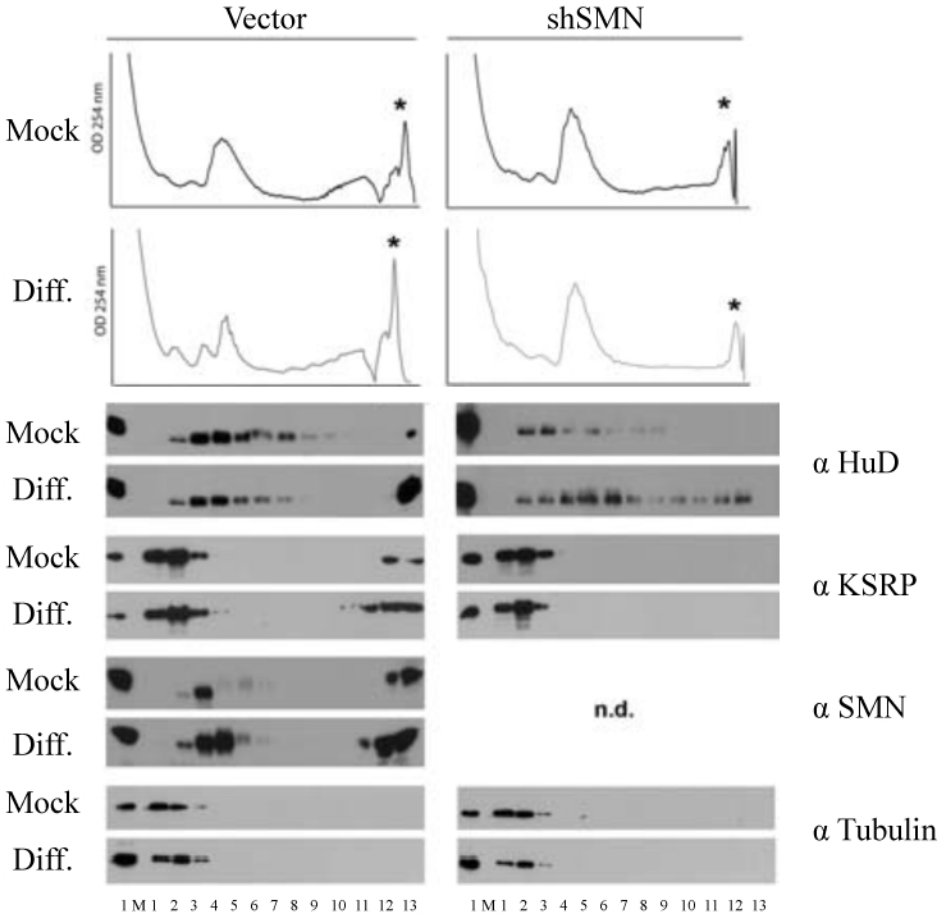
Vector
shSMN
Mock
Diff.
OD 254 nm
Mock
Diff.
α HuD
Mock
Diff.
α KSRP
Mock
Diff.
n.d.
α SMN
Mock
Diff.
α Tubulin
1 M 1 2 3 4 5 6 7 8 9 10 11 12 13
1 M 1 2 3 4 5 6 7 8 9 10 11 12 13

Figure 12. SMN is required for the localization of HuD into RNA granules. A sucrose density fractionation gradient was done on control vector (vector) and on SMN stable knockdown MN-1 cells (shSMN) that were left undifferentiated (Mock) or that had been differentiated (Diff.). The top panel demonstrates the representative profile of a sucrose density fractionation gradient and known component of the sucrose are indicated. They include mRNA ribonucleoprotein particules (mRNPs), small and large ribosomal subunits (40S and 60S), monosomes (80S), polyribosomes and dense RNA granules (*). The representative profiles of the vector control and shSMN left undifferentiated and differentiated are show in the middle panel. There is a relative enrichment in the RNA granules in vector control that add been differentiated whereas in shSMN cells this is not observed. Total proteins were extracted from each fraction, resolved by SDS-PAGE, and subjected to immunoblotting with the indicated antibodies. RNA granules component HuD and KSRP are seen enriched in fractions 11-13 upon differentiation of vector-transfected control cultures (left panels). In shSMN stable knockdown cells line there is a decrease in the translocation of HuD to these fractions whereas no translocation of KSRP is observed (right panels). SMN is also detected in the RNA granule fractions, while tubulin is only seen in mRNPs, as expected (n = 3).

Reduced translocation of β-actin mRNA to neuritic processes and growth cones has been observed in SMN-depleted cultured of neuronal cell lines and primary motoneurons derived from SMA model mice (Bowerman et al. 2007; Rossoll et al. 2003b). However, to date, no other mRNAs have been documented to be mislocalized in axons of SMA motoneurons. Since we found HuD to be misregulated in shSMN knockdown MN-1 cells, we next assessed if this also impacted some of its known axonal mRNA targets (Hector Valderrama-Carvajal, Janik Laframboise). The same approach as above was used except that total RNA was extracted from each collected fractions, which was then subjected to RT-PCR to monitor the distribution profiles of specific HuD mRNA targets (Figure 13). As a positive control to validate the procedure, the profile of β-actin mRNA was first assessed. As expected, β-actin mRNA was enriched in heavy fractions 11-13 following differentiation of control cells, while this redistribution was not observed in the shSMN knockdown samples (Figure 13, β-actin panels). Importantly, γ-actin mRNA, which does not translocate into neurites, was not detected in the heavy fractions under any conditions (Figure 13, γ-actin panels), confirming that the discrimination between cytoplasm and neuritic RNA granules mRNA populations is possible. The same fractions were next probed using RT-PCR to examine the distribution profiles in the sucrose gradient fractions of two known HuD targets, namely GAP43 and Tau. GAP43 mRNA was distributed more or less evenly in the gradient under Mock conditions and became more enriched in the heavy fractions following differentiation of MN-1 control cells (Figure 13, Vector, Mock and Diff. GAP43 panels). Although still detectable, this shift towards the dense RNA granules fractions was less pronounced in the absence of SMN (Figure 13, shSMN, Mock and Diff. GAP43 panels). Tau mRNA, on the other hand, was found largely enriched in the RNA granules fraction (lane 13), even in the absence of differentiation cues, although an

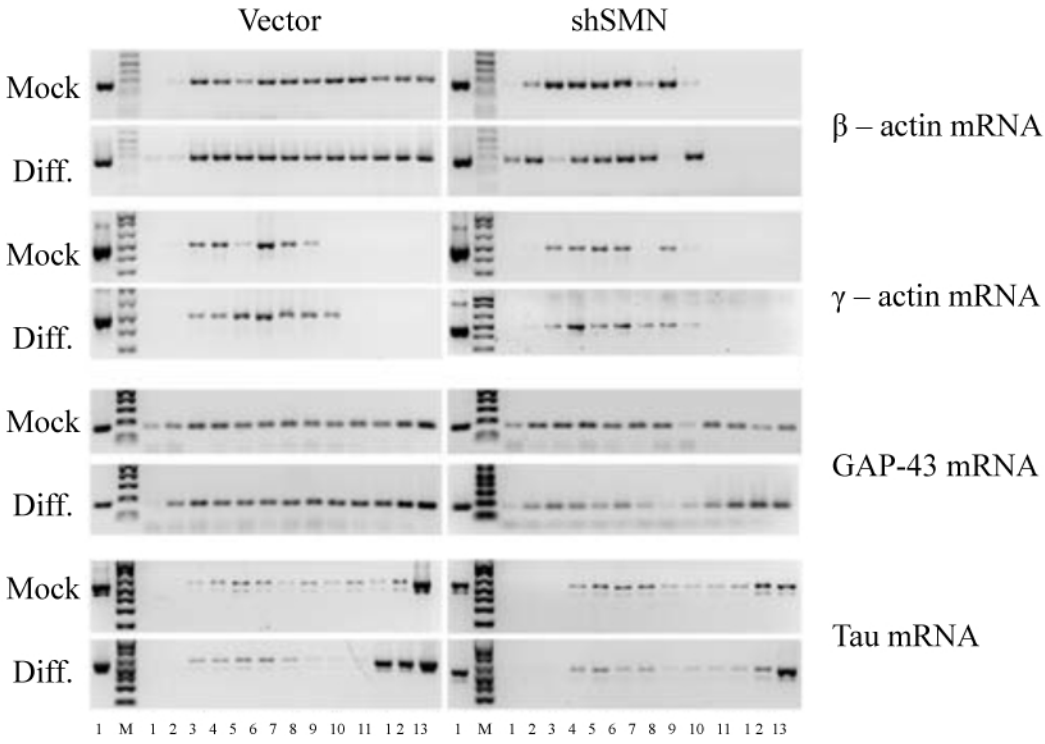
Vector
shSMN
Mock
Diff.
Mock
Diff.
Mock
Diff.
Mock
Diff.
β – actin mRNA
γ – actin mRNA
GAP-43 mRNA
Tau mRNA
1 M 1 2 3 4 5 6 7 8 9 10 11 12 13
1 M 1 2 3 4 5 6 7 8 9 10 11 12 13

Figure 13. Known mRNA molecules implicated in the differentiation process are mis-translocated to the RNA granules. Total mRNA was extracted from fractions of the sucrose density fractionation gradient done in vector control (vector) and MN-1 stable knockdown of SMN (shSMN) that had been left undifferentiated or had been differentiated. β – actin was used has a positive control and has expected was translocated to the RNA granules upon differentiation whereas in shSMN knockdown cells this translocation is not observed. γ – actin is not a known component of RNA granules; therefore it was used has a negative control. The accumulation of GAP-43 and Tau was observed in the RNA granules (fractions 11-13) of undifferentiated vector control cells demonstrating that these mRNA are present in these granules. Gap-43 and Tau translocates to the RNA granules (fractions 11-13) upon differentiation and has expected a decrease in their translocation is observed in SMA-like conditions (shSMN) (n = 3).

even greater accumulation was seen in fractions 11-13 after RA/GDNF treatment (Figure 13, Vector, Mock and Diff. Tau panels, respectively). Again, this enrichment of Tau mRNA in the RNA granules fractions was reduced in the MN-1 shSMN knockdown samples (Figure 13, shSMN, Mock and Diff. panels). These results imply that the defect in HuD recruitment to RNA granules observed in the face of reduced SMN expression, impacted on the fate of HuD mRNA targets GAP43 and Tau. This also constitutes the first identification of additional axonal mRNAs, apart from β-actin, that are misregulated in SMA-like conditions.

3.2 Identification and characterization of a novel SMN-interacting protein, SERBP1.

It has been reported that SMN localizes in neurites with a variety of RBPs (Fallini et al. 2011; Hubers et al. 2011; Tadesse et al. 2008) and that, in this context, SMN does not interact with Sm proteins (Fallini et al. 2011; Todd et al. 2010; Zhang et al. 2006) which suggest its role in neurites is independent of its well known function in snRNP biogenesis. As previously mentioned, we decided to investigate possible interacting proteins of SMN to shed light on a possible novel function for SMN in neurites. In the laboratory, it has previously been demonstrated that SMN interacts with the RBP KSRP (Tadesse et al. 2008) and HuD (Hubers et al. 2011), therefore it is possible that SMN interacts with other RNA-binding proteins. Data from a proteomic screen for SMN interacting proteins performed in the laboratory revealed that SMN might interact with the RBP SERBP1 which has recently been identified has a component of RNA granules purified from rat brain (Elvira et al. 2006a). SERBP1 has not been linked to any specific function in cells and it is possible that it interacts with SMN and therefore has a potential role in the SMA pathology. Hence, as

for HuD, I characterized the putative interaction between SMN and SERBP1 and determined the functional relevance of this interaction in motor neurons-derived cells.

3.2.1 SMN and SERBP1 interact in a direct fashion.

I first investigated whether an *in vitro* interaction potentially exists between SMN and SERBP1; therefore a GST pulldown experiment was performed. Protein extracts from WT MN-1 cells were first incubated with the purified GST-Tag proteins, the GST-SMN Tudor proteins or the GST-SMN Tudor E134K mutant found in severe type I SMA patients, respectively. Proteins retained on the column were then resolved by SDS-PAGE, transferred on a PVDF membrane and subjected to Western blot analysis using anti-SERBP1 antibodies. This clearly suggests that there is an *in vitro* interaction between the Tudor domain of SMN and SERBP1 and that the interaction observed is specific since the presence of only the GST-Tag did not retain SERBP1 (Figure 14). Importantly, the interaction between the E134K mutant of the Tudor domain and SERBP1 is completely abolished, hence suggesting that the Tudor domain is sufficient for the interaction between SMN and SERBP1 and therefore also potentially arginine methylation dependent. Since a non-physiological amounts of Tudor domain was added to the extract, it may drive an interaction that might not occur endogenously within cells. Therefore, I investigated whether an interaction is possible with endogenous proteins. To specifically assess this question, endogenous SMN proteins was immunoprecipitated from WT MN-1 cell extracts (Figure 15). As described above the immunoprecipitate was resolved by SDS-PAGE,

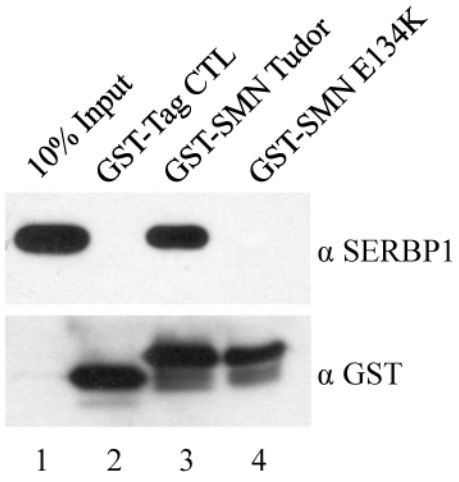
10% Input
GST-Tag CTL
GST-SMN Tudor
GST-SMN E134K
α SERBP1
α GST
1
2
3
4

Figure 14. The interaction between SMN and SERBP1 is dependent on the Tudor domain of SMN. SERBP1 interacts with the Tudor domain of SMN as determined by GST-pulldown experiments. A GST pulldown was done using total lysates from MN-1 cells. The lysates were incubated with purified GST (negative control), GST-SMN Tudor or GST-SMN E134K fusion proteins coupled to glutathione-agarose beads and subjected to Western blotting to probe for the presence of endogenous SERBP1. 10% of the total amount of lysate that was used is shown in lane 1. The anti-SERBP1 blot indicated that there is an interaction between the Tudor domain of SMN and SERBP1. The interaction is completely abolished when the lysate was incubated with GST-SMN E134K, a mutation of the Tudor domain found in severe SMA patients. The same membrane was stripped and blotted with anti-GST to verify the abundance of fusion proteins (n = 3).

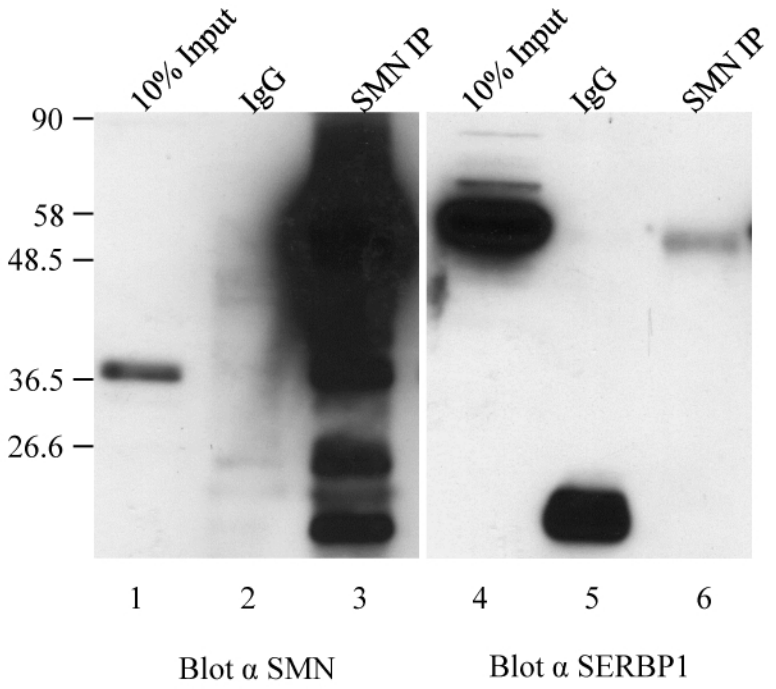
10% Input
IgG
SMN IP
10% Input
IgG
SMN IP
90
58
48.5
36.5
26.6
1
2
3
4
5
6
Blot α SMN
Blot α SERBP1

Figure 15. SMN and SERBP1 interact in motor neuron-derived cells. SMN and SERBP1 interact in motor neuron derived cells as determined by co-immunoprecipitation (co-IP) experiments. Endogenous SMN was immunoprecipitated from MN-1 cell lysates. Retained proteins following extensive washings were resolved by SDS-PAGE, transferred to PVDF and subjected to western blot analysis for the presence of either SMN (lanes 1-3) or SERBP1 (lanes 4-6). 10% of the amount of lysate used for IP is shown in lane 1 and lane 4. An IP was performed with purified non-immunogenic mouse immunoglobulins G (IgGs) as a negative control (n = 3).

transferred onto a PVDF membrane and subjected to Western blot analysis. The resulting anti-SERBP1 immunoblot suggest a possible interaction between endogenous SMN and SERBP1, while no interaction was seen in the IgG negative control. While this experiment shows that an interaction between SMN and SERBP1 exists, this interaction might be dependent on other proteins. To assess if there is an *in vitro* direct physical interaction between SMN and SERBP1, a Far Western/Blot overlay experiment using a large scale IP of endogenous SERBP1 was performed using WT MN-1 cells as described above for HuD (Figure 16). A direct interaction between the Tudor domain of SMN and SERBP1 was confirmed as the anti-GST immunoblot demonstrated a significant level of the Tudor domain binding to the SERBP1 protein and no other signals were observed in the SERBP1 IP lane. Therefore, taken together, these results suggest that SMN and SERBP1 can physically interact in motor neuron derived cells and that this interaction is potentially mediated through the Tudor domain of SMN.

3.2.2 SMN and SERBP1 physically interact in granular foci in neurites of motor neuron-derived cells.

The localization of SERBP1 in motor neurons has not been examined, therefore I characterized its localization in MN-1 cells using indirect immunofluorescence (IF) microscopy (Figure 17A). The IF performed on WT MN-1 cells shows that the endogenous localization of SERBP1 in motor neuron-like cells is mainly cytoplasmic with some week staining in the nucleus. Importantly, SERBP1 is also localizing to neurites of differentiated motor neuron-derived cells. This localization pattern is similar to what is observed for endogenous SMN in MN-1 cells; therefore an indirect immunofluorescence was carried out

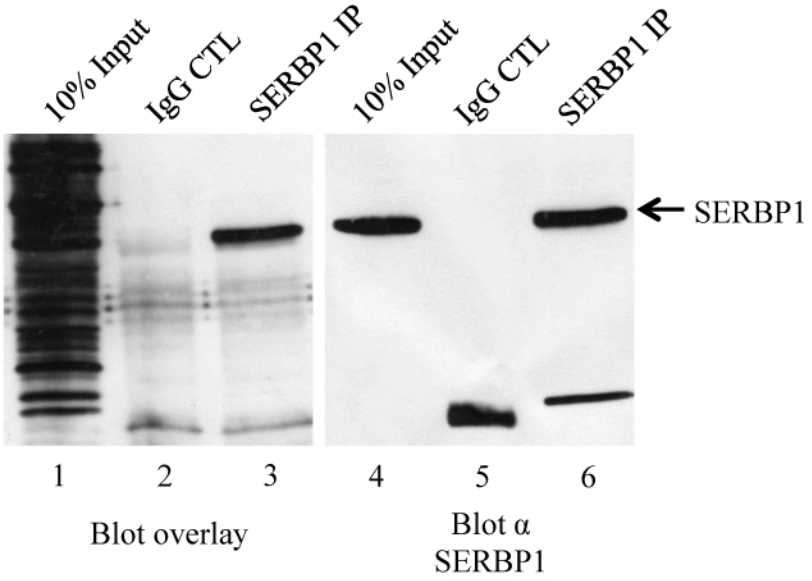
10% Input
IgG CTL
SERBP1 IP
10% Input
IgG CTL
SERBP1 IP
SERBP1
1
2
3
4
5
6
Blot overlay
Blot α
SERBP1

Figure 16. The Tudor domain of SMN can bind directly to SERBP1 *in vitro*. SERBP1 interacts directly with the Tudor domain of SMN as determined by a Blot overlay assay. A blot overlay experiment was carried out using a large scale IP of SERBP1 from MN-1 cell lysates. The IP was resolved by SDS-PAGE, transferred to nitrocellulose, which was then probed with purified GST-SMN Tudor. Immunoblotting against GST was performed and demonstrates that a significant amount of GST-SMN Tudor can bind directly to SERBP1. The membrane was stripped and blotted with anti-SERBP1 to determine where SERBP1 was migrating. 10% of the amount of lysate used for IP is shown in lane 1 and lane 4. An IP was performed with purified non-immunogenic mouse immunoglobulins G (IgGs) as a negative control (n = 3).

against SMN and SERBP1 in MN-1 cells that were induced to differentiate with a cocktail of Trans-Retinol and GDNF for 48 hours (Figure 17B). The resulting data suggests that there is co-localization of SMN and SERBP1 in the cytoplasm, and more importantly in foci-like structures along the neurites. Taken together, these results show that SERBP1 and SMN's localization in MN-1 cells is similar and that they co-localized in neurites of differentiated cells. Therefore, it is possible that the interaction between SMN and SERBP1 plays a role in neuronal differentiation, as it is the case for its interaction with HuD. SERBP1 and SMN interact in a direct fashion *in vitro* and are found in neuronal processes; therefore, in order to validate the endogenous direct interaction as well as assess the localization of this interaction, a BiFC experiment was performed. As discussed previously, the BiFC experiment can be used to visualize the localization of a direct interaction between two putative proteins. First, all the fusion constructs were transfected individually in MN-1 cells to verify that no reconstitution of the YFP signal was observed in the absence of a physical interaction. As expected, imaging these cells after 24 hours demonstrated no discernible signal, showing that the signal is specific (Figure 18B). Furthermore, the level of expression of each fusion constructs was verified by immunoblotting (Figure 18A). As the dimerization of SERBP1 has not yet been reported, the Cyfp-SERBP1 and Nyfp-SERBP1 were first co-transfected in WT MN-1 cells to assess whether, like for HuD, this takes place in motor neurons. Surprisingly, after fixation of these transfected cells and imaging, SERBP1 was shown to dimerize and this dimerization takes place mainly in the cytoplasm, but it is also observed along neurites of motor neuron-derived cells (Figure 19, panel J to L). Next, the Nyfp-SMN and the Cyfp-SERBP1 were co-transfected in WT MN-1 cells and cells were prepared for imaging. The resulting data showed that there is a direct endogenous interaction between these two proteins in motor

A

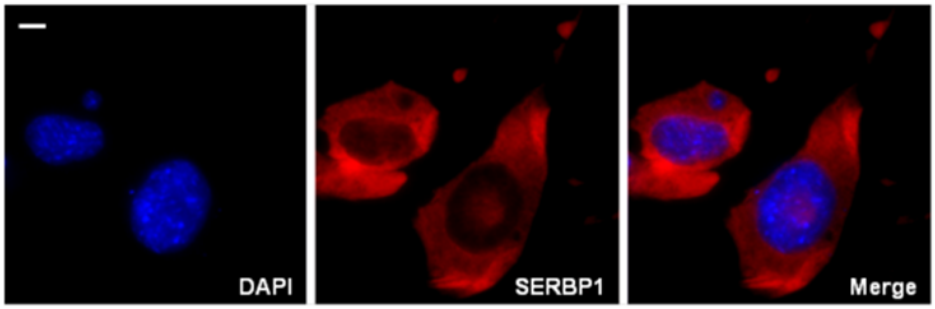

B

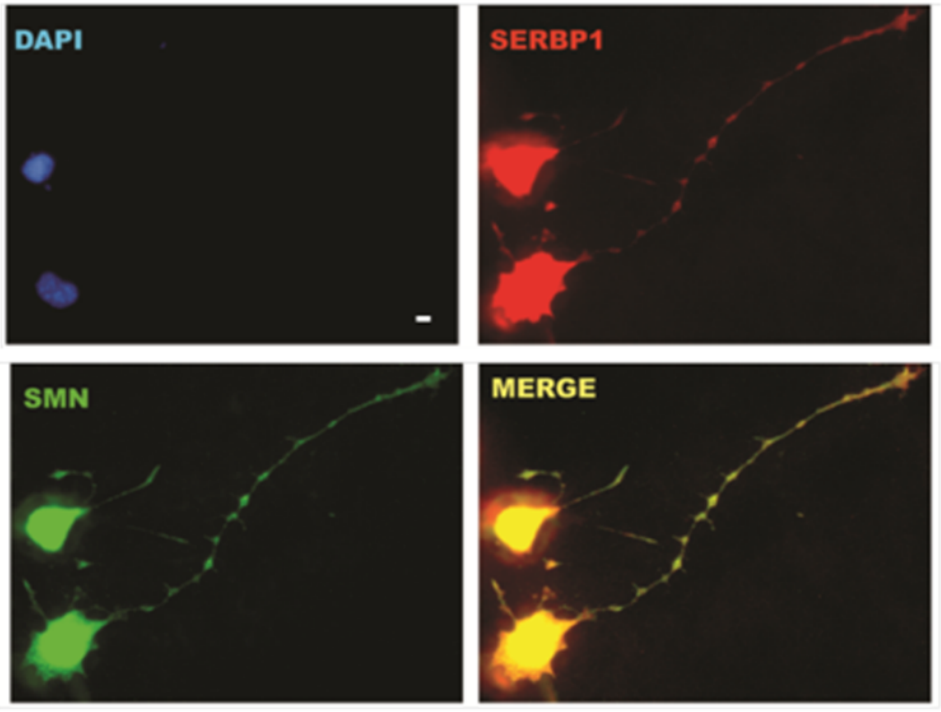

Figure 17. SERBP1 and SMN co-localize in granular foci along neurites of differentiated motor neuron derived cells. A. Representative immunofluorescence microscopy showing the localization of endogenous SERBP1 in undifferentiated MN-1 cells. Localization of this protein is mostly cytoplasmic with a low level of expression in the nucleus. Bar = 5 μm. **B.** Indirect immunofluorescence against SMN and SERBP1 performed on differentiated MN-1 cells shows that these proteins co-localize in granular foci along neurites of motor neuron derived cells. Bar = 5 μm (n = 3).

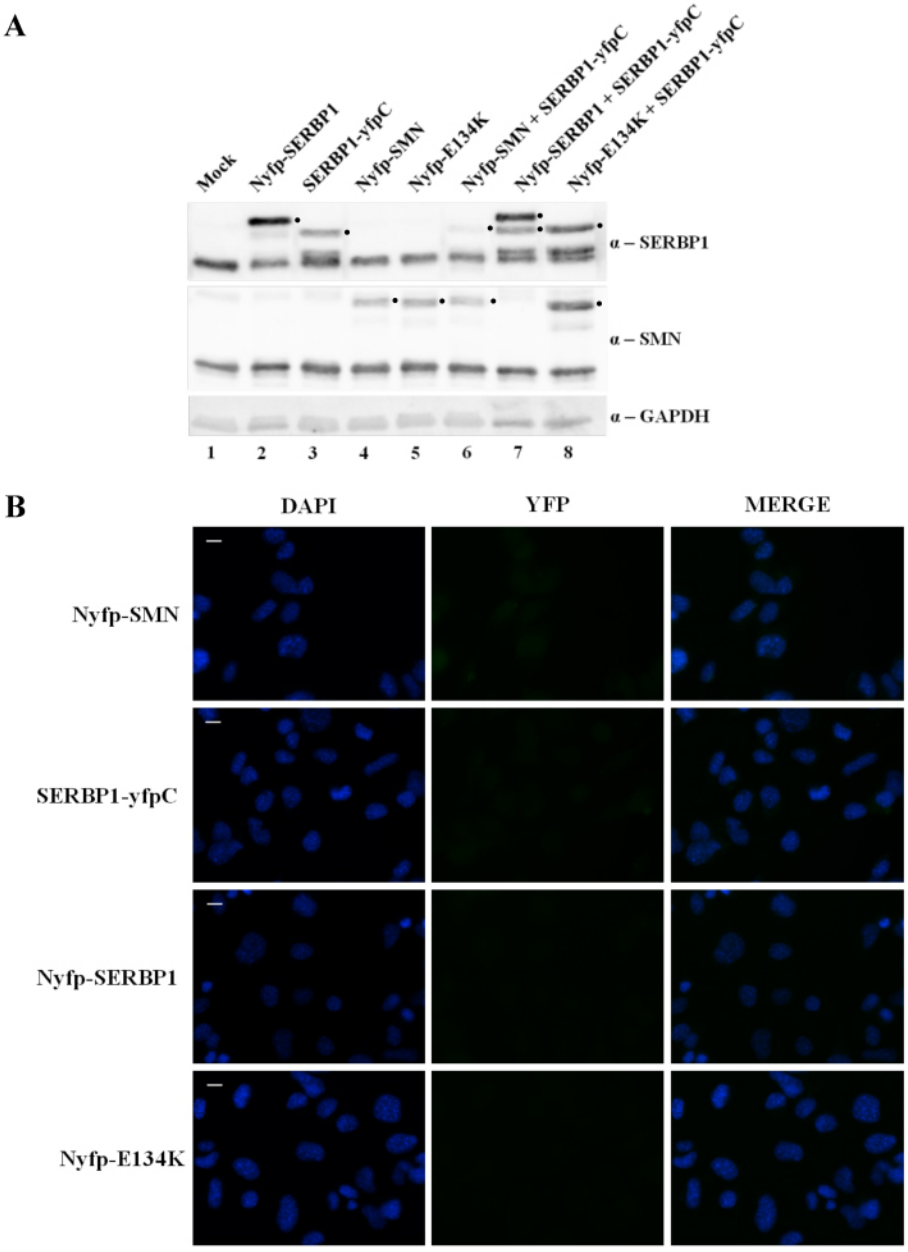
A
Mock
Nyfp-SERBP1
SERBP1-yfpC
Nyfp-SMN
Nyfp-E134K
Nyfp-SMN + SERBP1-yfpC
Nyfp-SERBP1 + SERBP1-yfpC
Nyfp-E134K + SERBP1-yfpC
α – SERBP1
α – SMN
α – GAPDH
1 2 3 4 5 6 7 8
B
DAPI
YFP
MERGE
Nyfp-SMN
SERBP1-yfpC
Nyfp-SERBP1
Nyfp-E134K

Figure 18. Expression of individual BiFC fusion constructs or combination of parental Nyfp and yfpC proteins does not reconstitute YFP fluorescence. **A.** The expression levels of each fusion construct were assessed by immunoblotting using anti-SERBP1 and anti-SMN antibodies. The endogenous SERBP1 and SMN proteins are indicated on the right and the expressing constructs are indicated with a '•'. **B** The identity of the respective expression vectors transfected in MN-1 cells is indicated on the left. Cell nuclei were counter-stained with DAPI. Bar is 20 μm (n = 3).

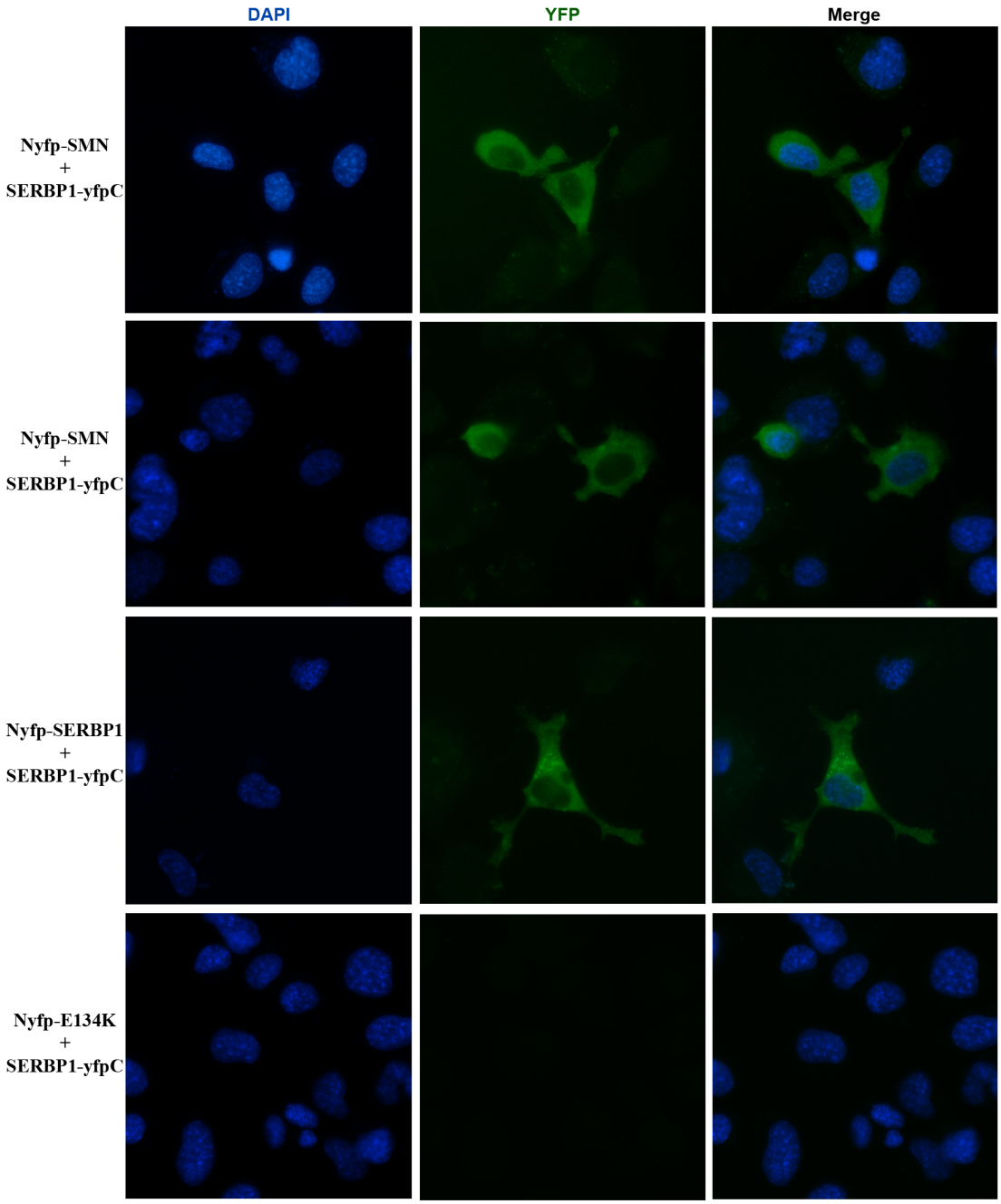
DAPI
YFP
Merge
Nyfp-SMN
+
SERBP1-yfpC
Nyfp-SMN
+
SERBP1-yfpC
Nyfp-SERBP1
+
SERBP1-yfpC
Nyfp-E134K
+
SERBP1-yfpC

Figure 19. SERBP1 and SMN physically interact in undifferentiated motor neuron-derived cells. Cyfp-SERBP1 and Nyfp-SMN were co-transfected in undifferentiated MN-1 cells and suggests that SMN and SERBP1 protein interact directly in motor neuron-derived cells. The localization of the interaction is mostly cytoplasmic with some degree of interaction in the nucleus and also in granular foci along the neurites (panel A to F; indicated by the arrows). When Cyfp-E134K, a well known mutation of the Tudor domain of SMN and Nyfp-SERBP1 were also co-transfected, it completely abolishes the interaction (panel G to I). Co-transfections of Nyfp-SERBP1 and Cyfp-SERBP1 (panel J to L) indicate that the dimerization of SERBP1 occurs in the cytoplasm but also in granular foci along the neurites as indicated by the arrow. Bar = 20 μm (n = 3).

neuron-derived cells, consistent with the *in vitro* Far Western/Blot overlay experiment. Importantly, the SMN/SERBP1 interaction localizes mainly in the cytoplasm with some evidence of interaction in the nucleus, but, as observed for HuD, it also localizes to granular foci along the axons (Figure 19, panel A to F). As I have suggested that the interaction is potentially mediated by the Tudor domain of SMN by performing GST pulldown experiments, I next co-transfect Nyfp-E134K and the Cyfp-SERBP1 in WT MN-1 cells to validate whether the interaction is dependent on this specific domain. As expected, when these two fusion constructs were co-transfected in MN-1 cells, no YFP signal was observed suggesting that the Tudor domain is required for the interaction between SMN and SERBP1 (Figure 19, panel G to I). Taken together, these results show for the first time that SERBP1 can dimerize and that this dimerization localizes to the cytoplasm, as well as in granular foci along neurites of motor neuron-like cells. Furthermore, I have uncovered a novel endogenous physical interaction between the causative gene for SMA, SMN and SERBP1, therefore establishing a potential implication of SERBP1 in the SMA pathology.

3.2.3 SERBP1 is down-regulated in an SMA cell culture model and can rescue SMA-like neuronal defects.

Since I discovered that SMN and SERBP1 interact directly with each other in motor neuron-derived cells, next, I investigated the possibility that this interaction has a role in the SMA pathology. It has been reported in numerous instances that in SMA-like conditions where SMN protein levels are low, the protein levels of its interacting partners decreases (Helmken et al. 2003; Tadesse et al. 2008); therefore this could also be the case for

A

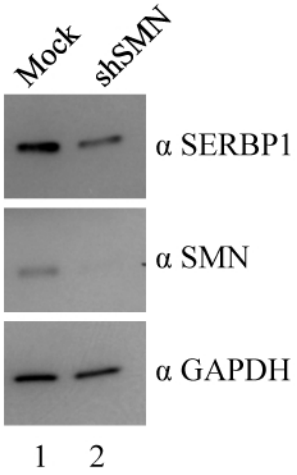
Mock
shSMN
α SERBP1
α SMN
α GAPDH
1
2

B

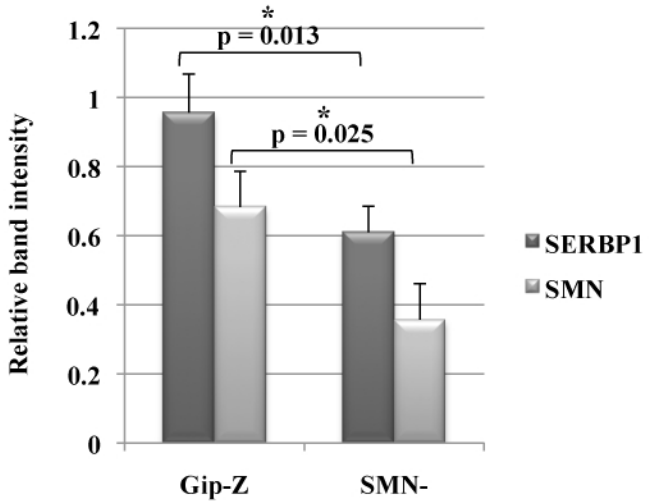
*
p = 0.013
*
p = 0.025
1.2
1
0.8
0.6
0.4
0.2
0
Relative band intensity
SERBP1
SMN
Gip-Z
SMN-

Figure 20. SERBP1 protein levels are reduced in SMA-like conditions. A. Representative Western blot demonstrating that in SMN stable knockdown MN-1 cells line, there is a significant decrease of SERBP1 protein levels. GAPDH was used has a loading control. **B.** Bar graph demonstrating that the decrease in SERBP1 and SMN protein levels are significant (n = 6).

SERBP1. To assess if reduced SMN protein levels affect SERBP1 protein levels, I used the previously described shSMN stable knockdown cells line. Lysates from vector control MN-1 cells and shSMN knockdown cells were resolved by SDS-PAGE, transferred on a nitrocellulose membrane and subjected to Western blot analysis or alternatively were also assessed by fluorescence immunoblotting (Licor). The resulting anti-SERBP1 immunoblot imply that in shSMN stable knockdown cells there is a significant decrease in the SERBP1 protein level compared to the vector control cells (Figure 20). Thus, this result suggests that in SMA-like conditions, SERBP1 protein levels decrease; therefore implying that SERBP1 could potential be implicated in the etiology of the disease. Since SERBP1 protein levels are down regulated in SMA-like conditions, I next determine the functional relevance of this result. A rescue experiment was carried out by transfecting the pcDNA 3.1-myc-SERBP1 construct in vector control MN-1 cells as well as in shSMN stable knockdown MN-1 cells to assess if restoring SERBP1 protein levels would be able to rescue SMA-like neuronal defects observed in these cells (Hubers et al. 2011). To obtain a quantitative measure of neuronal differentitation, a few specific parameters were monitored in those experiments. First, the cells with neurites double the length of the cell body as well as cells with neurites showing branching were counted. Additionally, the average length of neurites was measured. These three parameters have previously been used to measure the level of differentiation of MN-1 cells and other neuronal cell lines and can therefore be suitable to measure neurites outgrowth as well as neuronal differentiation (Hubers, L. et al., 2011; Tadesse, H. et al., 2008). In all the conditions used the level of expression of the myc epitope-tagged SERBP1 was assessed by Western blot analysis to insure comparable expression (Figure 21A). I first transfected vector control MN-1 cells that were left undifferentiated with the pcDNA 3.1-myc-SERBP1 construct. Phase contrast images were

A

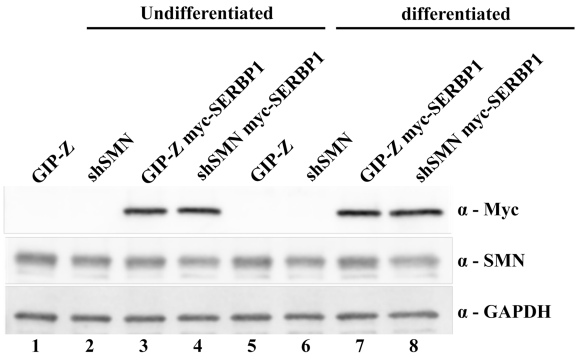
Undifferentiated
differentiated
GIP-Z
shSMN
GIP-Z myc-SERBP1
shSMN myc-SERBP1
GIP-Z
shSMN
GIP-Z myc-SERBP1
shSMN myc-SERBP1
α - Myc
α - SMN
α - GAPDH
1 2 3 4 5 6 7 8

B

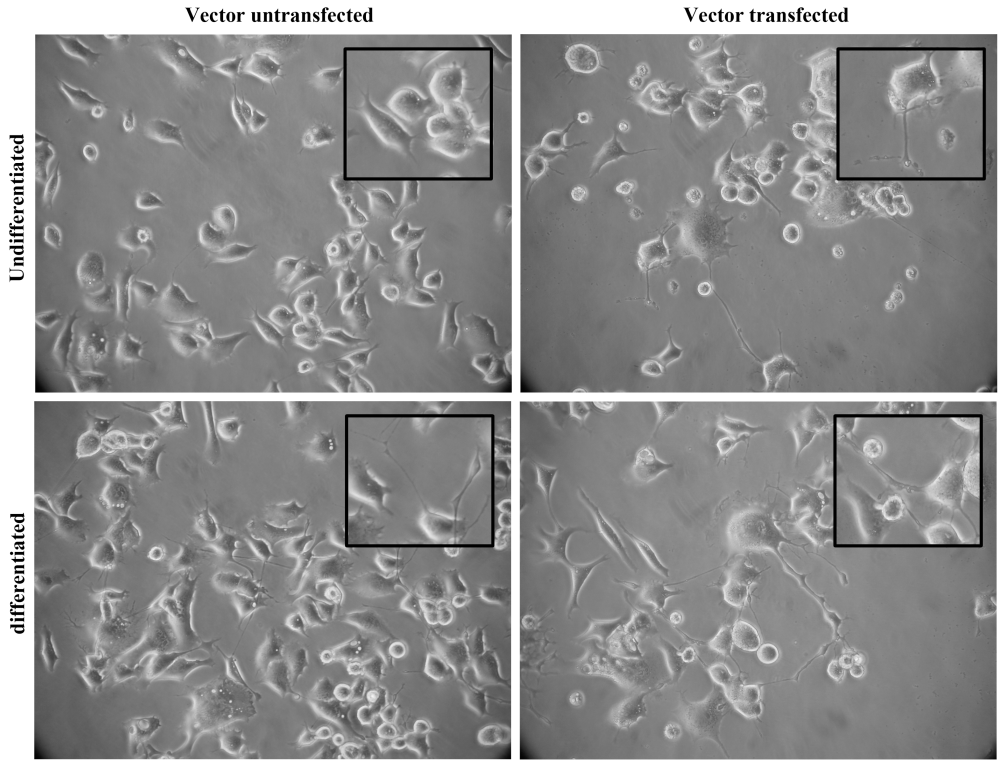
Vector untransfected
Vector transfected
Undifferentiated
differentiated

Figure 21. SERBP1 can rescue neurite outgrowth defects observed in SMA-like conditions. Vector control (GIP-Z) and shSMN stable knockdown MN-1 cells were transfected with the pcDNA 3.1-myc-SERBP1 construct which suggests that SERBP1 can rescue neurites outgrowth defects observed in shSMN stable knockdown MN-1 cells. **A.** Western blot analysis demonstrates that the pcDNA 3.1-myc-SERBP1 (myc-SERBP1) is expressed at comparable levels in transfected MN-1 cells that were left untreated or treated with differentiation media using an anti-myc antibody. The same membrane was stripped and reblotted with anti-SMN to verify the level of knockdown of SMN in shSMN MN-1 cells. GAPDH was used as a loading control. **B.** Representative phase contrast images demonstrating the increased number and length of neurites in transfected/undifferentiated and transfected/differentiated vector control (n=5).

C

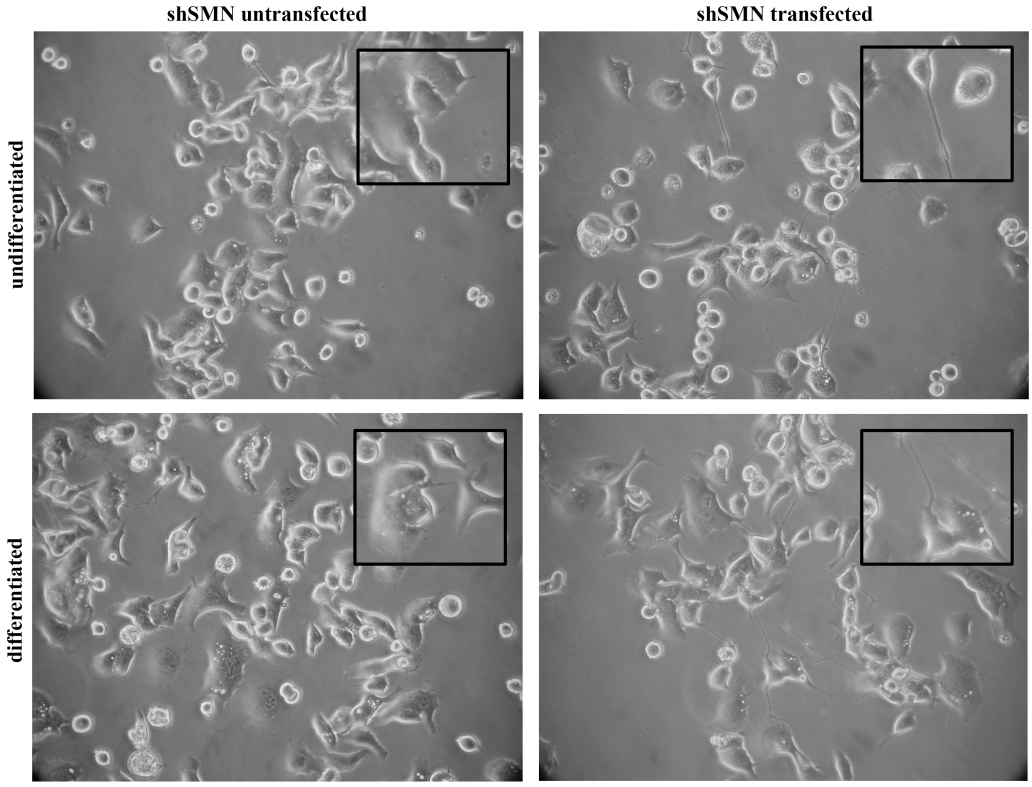
shSMN untransfected
shSMN transfected
undifferentiated
differentiated

Figure 21. SERBP1 can rescue neurite outgrowth defects observed in SMA-like conditions (continued). C. Vector control (GIP-Z) and shSMN stable knockdown MN-1 cells were transfected with the pcDNA 3.1-myc-SERBP1 construct which suggests that SERBP1 can rescue neurites outgrowth defects observed in shSMN stable knockdown MN-1 cells. Representative phase contrast images demonstrating the increased number and length of neurites in transfected/undifferentiated and transfected/differentiated shSMN stable knockdown cell line (n=5).

taken (Figure 21B and C) and showed that there is an increase in all three parameters described above (Figure 21 D, E and F); therefore suggesting that SERBP1, even in the absence of differentiation stimulus, is capable of inducing differentiation of motor neuron-derived cells implying a potential role of SERBP1 in this specific pathway. Next, the vector control cells that were previously transfected were then induced to differentiate with a RA/GDNF cocktail. The resulting data suggests that SERBP1 is still increasing the three parameters but has less of an effect, since cells have likely reached their maximum differentiation level (Figure 21). Together, these results strongly suggests that the over-expression of SERBP1 in undifferentiated conditions, is capable of inducing neuronal differentiation and more specifically neurite outgrowth, thus implying that SERBP1 might be implicated in neuronal differentiation of motor neuron-derived cells.

As previously reported, SMN depletion reduces the efficiency of differentiation and in cell culture models, defects in neurite outgrowth have been reported (Zhang et al. 2003; Zhang et al. 2007; Rossoll et al. 2003). Hence, next I assessed whether the over-expression of SERBP1 might rescue these specific defects. In order to verify this hypothesis, I transfected undifferentiated shSMN stable knockdown cells with the pcDNA 3.1-myc-SERBP1 construct. Interestingly, I observed a significant increase in all three parameters described above suggesting that SERBP1 is capable of rescuing neurite outgrowth defects observed in the face of low SMN levels (Figure 21). I then differentiated the previously tranfected shSMN stable knockdown cells. Precisely, all three parameters increased and this effect was even greater than what was observed for undifferentiated cells (Figure 21). Taken together, these results imply that over-expression of SERBP1 in shSMN stable knockdown cells, which have been reported to have numerous neurite outgrowth defects,

D

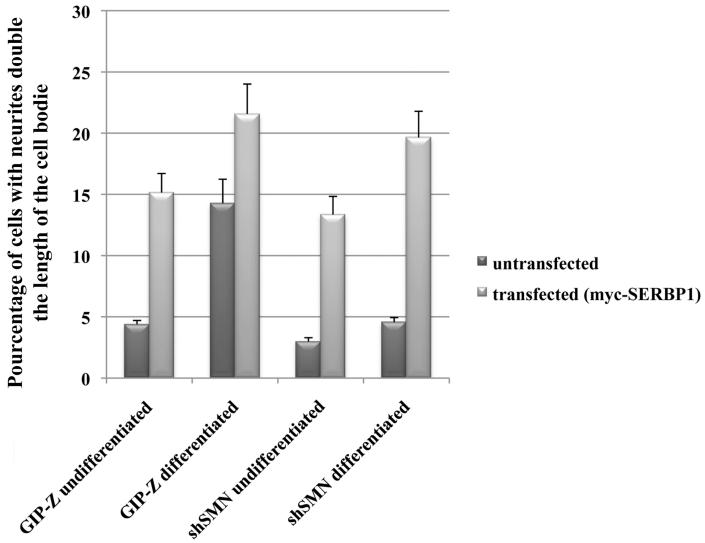
Pourcentage of cells with neurites double the length of the cell bodie
30
25
20
15
10
5
0
GIP-Z undifferentiated
GIP-Z differentiated
shSMN undifferentiated
shSMN differentiated
untransfected
transfected (myc-SERBP1)

E

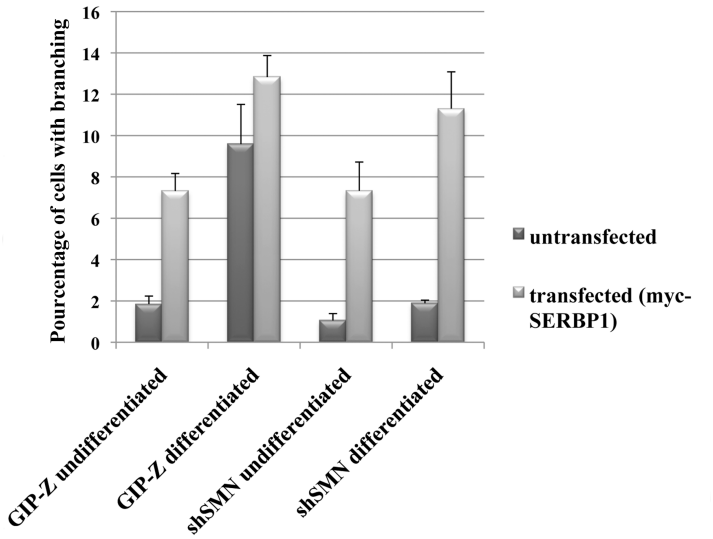
Pourcentage of cells with branching
16
14
12
10
8
6
4
2
0
GIP-Z undifferentiated
GIP-Z differentiated
shSMN undifferentiated
shSMN differentiated
untransfected
transfected (myc-SERBP1)

F

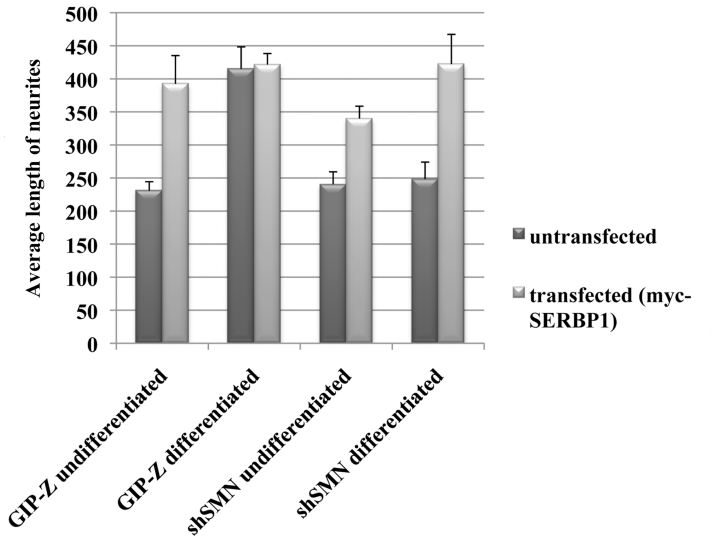
Average length of neurites
500
450
400
350
300
250
200
150
100
50
0
GIP-Z undifferentiated
GIP-Z differentiated
shSMN undifferentiated
shSMN differentiated
untransfected
transfected (myc-SERBP1)

Figure 21. SERBP1 can rescue defects in neurites outgrowth found in SMA-like conditions (continued). D. Bar graph showing quantification of the average percentage of cells with neurites double the length of the cell body (GIP-Z undifferentiated untransfected/transfected: p=0.0013; GIP-Z differentiated untransfected/transfected: p=0.0015; shSMN undifferentiated untransfected/transfected: p=0.0013; shSMN differentiated untrabsfected/transfected: p=0.0027). **E.** Bar graph showing quantification of the average percentage of cells with branching (GIP-Z undifferentiated untransfected/transfected: p=0.0056; GIP-Z differentiated untransfected/transfected: p=0.0622; shSMN undifferentiated untransfected/transfected: p=0.0131; shSMN differentiated untrabsfected/transfected: p=0.0050). **F.** Bar graph showing quantification of the average length of neurites (GIP-Z undifferentiated untransfected/transfected: p=0.0307; GIP-Z differentiated untransfected/transfected: p=0.7344; shSMN undifferentiated untransfected/transfected: p=0.0399; shSMN differentiated untrabsfected/transfected: p=0.0080) (n=5).

can rescue these SMA-like defects. Therefore, I speculate that SERBP1 plays an important role in neuronal differentiation, and, more importantly, could represent a novel target for the development of therapeutic strategies to treat and/or cure SMA.

Chapter 4: Discussion

4.1 Summary

Since SMN plays a housekeeping role in all cells as it functions as a molecular chaperone in snRNP biogenesis, it remains unclear why SMA specifically affects lower motor neurons. Hence, it has been postulated that SMN might play an additional function in motor neurons. In order to gain insight on this potential role, investigation of possible interacting partners of SMN in motor neuron-derived cells seemed essential. We have uncovered that HuD and SERBP1, two RNA-binding proteins, are physically interacting with SMN in MN-1 cells and that these specific interactions are occurring in granular foci along neurites, thought to be RNA granules. Furthermore, we were able to show that SMN is potentially crucial for the proper localization of KSRP and HuD (along with some of its mRNA targets) in RNA granules, consistent with a role for SMN in the assembly of these specific granules. Moreover, I also showed that SERBP1 can promote neuronal differentiation, as it was able to induce differentiation in absence of differentiation stimuli and was capable of rescuing neurite outgrowth defects observed in MN-1 shSMN stable knockdown cells. Together, these results suggest that SMN, through its interaction with

specific RNA-binding protein partners including HuD and SERBP1, plays a crucial role in promoting differentiation of motor neurons.

4.2 SMN physically interacts with two novel RNA-binding proteins and these interactions occur in RNA granules of motor neurons-derived cells.

SMN has been shown to colocalize with Ribosomal RNA, poly (A+) mRNAs and PABP in axons of motor neurons (Zhang et al., 2003; Zhang et al., 2007). Furthermore, SMN was also demonstrated to colocalize with hnRNP Q and hnRNP R in axonal processes, suggesting a possible functional implication of SMN in neuronal RNA granules (Rossoll et al., 2002). Our laboratory has previously reported the characterization of the interaction between SMN and KSRP; a known component of these neuronal RNA granules (Tadesse et al., 2008). More recently, I have participated in the biochemical and functional characterization of a novel interaction between SMN and HuD, another known component of RNA granules (Hubers et al., 2010) following up on the work of a former graduate student in the laboratory (Lisa Hubers). More specifically, through the use of various biochemical and cell biology approaches, I have helped demonstrate that SMN and HuD physically interact with each other in the cytoplasm and in axonal foci of motoneuron-derived MN-1 cells. Intriguingly, although it was speculated that this interaction might take place in the context of an mRNP complex, I found that the interaction was resistant to RNase treatment suggesting that this specific interaction is not mediated by an mRNA molecule. This is in contrast to what was observed before by the previous student, who had demonstrated that the interaction between SMN and HuD was sensitive to RNase A treatment, when assessed by GST-pulldown assays (Hubers et al. 2011). It is possible that

in a cellular context, the interaction between SMN and HuD is part of a larger complex that contains additional proteins capable of stabilizing the interaction. Alternatively, a large multi-protein complex might block the access to RNase A. As was demonstrated in the recent paper (Hubers et al., 2010), HuD is methylated by CARM1, therefore it was speculated that arginine methylation of HuD could potentially regulate its interaction with the Tudor domain of SMN. However, co-IP experiments performed with lysate of shCARM1 stable knockdown cells suggest that CARM1 is not absolutely required for the interaction between SMN and HuD to take place. Nevertheless, there is still some CARM1 present in our stable knockdown line and it is possible that these low levels would be sufficient to promote binding of HuD to the Tudor domain of SMN. Alternatively, a distinct PRMT might be responsible for regulating this interaction. Interestingly, while we have shown that CARM1 levels are normally down-regulated upon motoneuron differentiation (Hubers et al., 2010), we have preliminary evidence that PRMT8 expression is gradually up-regulated during this process. A former graduate student in the laboratory has performed experiments which suggests that HuD is unlikely methylated by another PRMT apart from CARM1 (Hubers et al. 2011). However, the approach that was used for those experiments involved sonication to prepare cellular extracts, and it is possible that these treatments may have inhibited the activity of certain PRMTs. Therefore, I cannot rule out the possibility that HuD may be methylated by other PRMTs, like e.g. PRMT8, and additional experiments will be required to clarify this question.

I have also biochemically characterized a novel interaction between SMN and the RNA-binding protein SERBP1, another known component of RNA granules. Following essentially the same experimental scheme as for HuD, I have shown that SMN and

SERBP1 also interact in a direct fashion *in vitro* and in the cytoplasm and axons of motoneuron-derived cells. However, in contrast to what was observed for HuD, it was found that the interaction between SMN and SERBP1 was not sensitive to RNase A treatment, even when assessed *in vitro* using GST-pulldown assays (Dr. Hector Valderrama-Carvajal, data not shown), therefore this was not tested further using co-IPs. A similar situation was also observed previously by our laboratory for the interaction between SMN and KSRP (Tadesse et al. 2008), suggesting that overall, interactions between SMN and components of neuronal RNA granules is likely not bridged by RNA.

A Far Western/Blot overlay was performed as one of two experimental approaches to address whether the interactions between SMN and HuD/SERBP1 were direct. The signal obtained for SERBP1 in these experiments was generally more intense compared with HuD, which could suggest that the binding of the Tudor domain of SMN with SERBP1 is stronger. However, it is difficult to compare these two separate blot overlays since the amount of antibody used for IP and the efficiency of the antibody can vary. Furthermore, in cells, the level of expression of different proteins can differ; therefore increased binding of the Tudor domain of SMN to SERBP1 could simply reflect a higher expression level in motor neurons. Binding experiments (e.g. using surface plasmon resonance, fluorescence polarization, or isothermal titration calorimetry) with known amounts of purified proteins would be needed to obtain a precise quantitative measure of binding affinity/strength between these proteins and the Tudor domain of SMN. Intriguingly, I have observed that in the case of HuD, the Tudor domain of SMN interacts directly with a slower-migrating form of HuD. This could possibly be due to post-translational modifications of HuD. In fact, HuD can be methylated by CARM1 and this

methylation can be recognized by the Tudor domain of SMN (Hubers et al. 2011); therefore this could explain the data observed. However, we cannot exclude the possibility that the slower migrating form of HuD can potentially be due to another form of post-translationnal modification like for example phosphorylation. It has also been reported that HuD can by alternatively spliced to produce three splicing variants (Wang et al. 2010), which could suggest that SMN might interact specifically with only one of these isoforms. Although previous experiments from our laboratory have essentially ruled out this possibility (L. Hubers, M.Sc. Cellular and Molecular Medicine, 2010), we cannot rule out that this slower migrating band could represent a yet-uncharacterized isoform of HuD. Thus, further analysis will be needed to determine the precise nature of the HuD form that is bound by the Tudor domain of SMN in motor neurons.

Lastly, BiFC experiments were carried out and suggest a direct interaction between SMN and these interacting RBPs. Interestingly, no interaction between SMN and these proteins were observed within Cajal bodies, even though SMN is highly concentrated in these nuclear bodies that are known sites of maturation for partially assembled snRNPs. This strongly suggests that these interactions do not take place in the context of snRNP biogenesis; therefore supporting the growing evidence that SMN might play an additional role in motor neurons. It is likely that the granular foci where we detected an interaction using BiFC represent RNA granules since HuD and SERBP1 have both been shown to be components of RNA granules biochemically purified from rat brains (Elvira et al. 2006a). Altogether, my results are in line with recent literature suggesting that SMN is likely a bona fide component of neuronal RNA granules (Tadesse et al., 2008; Hubers et al., 2010; Akten et al., 2011; Fallini et al., 2011; Rossoll et al., 2003). They further indicates that within

those structures, SMN interacts directly with a number of RNA-binding proteins through its Tudor domain, supporting the notion that it might serve as a scaffold to stabilize these complexes and/or serve as a chaperone to promote their assembly.

4.3 SMN is potentially required for the translocation of RNA-binding proteins to RNA granules.

There is growing evidence for the association of SMN with RNA granules. However the role it might play in this specific pathway is largely unknown. The Kosik group has documented a method that can potentially fractionate RNA granules (Krichevsky and Kosik 2001). Precisely, the ultracentrifugation through sucrose density gradient, which is most commonly used to assess polysome profiles, contains in its 'super heavy' fractions RNA granules (Krichevsky and Kosik 2001). The observation of HuD and KSRP, two known components of RNA granules, in these fraction and the drastic increase of the accumulation of these proteins when MN-1 cells were induced to differentiate, supports that these specific fractions contain RNA granules. Importantly, in accordance with the possible function of SMN in mRNP assembly, SMN accumulates in these fractions and as observed for KSRP and HuD, the translocation of SMN to these specific fraction increases upon neuronal differentiation strongly suggesting a possible functional implication of SMN in motor neuron differentiation. Interestingly, in SMA-like condition, the translocation of both HuD and KSRP to these fractions is decreased. In the case of HuD, a fraction of the total HuD protein is still present in these heavy fractions containing RNA granules. It is possible that the pool of SMN still expressed in these knockdown cells is monopolized for the assembly HuD-containing RNA granules. Interestingly, following publication of our

study, Fallini and Colleagues also reported reduced localization of HuD in motor neuron axons in the absence of SMN, using a microscopy approach (Fallini et al., J. Neurosci, 2011). Therefore, these results suggest that SMN plays a determinant role in the assembly of RNA granules and/or promotes the specific recruitment of KSRP and HuD to these structures. However, this does not pin point the specific role of SMN in this process. Gemins, known components of the core SMN complex are found with SMN in neurites of motor neurons (Todd et al. 2010; Zhang et al. 2006), which could suggest that it might act as a molecular chaperone that mediate the assembly of RNA granules, through a mechanism reminiscent of the role the SMN complex plays in snRNP biogenesis. Alternatively, SMN could also be required for the stabilization of RNA granules, which would be compatible with the fact that it actually stays associated with these structures after they are assembled. This might also suggest that SMN could have a more functional role within RNA granules. For example, SMN could be implicated in the transport of RNA granules along the growing neurites, since a link as been made between components of the cytoskeleton and SMA-like defects (Torres-Benito et al. 2011; Wen et al. 2010). Furthermore, SMN could also be implicated in the regulation of local translation within RNA granules and/or at growth cones as our lab has recently shown that SMN can serve as a translational repressor for certain mRNAs (Sanchez et al., HMG, 2012). Taken together, these results strongly suggest that SMN is a major player in the proper assembly, Stability, and/or function of RNA granules present along neurites of motor neuron-derived cells, but clearly, more experiments will be required to start getting an appreciation of the precise molecular mechanisms involved.

Accordingly, some of HuD mRNA targets known to be transported to the growth cones were analysed. GAP-43 and Tau translocation to RNA granules was observed, thus suggesting that some of HuD's targets are part of this specific mRNP complex. As could be expected, when shSMN stable knockdown cells were used, there was a decrease in the presence of these targets in RNA granules. Consistent with the low levels of HuD still present in granules in the absence of SMN, a fraction of these mRNAs are also still present in heavy fractions, strongly suggesting that the localization of these mRNAs within RNA granules is dependent on the interaction between HuD and SMN. However, we cannot rule out the possibility that these targets are also recognized and bound by other RBPs that can transport them to RNA granules even under SMA-like conditions. Strikingly, this represented the first identification of mRNAs mis-regulated in SMA motor neurons besides the well-documented mis-localization of β-actin mRNA (Rossoll et al., 2003). Following publication of our study, Akten and colleagues also identified cpg-15 as a novel mRNA that is mis-regulated in axons of motor neurons in the absence of SMN (Akten et al., PNAS, 2011), and Fallini and Colleagues demonstrated that in fact an overall decrease of the poly(A)+ mRNA signal normally present in motor neuron axons is decreased in SMA-like conditions (Fallini et al. 2011), suggesting a significant number of mRNA targets are indeed mis-regulated in SMA motor neuron axons. Interestingly, it is known that KSRP and HuD recognize ARE motifs present in the 3'untranslated region of their specific mRNA targets and GAP-43, Tau as well as cpg-15 are all known ARE-containing mRNAs (Akten et al. 2011; Hubers et al. 2011; Rossoll et al. 2003a). Thus, it will be interesting to determine if a greater proportion of ARE-containing messages are actually present in RNA granules, and more importantly, if they constitute a major subset of mRNAs mis-regulated in SMA motor neuron axons. Together these results, this strongly suggests that there are

defects in the axonal transport of some of HuD targets and that SMN plays a essential role in this process in motor neurons.

4.4 SERBP1 protein levels decrease in SMA-like conditions.

I have demonstrated that SMN physically interacts with SERBP1 and that this specific interaction localizes to granular foci along axons, thought to be RNA granules since SERBP1 is known to be a constituent of these specific granules (Elvira et al. 2006a). However, for SERBP1, the ultracentrifugation through sucrose density gradients assay was not carried out; therefore we can only speculate that SMN might be implicated in the translocation of SERBP1 into RNA granules as was observed for HuD and KSRP. Nevertheless, it has previously been demonstrated by our laboratory and other groups that the protein levels of some of SMN RBP interacting partners (e.g. KSRP and hnRNP Q) decreased under SMA-like conditions; therefore possibly implicating these specific RBP in the SMA pathology (Helmken et al. 2003; Tadesse et al. 2008). Hence, this could potentially be the case for SERBP1. As expected, in shSMN stable knockdown cell line, which have some of the characteristics of the SMA pathology, there was a significant decrease of SERBP1 compared to the vector control cells, therefore possibly linking SERBP1 to the pathophysiology of SMA. The mRNA levels of SERBP1 were also assessed and even though the levels seem to stay the same in vector control and in shSMN knockdown cells, there was too much variability to obtain a statistically significant result (data not shown), therefore I was not able to conclusively determine at which level the regulation occurs. The decrease in the amount of SERBP1 proteins observed could therefore be at the level of transcription or mRNA stability, but also at the level of either

proteins stability or translational regulation. A conceivable explanation for this decrease could be that SMN is not present to bring additional stabilization to a multi-protein complex containing SERBP1, leading to SERBP1 protein degradation. As mentioned above, it was demonstrated for KSRP and hnRNP Q that in SMA-like conditions the proteins levels of these specific RBPs decrease dramatically (Helmken et al. 2003; Tadesse et al. 2008). Furthermore, our laboratory has uncovered in a whole proteome screen that CARM1, CDK2 and CKAP5 protein levels are up-regulated in SMA-like conditions and that, at least for CARM1, this increase is at the translation level, suggestive of a role for SMN in translational regulation (Sanchez et al., HMG 2012 and unpublished results). Therefore, my work has identified a novel molecular defect in SMA and it will be important in future work to assess the functional consequences of reduced SERBP1 levels and how it might relate to the SMA pathology.

4.5 SERBP1 as a novel regulator of neuronal differentiation.

I was able for the first time, to potentially implicate SERBP1 in the SMA pathology. However, the pathway in which SERBP1 might function in motor neurons that would be affected in SMA still remains unclear. We observed that SERBP1 is capable of inducing neuronal differentiation even in the absence of differentiation stimulus since overexpression of SERBP1 increased the number of neurites double the length of the cell body, the number of cells with branching as well as the average length of neurites. When these transfected cells were induced to differentiate, as expected, SERBP1 did not increase the level of differentiation as drastically as in undifferentiated cells since, for this type of cells, the highest level of differentiation was likely reached already. Hence, this suggests

that SERBP1 potentially plays a role in motor neuron differentiation. Furthermore, a previous graduate student in the laboratory demonstrated that HuD can also induce neuronal differentiation even without differentiation stimulus. Precisely, she showed that over-expression of HuD can increase the percentage of cells with neurites double the length of the cells body and significantly increase p21 mRNA levels which in turn triggers cell cycle exit (Hubers et al. 2011). Taken together, for the first time, we were able to implicate SERBP1 in neuronal differentiation, although further experiments will be needed to gain mechanistic insights into how, and at what level, this effect is mediated.

Strikingly, overexpression of SERBP1 was also able to rescue the neurite outgrowth defects observed in our cell culture model of SMA. It is possible that SERBP1 might be capable of monopolizing the SMN left in these stable knockdown cells and bring it to play its crucial role in motor neuron differentiation. However, SERBP1 might also act downstream of SMN in this specific pathway, and when the level of expression of SERBP1 is increased, it is capable of bypassing SMN and therefore promote neurite outgrowth. In cell culture, SMN has been reported to possibly play a crucial role in neurite outgrowth (McWhorter et al. 2003; Rossoll et al. 2003a; Winkler et al. 2005; Ymlahi-Ouazzani et al. 2010; Zhang et al. 2007a; Zhang et al. 2003); however, *in vivo,* these specific defects are not observed in all animal models. Therefore, it is possible that, *in vivo,* an alternative pathway and/or support system might compensate for this specific defect which leads to a normal elongation of neurites. Nevertheless, motor neurons of SMA patients still die which would imply that another molecular mechanism is defective in motor neurons. Interestingly, SMN potentially plays a crucial role in the formation and function of neuromuscular junctions, since it was observed in SMA models that there was pronounced

synaptic defects. Actually, phosphorylated neurofilament aggregation, altered calcium homeostasis and impaired neurotransmitter release were observed, underlying the importance of SMN in neuromuscular junction activity (Kariya et al. 2008). It was also observed that, under decreased SMN protein levels, presynaptic vesicles are not organized correctly at the nerve terminal (Kariya et al. 2008; Kong et al. 2009) and neuromuscular junction maturation is delayed in SMA model mice (McGovern et al. 2008; Murray et al. 2010). Therefore SMN, apart from its role in snRNP biogenesis, could play an important role in the transport of specific mRNAs within RNA granules to the growth cone leading to defects in neuromuscular junction maturation and maintenance. Thus, the molecular mechanism which leads to motor neuron death in SMA could be linked to defects in mRNA transports which lead to defect in the development, function and maintenance of neuromuscular junction. Together, these results demonstrates that SERBP1 is capable of rescuing neurite outgrowth defects found in SMA-like conditions, and therefore could potentially be a good therapeutic approach for curing SMA.

4.6 Future work

4.6.1 Determination of the effects of over-expression of HuD on a SMA model mouse.

We have demonstrated that a decrease in SMN protein levels affects the translocation of HuD into RNA granules. Furthermore, a sucrose density fractionation assay done on SMN stable knockdown cells over-expressing WT HuD or its methylation mutants demonstrated that HuD can partially rescue SMA-like defects (Hubers et al. 2011). Precisely, the methylation mutant R248K, which mimics a protein that cannot be

methylated by CARM1, shows a significant increase in neurites double the length of the cell body and a drastic increase in the level of p21 demonstrating that the cells are exiting the cell cycle and entering the differentiation process. Furthermore, the defects observed on the translocation of HuD and its mRNA target to the neurites in shSMN knockdown cells, is significantly rescued by over-expression of HuD in MN-1 cells, hence leading us to speculate that HuD might be a very interesting therapeutic approach for SMA. Therefore, a transgenic mouse over-expressing HuD in a SMA-like background could be generated to investigate whether HuD is capable of restoring neuromuscular junction defects, translocation of specific RBPs and their mRNA targets to growth cones and possibly other defects found in severe SMA mice. Thus, this work could help shed light on novel functions of HuD as well as provide information on a possible novel therapeutic approach that could help relieve symptoms of SMA or even help finding a cure for this devastating disease.

4.6.2 Determination of the function of SERBP1 in motor neurons.

SERBP1 is an RNA-binding protein for which the precise cellular function remains unknown. Furthermore, not much is known about the mRNA targets that SERBP1 regulates and how it might regulate them. We report here that SERBP1 is a novel interacting protein of SMN and that over-expression of SERBP1 can induce neuronal differentiation and can also rescue SMA-like neuronal defects observed in our cell culture model of the disease. Therefore further experiments could be done to investigate the specific contribution of SERBP1 in the SMA pathology. First, an ultracentrifugation through sucrose density gradients experiment could be done on vector control and shSMN stable knockdown MN-1

cells. This would clarify whether, like HuD and KSRP, SERBP1 could present translocation defects to RNA granules under SMA-like conditions, hence demonstrating that it is possible that numerous or all RBPs implicated in the translocation of mRNA to growth cones present these specific defects in SMA-like conditions. Furthermore, a 'RIP-Seq' or 'CLIP-Seq' experiment could be done to identify SERBP1 mRNA targets in motor neurons. The mRNA targets could next be screened for possible implication in neuronal differentiation, and a sucrose gradient fractionation experiment could be done in vector control and shSMN stable knockdown MN-1 cells to see if these targets are also presenting translocation defects in the face of low levels of SMN. Taken together, these experiments would potentially give us information on the targets of SERBP1 and their implication in neuronal differentiation. Additionally, this could identify some novel therapeutic targets that are mis-regulated in SMA conditions.

4.7 Conclusion

We have identified two RNA-binding proteins, HuD and SERBP1, that interact with the causative gene for SMA, SMN in axons of motoneuron-like cells. Furthermore, we have shown that SMN is required for the proper translocation of HuD and at least some of its mRNA targets in axonal RNA granules. In contrast, SMN is required for maintaining normal protein levels of SERBP1. Strikingly, over-expression of either of these proteins can rescue SMA-like axonal defects underlying the potential therapeutic benefits of these RNA-binding proteins for the treatment of SMA. The findings presented in this thesis support our initial hypothesis and the objectives were fully fulfilled. The novel function, in which SMN is hypothesized to contribute, should help the scientific community understand

the specificity of the pathology on motor neuron and help develop novel therapeutic approaches for the treatment of SMA. My work has supported growing evidence on the role of SMN in neuronal mRNP assembly and/or translocation and has paved the road for future, more mechanistic studies.

References

Akamatsu W, Fujihara H, Mitsuhashi T, Yano M, Shibata S, Hayakawa Y, Okano HJ, Sakakibara S, Takano H, Takano T, Takahashi T, Noda T, Okano H (2005) The RNA-binding protein HuD regulates neuronal cell identity and maturation. Proc Natl Acad Sci U S A 102:4625-4630.

Akten B, Kye MJ, Hao le T, Wertz MH, Singh S, Nie D, Huang J, Merianda TT, Twiss JL, Beattie CE, Steen JA, Sahin M (2011) Interaction of survival of motor neuron (SMN) and HuD proteins with mRNA cpg15 rescues motor neuron axonal deficits. Proc Natl Acad Sci U S A 108:10337-10342.

Anderson KD, Merhege MA, Morin M, Bolognani F, Perrone-Bizzozero NI (2003) Increased expression and localization of the RNA-binding protein HuD and GAP-43 mRNA to cytoplasmic granules in DRG neurons during nerve regeneration. Exp Neurol 183:100-108.

Anderson KD, Sengupta J, Morin M, Neve RL, Valenzuela CF, Perrone-Bizzozero NI (2001) Overexpression of HuD accelerates neurite outgrowth and increases GAP-43 mRNA expression in cortical neurons and retinoic acid-induced embryonic stem cells in vitro. Exp Neurol 168:250-258.

Anderson KD, Morin MA, Beckel-Mitchener A, Mobarak CD, Neve RL, Furneaux HM, Burry R, Perrone-Bizzozero NI (2000) Overexpression of HuD, but not of its truncated form HuD I+II, promotes GAP-43 gene expression and neurite outgrowth in PC12 cells in the absence of nerve growth factor. J Neurochem 75:1103-1114.

Antic D, Keene JD (1998) Messenger ribonucleoprotein complexes containing human ELAV proteins: interactions with cytoskeleton and translational apparatus. J Cell Sci 111 (Pt 2):183-197.

Antic D, Keene JD (1997) Embryonic lethal abnormal visual RNA-binding proteins involved in growth, differentiation, and posttranscriptional gene expression. Am J Hum Genet 61:273-278.

Aranda-Abreu GE, Behar L, Chung S, Furneaux H, Ginzburg I (1999) Embryonic lethal abnormal vision-like RNA-binding proteins regulate neurite outgrowth and tau expression in PC12 cells. J Neurosci 19:6907-6917.

Aronov S, Aranda G, Behar L, Ginzburg I (2002) Visualization of translated tau protein in the axons of neuronal P19 cells and characterization of tau RNP granules. J Cell Sci 115:3817-3827.

Barreau C, Paillard L, Osborne HB (2006) AU-rich elements and associated factors: are there unifying principles?. Nucleic Acids Res 33:7138-7150.

Barth S, Liss M, Voss MD, Dobner T, Fischer U, Meister G, Grasser FA (2003) Epstein-Barr virus nuclear antigen 2 binds via its methylated arginine-glycine repeat to the survival motor neuron protein. J Virol 77:5008-5013.

Baumer D, Lee S, Nicholson G, Davies JL, Parkinson NJ, Murray LM, Gillingwater TH, Ansorge O, Davies KE, Talbot K (2009) Alternative splicing events are a late feature of pathology in a mouse model of spinal muscular atrophy. PLoS Genet 5:e1000773.

Bedford MT (2007) Arginine methylation at a glance. J Cell Sci 120:4243-4246.

Bedford MT, Richard S (2005) Arginine methylation an emerging regulator of protein function. Mol Cell 18:263-272.

Bedford MT, Frankel A, Yaffe MB, Clarke S, Leder P, Richard S (2000) Arginine methylation inhibits the binding of proline-rich ligands to Src homology 3, but not WW, domains. J Biol Chem 275:16030-16036.

Boulisfane N, Choleza M, Rage F, Neel H, Soret J, Bordonne R (2011) Impaired minor tri-snRNP assembly generates differential splicing defects of U12-type introns in lymphoblasts derived from a type I SMA patient. Hum Mol Genet 20:641-648.

Bowerman M, Shafey D, Kothary R (2007) Smn depletion alters profilin II expression and leads to upregulation of the RhoA/ROCK pathway and defects in neuronal integrity. J Mol Neurosci 32:120-131.

Brahms H, Meheus L, de Brabandere V, Fischer U, Luhrmann R (2001) Symmetrical dimethylation of arginine residues in spliceosomal Sm protein B/B' and the Sm-like protein LSm4, and their interaction with the SMN protein. RNA 7:1531-1542.

Briese M, Esmaeili B, Sattelle DB (2005) Is spinal muscular atrophy the result of defects in motor neuron processes?. Bioessays 27:946-957.

Brzustowicz LM, Lehner T, Castilla LH, Penchaszadeh GK, Wilhelmsen KC, Daniels R, Davies KE, Leppert M, Ziter F, Wood D (1990) Genetic mapping of chronic childhood-onset spinal muscular atrophy to chromosome 5q11.2-13.3. Nature 344:540-541.

BYERS RK, BANKER BQ (1961) Infantile muscular atrophy. Arch Neurol 5:140-164.

Calvanese V, Lara E, Suarez-Alvarez B, Abu Dawud R, Vazquez-Chantada M, Martinez-Chantar ML, Embade N, Lopez-Nieva P, Horrillo A, Hmadcha A, Soria B, Piazzolla D, Herranz D, Serrano M, Mato JM, Andrews PW, Lopez-Larrea C, Esteller M, Fraga MF (2010) Sirtuin 1 regulation of developmental genes during differentiation of stem cells. Proc Natl Acad Sci U S A 107:13736-13741.

Campion Y, Neel H, Gostan T, Soret J, Bordonne R (2010) Specific splicing defects in S. pombe carrying a degron allele of the Survival of Motor Neuron gene. EMBO J 29:1817-1829.

Cartegni L, Krainer AR (2002) Disruption of an SF2/ASF-dependent exonic splicing enhancer in SMN2 causes spinal muscular atrophy in the absence of SMN1. Nat Genet 30:377-384.

Carvalho T, Almeida F, Calapez A, Lafarga M, Berciano MT, Carmo-Fonseca M (1999) The spinal muscular atrophy disease gene product, SMN: A link between snRNP biogenesis and the Cajal (coiled) body. J Cell Biol 147:715-728.

Cauchi RJ (2010) SMN and Gemins: 'we are family' ... or are we?: insights into the partnership between Gemins and the spinal muscular atrophy disease protein SMN. Bioessays 32:1077-1089.

Chagnovich D, Fayos BE, Cohn SL (1996) Differential activity of ELAV-like RNA-binding proteins in human neuroblastoma. J Biol Chem 271:33587-33591.

Chari A, Golas MM, Klingenhager M, Neuenkirchen N, Sander B, Englbrecht C, Sickmann A, Stark H, Fischer U (2008) An assembly chaperone collaborates with the SMN complex to generate spliceosomal SnRNPs. Cell 135:497-509.

Chen D, Ma H, Hong H, Koh SS, Huang SM, Schurter BT, Aswad DW, Stallcup MR (1999) Regulation of transcription by a protein methyltransferase. Science 284:2174-2177.

Cheng D, Cote J, Shaaban S, Bedford MT (2007) The arginine methyltransferase CARM1 regulates the coupling of transcription and mRNA processing. Mol Cell 25:71-83.

Chung S, Eckrich M, Perrone-Bizzozero N, Kohn DT, Furneaux H (1997) The Elav-like proteins bind to a conserved regulatory element in the 3'-untranslated region of GAP-43 mRNA. J Biol Chem 272:6593-6598.

Cimato TR, Ettinger MJ, Zhou X, Aletta JM (1997) Nerve growth factor-specific regulation of protein methylation during neuronal differentiation of PC12 cells. J Cell Biol 138:1089-1103.

Coady TH, Lorson CL (2011) SMN in spinal muscular atrophy and snRNP biogenesis. Wiley Interdiscip Rev RNA 2(4):546-564.

Coovert DD, Le TT, McAndrew PE, Strasswimmer J, Crawford TO, Mendell JR, Coulson SE, Androphy EJ, Prior TW, Burghes AH (1997) The survival motor neuron protein in spinal muscular atrophy. Hum Mol Genet 6:1205-1214.

Cote J, Richard S (2005) Tudor domains bind symmetrical dimethylated arginines. J Biol Chem 280:28476-28483.

Dalmau J, Furneaux HM, Gralla RJ, Kris MG, Posner JB (1990) Detection of the anti-Hu antibody in the serum of patients with small cell lung cancer--a quantitative western blot analysis. Ann Neurol 27:544-552.

Deschenes-Furry J, Perrone-Bizzozero N, Jasmin BJ (2006) The RNA-binding protein HuD: a regulator of neuronal differentiation, maintenance and plasticity. Bioessays 28:822-833.

Deschenes-Furry J, Belanger G, Perrone-Bizzozero N, Jasmin BJ (2003) Post-transcriptional regulation of acetylcholinesterase mRNAs in nerve growth factor-treated PC12 cells by the RNA-binding protein HuD. J Biol Chem 278:5710-5717.

Elvira G, Wasiak S, Blandford V, Tong XK, Serrano A, Fan X, del Rayo Sanchez-Carbente M, Servant F, Bell AW, Boismenu D, Lacaille JC, McPherson PS, DesGroseillers L, Sossin WS (2006a) Characterization of an RNA granule from developing brain. Mol Cell Proteomics 5:635-651.

Elvira G, Wasiak S, Blandford V, Tong XK, Serrano A, Fan X, del Rayo Sanchez-Carbente M, Servant F, Bell AW, Boismenu D, Lacaille JC, McPherson PS, DesGroseillers L, Sossin WS (2006b) Characterization of an RNA granule from developing brain. Mol Cell Proteomics 5:635-651.

Fallini C, Zhang H, Su Y, Silani V, Singer RH, Rossoll W, Bassell GJ (2011) The survival of motor neuron (SMN) protein interacts with the mRNA-binding protein HuD and regulates localization of poly(A) mRNA in primary motor neuron axons. J Neurosci 31:3914-3925.

Fallini C, Bassell GJ, Rossoll W (2010) High-efficiency transfection of cultured primary motor neurons to study protein localization, trafficking, and function. Mol Neurodegener 5:17.

Feldkotter M, Schwarzer V, Wirth R, Wienker TF, Wirth B (2002) Quantitative analyses of SMN1 and SMN2 based on real-time lightCycler PCR: fast and highly reliable carrier testing and prediction of severity of spinal muscular atrophy. Am J Hum Genet 70:358-368.

Fialcowitz-White EJ, Brewer BY, Ballin JD, Willis CD, Toth EA, Wilson GM (2007) Specific protein domains mediate cooperative assembly of HuR oligomers on AU-rich mRNA-destabilizing sequences. J Biol Chem 282:20948-20959.

Figueroa A, Cuadrado A, Fan J, Atasoy U, Muscat GE, Munoz-Canoves P, Gorospe M, Munoz A (2003) Role of HuR in skeletal myogenesis through coordinate regulation of muscle differentiation genes. Mol Cell Biol 23:4991-5004.

Fujiwara T, Fukao A, Sasano Y, Matsuzaki H, Kikkawa U, Imataka H, Inoue K, Endo S, Sonenberg N, Thoma C, Sakamoto H (2012) Functional and direct interaction between the RNA binding protein HuD and active Akt1. Nucleic Acids Res 40:1944-1953.

Fujiwara T, Mori Y, Chu DL, Koyama Y, Miyata S, Tanaka H, Yachi K, Kubo T, Yoshikawa H, Tohyama M (2006) CARM1 regulates proliferation of PC12 cells by methylating HuD. Mol Cell Biol 26:2273-2285.

Fukao A, Sasano Y, Imataka H, Inoue K, Sakamoto H, Sonenberg N, Thoma C, Fujiwara T (2009) The ELAV protein HuD stimulates cap-dependent translation in a Poly(A)- and eIF4A-dependent manner. Mol Cell 36:1007-1017.

Gabanella F, Butchbach ME, Saieva L, Carissimi C, Burghes AH, Pellizzoni L (2007) Ribonucleoprotein assembly defects correlate with spinal muscular atrophy severity and preferentially affect a subset of spliceosomal snRNPs. PLoS One 2:e921.

Gabanella F, Carissimi C, Usiello A, Pellizzoni L (2005) The activity of the spinal muscular atrophy protein is regulated during development and cellular differentiation. Hum Mol Genet 14:3629-3642.

Giavazzi A, Setola V, Simonati A, Battaglia G (2006) Neuronal-specific roles of the survival motor neuron protein: evidence from survival motor neuron expression patterns in the developing human central nervous system. J Neuropathol Exp Neurol 65:267-277.

Goulet I, Boisvenue S, Mokas S, Mazroui R, Cote J (2008) TDRD3, a novel Tudor domain-containing protein, localizes to cytoplasmic stress granules. Hum Mol Genet 17:3055-3074.

Grohmann K, Schuelke M, Diers A, Hoffmann K, Lucke B, Adams C, Bertini E, Leonhardt-Horti H, Muntoni F, Ouvrier R, Pfeufer A, Rossi R, Van Maldergem L, Wilmshurst JM, Wienker TF, Sendtner M, Rudnik-Schoneborn S, Zerres K, Hubner C (2001) Mutations in the gene encoding immunoglobulin mu-binding protein 2 cause spinal muscular atrophy with respiratory distress type 1. Nat Genet 29:75-77.

Heaton JH, Dlakic WM, Dlakic M, Gelehrter TD (2001) Identification and cDNA cloning of a novel RNA-binding protein that interacts with the cyclic nucleotide-responsive sequence in the Type-1 plasminogen activator inhibitor mRNA. J Biol Chem 276:3341-3347.

Hebert MD, Shpargel KB, Ospina JK, Tucker KE, Matera AG (2002) Coilin methylation regulates nuclear body formation. Dev Cell 3:329-337.

Helmken C, Hofmann Y, Schoenen F, Oprea G, Raschke H, Rudnik-Schoneborn S, Zerres K, Wirth B (2003) Evidence for a modifying pathway in SMA discordant families: reduced SMN level decreases the amount of its interacting partners and Htra2-beta1. Hum Genet 114:11-21.

Hinman MN, Lou H (2008) Diverse molecular functions of Hu proteins. Cell Mol Life Sci 65:3168-3181.

Hoffman J (1892) Ueber chronische spinal muskelatrophie im kindesalter auf familiarer basis. Dtsch Z Nervenheilkd 3:427-470.

Hubers L, Valderrama-Carvajal H, Laframboise J, Timbers J, Sanchez G, Cote J (2011) HuD interacts with survival motor neuron protein and can rescue spinal muscular atrophy-like neuronal defects. Hum Mol Genet 20:553-579.

Jodelka FM, Ebert AD, Duelli DM, Hastings ML (2010) A feedback loop regulates splicing of the spinal muscular atrophy-modifying gene, SMN2. Hum Mol Genet 19:4906-4917.

Kariya S, Park GH, Maeno-Hikichi Y, Leykekhman O, Lutz C, Arkovitz MS, Landmesser LT, Monani UR (2008) Reduced SMN protein impairs maturation of the neuromuscular junctions in mouse models of spinal muscular atrophy. Hum Mol Genet 17:2552-2569.

Kasashima K, Sakashita E, Saito K, Sakamoto H (2002) Complex formation of the neuron-specific ELAV-like Hu RNA-binding proteins. Nucleic Acids Res 30:4519-4526.

Kasashima K, Terashima K, Yamamoto K, Sakashita E, Sakamoto H (1999) Cytoplasmic localization is required for the mammalian ELAV-like protein HuD to induce neuronal differentiation. Genes Cells 4:667-683.

Kashima T, Manley JL (2003) A negative element in SMN2 exon 7 inhibits splicing in spinal muscular atrophy. Nat Genet 34:460-463.

Kerppola TK (2009) Visualization of molecular interactions using bimolecular fluorescence complementation analysis: characteristics of protein fragment complementation. Chem Soc Rev 38:2876-2886.

Kerppola TK (2006) Design and implementation of bimolecular fluorescence complementation (BiFC) assays for the visualization of protein interactions in living cells. Nat Protoc 1:1278-1286.

Khoo B, Akker SA, Chew SL (2003) Putting some spine into alternative splicing. Trends Biotechnol 21 (8):328-330.

Kiebler MA, Bassell GJ (2006) Neuronal RNA granules: movers and makers. Neuron 51:685-690.

Kim J, Daniel J, Espejo A, Lake A, Krishna M, Xia L, Zhang Y, Bedford MT (2006) Tudor, MBT and chromo domains gauge the degree of lysine methylation. EMBO Rep 7:397-403.

Kobarg J, Schnittger S, Fonatsch C, Lemke H, Bowen MA, Buck F, Hansen HP (1997) Characterization, mapping and partial cDNA sequence of the 57-kD intracellular Ki-1 antigen. Exp Clin Immunogenet 14:273-280.

Kong L, Wang X, Choe DW, Polley M, Burnett BG, Bosch-Marce M, Griffin JW, Rich MM, Sumner CJ (2009) Impaired synaptic vesicle release and immaturity of neuromuscular junctions in spinal muscular atrophy mice. J Neurosci 29:842-851.

Krichevsky AM, Kosik KS (2001) Neuronal RNA granules: a link between RNA localization and stimulation-dependent translation. Neuron 32:683-696.

Lal A, Mazan-Mamczarz K, Kawai T, Yang X, Martindale JL, Gorospe M (2004) Concurrent versus individual binding of HuR and AUF1 to common labile target mRNAs. EMBO J 23:3092-3102.

Lee EK (2012) Post-translational Modifications of RNA-Binding Proteins and their Roles in RNA Granules. Curr Protein Pept Sci 13:331-336.

Lee YJ, Hsieh WY, Chen LY, Li C (2012) Protein arginine methylation of SERBP1 by protein arginine methyltransferase 1 affects cytoplasmic/nuclear distribution. J Cell Biochem 113:2721-2728.

Lefebvre S, Burglen L, Frezal J, Munnich A, Melki J (1998) The role of the SMN gene in proximal spinal muscular atrophy. Hum Mol Genet 7:1531-1536.

Lefebvre S, Burlet P, Liu Q, Bertrandy S, Clermont O, Munnich A, Dreyfuss G, Melki J (1997) Correlation between severity and SMN protein level in spinal muscular atrophy. Nat Genet 16:265-269.

Lefebvre S, Burglen L, Reboullet S, Clermont O, Burlet P, Viollet L, Benichou B, Cruaud C, Millasseau P, Zeviani M (1995) Identification and characterization of a spinal muscular atrophy-determining gene. Cell 80:155-165.

Liu Q, Fischer U, Wang F, Dreyfuss G (1997) The spinal muscular atrophy disease gene product, SMN, and its associated protein SIP1 are in a complex with spliceosomal snRNP proteins. Cell 90:1013-1021.

Liu Q, Dreyfuss G (1996) A novel nuclear structure containing the survival of motor neurons protein. EMBO J 15:3555-3565.

Liu-Yesucevitz L, Bassell GJ, Gitler AD, Hart AC, Klann E, Richter JD, Warren ST, Wolozin B (2011) Local RNA translation at the synapse and in disease. J Neurosci 31:16086-16093.

Lorson CL, Strasswimmer J, Yao JM, Baleja JD, Hahnen E, Wirth B, Le T, Burghes AH, Androphy EJ (1998) SMN oligomerization defect correlates with spinal muscular atrophy severity. Nat Genet 19:63-66.

McAndrew PE, Parsons DW, Simard LR, Rochette C, Ray PN, Mendell JR, Prior TW, Burghes AH (1997) Identification of proximal spinal muscular atrophy carriers and patients by analysis of SMNT and SMNC gene copy number. Am J Hum Genet 60:1411-1422.

McGovern VL, Gavrilina TO, Beattie CE, Burghes AH (2008) Embryonic motor axon development in the severe SMA mouse. Hum Mol Genet 17:2900-2909.

McWhorter ML, Monani UR, Burghes AH, Beattie CE (2003) Knockdown of the survival motor neuron (Smn) protein in zebrafish causes defects in motor axon outgrowth and pathfinding. J Cell Biol 162:919-931.

Meister G, Eggert C, Buhler D, Brahms H, Kambach C, Fischer U (2001) Methylation of Sm proteins by a complex containing PRMT5 and the putative U snRNP assembly factor pICln. Curr Biol 11:1990-1994.

Melki J (1997) Spinal muscular atrophy. Curr Opin Neurol 10:381-385.

Mobarak CD, Anderson KD, Morin M, Beckel-Mitchener A, Rogers SL, Furneaux H, King P, Perrone-Bizzozero NI (2000) The RNA-binding protein HuD is required for GAP-43 mRNA stability, GAP-43 gene expression, and PKC-dependent neurite outgrowth in PC12 cells. Mol Biol Cell 11:3191-3203.

Mohaghegh P, Rodrigues NR, Owen N, Ponting CP, Le TT, Burghes AH, Davies KE (1999) Analysis of mutations in the tudor domain of the survival motor neuron protein SMN. Eur J Hum Genet 7:519-525.

Monani UR (2005) Spinal muscular atrophy: a deficiency in a ubiquitous protein; a motor neuron-specific disease. Neuron 48:885-896.

Mouaikel J, Narayanan U, Verheggen C, Matera AG, Bertrand E, Tazi J, Bordonne R (2003) Interaction between the small-nuclear-RNA cap hypermethylase and the spinal muscular atrophy protein, survival of motor neuron. EMBO Rep 4:616-622.

Mowen KA, Tang J, Zhu W, Schurter BT, Shuai K, Herschman HR, David M (2001) Arginine methylation of STAT1 modulates IFNalpha/beta-induced transcription. Cell 104:731-741.

Murray LM, Lee S, Baumer D, Parson SH, Talbot K, Gillingwater TH (2010) Pre-symptomatic development of lower motor neuron connectivity in a mouse model of severe spinal muscular atrophy. Hum Mol Genet 19:420-433.

Najbauer J, Johnson BA, Young AL, Aswad DW (1993) Peptides with sequences similar to glycine, arginine-rich motifs in proteins interacting with RNA are efficiently recognized by methyltransferase(s) modifying arginine in numerous proteins. J Biol Chem 268:10501-10509.

Narayanan U, Achsel T, Luhrmann R, Matera AG (2004) Coupled in vitro import of U snRNPs and SMN, the spinal muscular atrophy protein. Mol Cell 16:223-234.

Ogawa C, Usui K, Ito F, Itoh M, Hayashizaki Y, Suzuki H (2009) Role of survival motor neuron complex components in small nuclear ribonucleoprotein assembly. J Biol Chem 284:14609-14617.

Okano HJ, Darnell RB (1997) A hierarchy of Hu RNA binding proteins in developing and adult neurons. J Neurosci 17:3024-3037.

Otter S, Grimmler M, Neuenkirchen N, Chari A, Sickmann A, Fischer U (2007) A comprehensive interaction map of the human survival of motor neuron (SMN) complex. J Biol Chem 282:5825-5833.

Pagliardini S, Giavazzi A, Setola V, Lizier C, Di Luca M, DeBiasi S, Battaglia G (2000) Subcellular localization and axonal transport of the survival motor neuron (SMN) protein in the developing rat spinal cord. Hum Mol Genet 9:47-56.

Pahlich S, Zakaryan RP, Gehring H (2006) Protein arginine methylation: Cellular functions and methods of analysis. Biochim Biophys Acta 1764:1890-1903.

Pascale A, Gusev PA, Amadio M, Dottorini T, Govoni S, Alkon DL, Quattrone A (2004) Increase of the RNA-binding protein HuD and posttranscriptional up-regulation of the GAP-43 gene during spatial memory. Proc Natl Acad Sci U S A 101:1217-1222.

Pearn J (1980) Classification of spinal muscular atrophies. Lancet 1:919-922.

Pellizzoni L (2007) Chaperoning ribonucleoprotein biogenesis in health and disease. EMBO Rep 8:340-345.

Pellizzoni L, Kataoka N, Charroux B, Dreyfuss G (1998) A novel function for SMN, the spinal muscular atrophy disease gene product, in pre-mRNA splicing. Cell 95:615-624.

Perrone-Bizzozero N, Bolognani F (2002) Role of HuD and other RNA-binding proteins in neural development and plasticity. J Neurosci Res 68:121-126.

Piazzon N, Rage F, Schlotter F, Moine H, Branlant C, Massenet S (2008) In vitro and in cellulo evidences for association of the survival of motor neuron complex with the fragile X mental retardation protein. J Biol Chem 283:5598-5610.

Prigge JR, Iverson SV, Siders AM, Schmidt EE (2009) Interactome for auxiliary splicing factor U2AF(65) suggests diverse roles. Biochim Biophys Acta 1789:487-492.

Quattrone A, Pascale A, Nogues X, Zhao W, Gusev P, Pacini A, Alkon DL (2001) Posttranscriptional regulation of gene expression in learning by the neuronal ELAV-like mRNA-stabilizing proteins. Proc Natl Acad Sci U S A 98:11668-11673.

Renvoise B, Khoobarry K, Gendron MC, Cibert C, Viollet L, Lefebvre S (2006) Distinct domains of the spinal muscular atrophy protein SMN are required for targeting to Cajal bodies in mammalian cells. J Cell Sci 119:680-692.

Roberts DF, Chavez J, Court SD (1970) The genetic component in child mortality. Arch Dis Child 45:33-38.

Robinow S, Campos AR, Yao KM, White K (1988) The elav gene product of Drosophila, required in neurons, has three RNP consensus motifs. Science 242:1570-1572.

Rossoll W, Jablonka S, Andreassi C, Kroning AK, Karle K, Monani UR, Sendtner M (2003a) Smn, the spinal muscular atrophy-determining gene product, modulates axon growth and localization of beta-actin mRNA in growth cones of motoneurons. J Cell Biol 163:801-812.

Rossoll W, Jablonka S, Andreassi C, Kroning AK, Karle K, Monani UR, Sendtner M (2003b) Smn, the spinal muscular atrophy-determining gene product, modulates axon growth and localization of beta-actin mRNA in growth cones of motoneurons. J Cell Biol 163:801-812.

Ruggiu M, McGovern VL, Lotti F, Saieva L, Li DK, Kariya S, Monani UR, Burghes AH, Pellizzoni L (2012) A role for SMN exon 7 splicing in the selective vulnerability of motor neurons in spinal muscular atrophy. Mol Cell Biol 32:126-138.

Sambuughin N, Sivakumar K, Selenge B, Lee HS, Friedlich D, Baasanjav D, Dalakas MC, Goldfarb LG (1998) Autosomal dominant distal spinal muscular atrophy type V (dSMA-V) and Charcot-Marie-Tooth disease type 2D (CMT2D) segregate within a single large kindred and map to a refined region on chromosome 7p15. J Neurol Sci 161:23-28.

Schuman EM (1999) mRNA trafficking and local protein synthesis at the synapse. Neuron 23:645-648.

Selenko P, Sprangers R, Stier G, Buhler D, Fischer U, Sattler M (2001) SMN tudor domain structure and its interaction with the Sm proteins. Nat Struct Biol 8:27-31.

Setola V, Terao M, Locatelli D, Bassanini S, Garattini E, Battaglia G (2007) Axonal-SMN (a-SMN), a protein isoform of the survival motor neuron gene, is specifically involved in axonogenesis. Proc Natl Acad Sci U S A 104:1959-1964.

Sharma A, Lambrechts A, Hao le T, Le TT, Sewry CA, Ampe C, Burghes AH, Morris GE (2005) A role for complexes of survival of motor neurons (SMN) protein with gemins and profilin in neurite-like cytoplasmic extensions of cultured nerve cells. Exp Cell Res 309:185-197.

Smith CL, Afroz R, Bassell GJ, Furneaux HM, Perrone-Bizzozero NI, Burry RW (2004) GAP-43 mRNA in growth cones is associated with HuD and ribosomes. J Neurobiol 61:222-235.

Tadesse H, Deschenes-Furry J, Boisvenue S, Cote J (2008) KH-type splicing regulatory protein interacts with survival motor neuron protein and is misregulated in spinal muscular atrophy. Hum Mol Genet 17:506-524.

Todd AG, Shaw DJ, Morse R, Stebbings H, Young PJ (2010) SMN and the Gemin proteins form sub-complexes that localise to both stationary and dynamic neurite granules. Biochem Biophys Res Commun 394:211-216.

Torres-Benito L, Neher MF, Cano R, Ruiz R, Tabares L (2011) SMN requirement for synaptic vesicle, active zone and microtubule postnatal organization in motor nerve terminals. PLoS One 6:e26164.

van Bergeijk J, Rydel-Konecke K, Grothe C, Claus P (2007) The spinal muscular atrophy gene product regulates neurite outgrowth: importance of the C terminus. FASEB J 21:1492-1502.

van der Vleuten AJ, van Ravenswaaij-Arts CM, Frijns CJ, Smits AP, Hageman G, Padberg GW, Kremer H (1998) Localisation of the gene for a dominant congenital spinal muscular atrophy predominantly affecting the lower limbs to chromosome 12q23-q24. Eur J Hum Genet 6:376-382.

Viollet L, Barois A, Rebeiz JG, Rifai Z, Burlet P, Zarhrate M, Vial E, Dessainte M, Estournet B, Kleinknecht B, Pearn J, Adams RD, Urtizberea JA, Cros DP, Bushby K, Munnich A, Lefebvre S (2002) Mapping of autosomal recessive chronic distal spinal muscular atrophy to chromosome 11q13. Ann Neurol 51:585-592.

Wan L, Battle DJ, Yong J, Gubitz AK, Kolb SJ, Wang J, Dreyfuss G (2005) The survival of motor neurons protein determines the capacity for snRNP assembly: biochemical deficiency in spinal muscular atrophy. Mol Cell Biol 25:5543-5551.

Wang H, Molfenter J, Zhu H, Lou H (2010) Promotion of exon 6 inclusion in HuD pre-mRNA by Hu protein family members. Nucleic Acids Res 38:3760-3770.

Wang H, Huang ZQ, Xia L, Feng Q, Erdjument-Bromage H, Strahl BD, Briggs SD, Allis CD, Wong J, Tempst P, Zhang Y (2001) Methylation of histone H4 at arginine 3 facilitating transcriptional activation by nuclear hormone receptor. Science 293:853-857.

Wein G, Rossler M, Klug R, Herget T (2003) The 3'-UTR of the mRNA coding for the major protein kinase C substrate MARCKS contains a novel CU-rich element interacting with the mRNA stabilizing factors HuD and HuR. Eur J Biochem 270:350-365.

Wen HL, Lin YT, Ting CH, Lin-Chao S, Li H, Hsieh-Li HM (2010) Stathmin, a microtubule-destabilizing protein, is dysregulated in spinal muscular atrophy. Hum Mol Genet 19:1766-1778.

Werdnig G (1892) Zwei Fruhinfantile hereditare falle von progressiver muskelatrophie unter dem bilde der dystrophie, ager auf neurotischer grunglace. Arch Psychiatr 22:437-481.

Winkler C, Eggert C, Gradl D, Meister G, Giegerich M, Wedlich D, Laggerbauer B, Fischer U (2005) Reduced U snRNP assembly causes motor axon degeneration in an animal model for spinal muscular atrophy. Genes Dev 19:2320-2330.

Wolf SS (2009) The protein arginine methyltransferase family: an update about function, new perspectives and the physiological role in human. Cell Mol Life Sci 66:2109-2121.

Wolstencroft EC, Mattis V, Bajer AA, Young PJ, Lorson CL (2005) A non-sequence-specific requirement for SMN protein activity: the role of aminoglycosides in inducing elevated SMN protein levels. Hum Mol Genet 14:1199-1210.

Xie B, Invernizzi CF, Richard S, Wainberg MA (2007) Arginine methylation of the human immunodeficiency virus type 1 Tat protein by PRMT6 negatively affects Tat Interactions with both cyclin T1 and the Tat transactivation region. J Virol 81:4226-4234.

Ymlahi-Ouazzani Q, J Bronchain O, Paillard E, Ballagny C, Chesneau A, Jadaud A, Mazabraud A, Pollet N (2010) Reduced levels of survival motor neuron protein leads to aberrant motoneuron growth in a Xenopus model of muscular atrophy. Neurogenetics 11:27-40.

Yong J, Kasim M, Bachorik JL, Wan L, Dreyfuss G (2010) Gemin5 delivers snRNA precursors to the SMN complex for snRNP biogenesis. Mol Cell 38:551-562.

Young PJ, Man NT, Lorson CL, Le TT, Androphy EJ, Burghes AH, Morris GE (2000) The exon 2b region of the spinal muscular atrophy protein, SMN, is involved in self-association and SIP1 binding. Hum Mol Genet 9:2869-2877.

Yun CY, Fu XD (2000) Conserved SR protein kinase functions in nuclear import and its action is counteracted by arginine methylation in Saccharomyces cerevisiae. J Cell Biol 150:707-718.

Zhang H, Xing L, Singer RH, Bassell GJ (2007a) QNQKE targeting motif for the SMN-Gemin multiprotein complexin neurons. J Neurosci Res 85:2657-2667.

Zhang H, Xing L, Singer RH, Bassell GJ (2007b) QNQKE targeting motif for the SMN-Gemin multiprotein complexin neurons. J Neurosci Res 85:2657-2667.

Zhang H, Xing L, Rossoll W, Wichterle H, Singer RH, Bassell GJ (2006) Multiprotein complexes of the survival of motor neuron protein SMN with Gemins traffic to neuronal processes and growth cones of motor neurons. J Neurosci 26:8622-8632.

Zhang HL, Pan F, Hong D, Shenoy SM, Singer RH, Bassell GJ (2003) Active transport of the survival motor neuron protein and the role of exon-7 in cytoplasmic localization. J Neurosci 23:6627-6637.

Zhang R, So BR, Li P, Yong J, Glisovic T, Wan L, Dreyfuss G (2011) Structure of a key intermediate of the SMN complex reveals Gemin2's crucial function in snRNP assembly. Cell 146:384-395.

Zhang Z, Lotti F, Dittmar K, Younis I, Wan L, Kasim M, Dreyfuss G (2008) SMN deficiency causes tissue-specific perturbations in the repertoire of snRNAs and widespread defects in splicing. Cell 133:585-600.

Appendix 1:

	GAPDH	γ-actin	β-actin	GAP-43	Tau
Initialization	98 ºC: 2 min	94 ºC: 3 min	94 ºC: 4 min	94 ºC: 5 min	94 ºC: 3 min
Denaturation	95 ºC: 30 sec	94 ºC: 30 sec	94 ºC: 1 min	94 ºC: 1 min	94 ºC: 30 sec
Annealing	60 ºC: 30 sec	64 ºC: 30 sec	60 ºC: 1 min	56.5ºC: 1 min	50 ºC: 30 sec
Extension /elongation	72ºC : 30 sec	72ºC : 1.5 min	72ºC : 1 min	72ºC : 1 min	72 ºC : 30 sec
	19 cycles of steps 2 to 4.	4 cycles of steps 2 to 4.	31 cycles of steps 2 to 4.	32 cycles of step 2 to 4.	29 cycles of steps 2 to 4.
Final elongation	72ºC: 10 min	94 ºC: 30 sec	72 ºC: 10 min	72ºC: 10 min	72 ºC: 10 min

Table 1. Polymerization chain reaction conditions (PCR) PCR conditions for GAPDH, γ-actin, β-actin, GAP-43 and Tau including the initialization, denaturation, annealing, extension/elongation and final elongation temperature used to amplify mRNA extracts as well as the number of cycles needed for the amplification.